# Dissecting Multi-Layered Mechanisms of Plant Growth Promotion by *Pseudomonas argentinensis* SA190

Doctoral thesis

for

the award of the doctoral degree

of the Faculty of Mathematics and Natural Sciences

of the University of Cologne

submitted by

Büsra Elkatmis

July 2026

**Thesis Advisory Committee**

**First Supervisor**

Prof. Dr. Stanislav Kopriva

**Second Supervisor**

Prof. Dr. Heribert Hirt

**Third Supervisor**

Prof. Dr. Vera Göhre

**Fourth Supervisor**

Dr. Maged Saad

**Thesis Committee**

**First Reviewer/Examiner**

Prof. Dr. Stanislav Kopriva

**Second Reviewer/Examiner**

Prof. Dr. Tatjana Hildebrandt

**Chair of the Examination Committee**

Prof. Dr. Andreas Beyer

**Minute Taker**

Dr. Daniela Ristova

**Date of the Oral Examination: 15.09.2026**

## List of Abbreviations

| | |
|---|---|
| ABA | Abscisic acid |
| ABF/AREB | ABRE-binding factors/ABA-responsive element-binding proteins |
| ABREs | ABA-responsive elements |
| ACC | 1-aminocyclopropane-1-carboxylate |
| AAI | Average amino acid identity |
| ANI | Average nucleotide identity |
| APX | Ascorbate peroxidase |
| APS | Adenosine 5′-phosphosulfate |
| AsA | Ascorbate |
| AsA-GSH | Ascorbate-glutathione |
| BRs | Brassinosteroids |
| BSO | Buthionine sulfoximine |
| CAT | Catalase |
| CFU | Colony-forming units |
| DHAR | Dehydroascorbate reductase |
| DREB | Dehydration-responsive element-binding |
| EPS | Exopolysaccharides |
| GBDP | Genome BLAST distance phylogeny |
| GR | Glutathione reductase |
| GS | Glutathione synthetase |
| GSH | Glutathione |
| GSSG | Glutathione disulfide |
| GST | Glutathione S-transferase |
| γ-EC | γ-glutamylcysteine |
| γ-ECS | γ-glutamylcysteine synthetase |
| $H_2O_2$ | Hydrogen peroxide |
| $H_2S$ | Hydrogen sulfide |
| H3K4me3 | Histone H3 lysine 4 trimethylation |

| | |
|---|---|
| HGAP | Hierarchical genome assembly process |
| IAA | Indole-3-acetic acid |
| KEGG | Kyoto encyclopedia of genes and genomes |
| KMBA | 2-keto-4-methylthiobutyric acid |
| MAPK | Mitogen-activated protein kinase |
| MDHAR | Monodehydroascorbate reductase |
| NBT | Nitroblue tetrazolium |
| OAS | O-acetylserine |
| ORFs | Open reading frames |
| P5CR | $\Delta^1$-pyrroline-5-carboxylate reductase |
| P5CS | $\Delta^1$-pyrroline-5-carboxylate synthetase |
| PAP | 3′-phosphoadenosine-5′-phosphate |
| PEG | Polyethylene glycol |
| PGPB | Plant growth-promoting bacteria |
| PIPs | Plasma membrane intrinsic proteins |
| PP2C | Protein phosphatase 2C |
| PYR/PYL | Pyrabactin resistance/PYR1-like |
| RATE-PCR | Random amplification of transposon ends |
| ROS | Reactive oxygen species |
| S | Sulfur |
| SMRT | Single-molecule real-time |
| SnRK2 | SNF1-related protein kinase 2 |
| $SO_3^{2-}$ | Sulfite |
| $SO_4^{2-}$ | Sulfate |
| SOB | Sulfur-oxidizing bacteria |
| SOD | Superoxide dismutase |
| SRB | Sulfate-reducing bacteria |
| SULTRs | Sulfate transporters |
| TIPs | Tonoplast intrinsic proteins |
| TYGS | Type strain genome server |

# Table of content

**Abstract** ..... 1

**Introduction** ..... 2

Physiological and molecular mechanisms of drought stress adaptation in plants ..... 2

Plant growth-promoting bacteria as modulators of drought stress tolerance and their underlying mechanisms ..... 4

Sulfur metabolism and its role in plant stress responses ..... 7

Bacterial sulfur metabolism and its role in soil sulfur cycling and plant nutrition ..... 9

Sulfur metabolism in plant-microbe interactions under abiotic stress ..... 10

*Pseudomonas argentinensis* SA190 as a model organism ..... 11

Aim of this study ..... 12

**Publications included in this thesis** ..... 14

**Chapter 1** ..... 15

Integrated genomic and mutagenesis analysis of *Pseudomonas argentinensis* SA190 reveals mechanisms of plant root colonization and stress resilience ..... 15

**Chapter 2** ..... 31

Comprehensive mapping of EZ-Tn5 transposon insertion sites in *Pseudomonas argentinensis* SA190 using RATE-PCR ..... 31

**Chapter 3** ..... 44

Root endophyte sulfur metabolites enhance redox balance and drought tolerance in Arabidopsis ..... 44

**Discussion** ..... 72

Plant growth-promoting traits of SA190 ..... 72

Role of biofilm formation in SA190 root colonization and plant growth promotion ..... 73

Role of sulfur metabolism in SA190-mediated drought tolerance ..... 75

Limitations and future directions ..... 78

*Experimental limitations and ecological relevance* ..... 79

*Unresolved mechanisms of sulfur metabolism in the Arabidopsis-SA190 interaction* ..... 79

*Sulfur flux analysis and future perspectives* ..... 80

*Future directions for biofilm and colonization studies* ..... 80

*Conclusion* ..... 80

**References** ..... 81

**Author contributions** ..... 93

**Acknowledgements** ..... 95

**Erklärung** ..... 97

**Appendix** ..... 98

## Abstract

Plants are in constant interaction with their surrounding environment and are strongly influenced by it. Climate change-driven alterations in environmental conditions are causing significant and often unavoidable reductions in plant growth and productivity. Therefore, developing strategies to support plant growth and maintain yield under adverse environmental conditions has become increasingly important. In this context, plant growth-promoting bacteria (PGPB) have emerged as a promising solution to enhance plant growth and development. Notably, the identification of PGPB and understanding the mechanisms they employ have become particularly important due to their potential to support the development of stress-resilient plants. To gain insight into these interactions, this thesis focuses on elucidating the multi-layered mechanisms underlying the plant growth-promoting (PGP) activity of the root endophyte *Pseudomonas argentinensis* SA190.

The first study investigated the PGP traits, biochemical characteristics and stress tolerance capacity of SA190. We then constructed a transposon library to identify the key microbial traits underlying the PGP activity of SA190. Our results showed that biofilm mutants, particularly disruption of the *wspC*, *rpoE*, and *fliD* genes, resulted in reduced stable attachment to *Arabidopsis thaliana* roots and impaired PGP activity under PEG-induced drought stress. Secondly, we optimized the RATE-PCR protocol for SA190 to identify the genomic locations of Tn5 insertions. Since transposon mutagenesis generates random insertions in the bacterial genome, identifying the insertion sites allowed us to improve our understanding of SA190 genes and link specific genes to PEG-stress tolerance.

The final study examined the impact of SA190 on *Arabidopsis thaliana* metabolism, with a particular focus on sulfur metabolism. We found that SA190 modulates sulfur metabolism and enhances tolerance to PEG-induced drought stress by improving glutathione (GSH)-mediated redox homeostasis. Collectively, the studies presented in this thesis provide insights into the multi-layered mechanisms underlying plant growth promotion by SA190 under PEG-induced drought stress. These findings improve our understanding of plant-microbe interactions under stress conditions and highlight the potential application of beneficial microbes and their mechanisms for the development of stress-resilient plants.

## Introduction

### Physiological and molecular mechanisms of drought stress adaptation in plants

Drought is one of the major abiotic stresses that negatively affects plant growth and development (Zhou et al., 2007; Zinta et al., 2014). Ongoing climate change, particularly global warming, has altered precipitation patterns, increased temperatures, and enhanced evaporation rates, thereby reducing soil moisture retention and intensifying drought stress (Duchenne-Moutien & Neetoo, 2021; Sánchez-Bermúdez et al., 2022; Sato et al., 2024). Consequently, crop yields decline with increasing drought severity, as plants undergo significant metabolic and physiological disruptions (Dietz et al., 2021; Qiao et al., 2024). Due to their sessile nature, plants cannot escape the adverse effects of drought stress (Zia et al., 2021). However, they have evolved a range of adaptive mechanisms to mitigate its impact (Fang & Xiong, 2015; Kooyers, 2015; Zia et al., 2021).

Drought stress severely influences water uptake and transport in plants (Aroca et al., 2012; Zia et al., 2021). Water uptake and transport in roots are mainly regulated by plasma membrane intrinsic proteins (PIPs) and tonoplast intrinsic proteins (TIPs) (Javot & Maurel, 2002; Li et al., 2025). A reduction in soil water potential decreases water uptake by roots and modulates the expression of PIP and TIP genes (Aroca et al., 2012). This significant reduction in water uptake leads to a decline in cell turgor pressure, contributing to drought stress signaling (Zia et al., 2021). These signals are subsequently transmitted from roots to shoots via hormonal pathways, particularly through abscisic acid (ABA) (Thompson et al., 2007; Zia et al., 2021). One of the earliest physiological responses is stomatal closure under drought conditions, primarily mediated by ABA, to maintain cellular water levels (Muhammad Aslam et al., 2022; Saradadevi et al., 2017; Thompson et al., 2007; Zia et al., 2021). While stomatal closure reduces water loss through transpiration, it simultaneously limits $CO_2$ uptake, thereby impairing the photosynthetic machinery and reducing photosynthetic efficiency (Lu et al., 2020; Qiao et al., 2024).

In addition to these immediate responses, plants employ three major drought-response strategies such as drought escape, drought avoidance, and drought tolerance (Fang & Xiong, 2015; Kooyers, 2015) (Figure 1). Drought escape involves acceleration of the life cycle, leading to early flowering and reproduction before the onset of severe stress (Kooyers, 2015; Shavrukov et al., 2017). Drought avoidance includes morphological and anatomical adaptations such as reduced stomatal density (Shahbaz et al., 2025), decreased leaf area (Wang et al., 2024), and

increased primary root length (Jiang et al., 2026), which enhance water uptake (Fang & Xiong, 2015). In contrast, drought tolerance involves a series of metabolic and biochemical adjustments that enable plants to endure cellular dehydration (Haghpanah et al., 2024). One of the key mechanisms of drought tolerance is the activation of antioxidant defense systems to mitigate reactive oxygen species (ROS) accumulation under stress conditions (Haghpanah et al., 2024; Laxa et al., 2019). Both enzymatic antioxidants, such as superoxide dismutase (SOD), catalase (CAT), and ascorbate peroxidase (APX), and non-enzymatic antioxidants, including glutathione (GSH), play crucial roles in limiting oxidative damage (Haghpanah et al., 2024; Hasanuzzaman et al., 2020; Laxa et al., 2019). Furthermore, plants synthesize osmoprotectants such as proline, glycine betaine, and polyamines to maintain osmotic balance and stabilize cellular structures during drought stress (Haghpanah et al., 2024; Jarin et al., 2024; Singh et al., 2015).

Plant hormones, including ABA, auxin, and brassinosteroids (BRs), also regulate drought responses by modulating water loss and reshaping root architecture to enhance water uptake (Ali et al., 2025; Sharma et al., 2025). Among these, ABA plays a central role in activating and regulating plant responses at the transcriptional level (Jiang et al., 2026; Khan, 2025; Yao et al., 2020). Transcriptional responses to drought stress are mediated through both ABA-dependent and ABA-independent pathways, particularly well characterized in *Arabidopsis thaliana* (Liu et al., 2018; Yao et al., 2020). In the ABA-dependent signaling pathway, ABA is perceived by pyrabactin resistance/PYR1-like (PYR/PYL) receptors (Liu et al., 2018; Yao et al., 2020). Upon ABA binding, these receptors inhibit protein phosphatase 2C (PP2C), a negative regulator of the pathway, thereby relieving its suppression of SNF1-related protein kinase 2 (SnRK2) (Liu et al., 2018; Yao et al., 2020). Consequently, SnRK2 becomes activated and phosphorylates downstream transcription factors, including ABRE-binding factors/ABA-responsive element-binding proteins (ABF/AREB), which bind to ABA-responsive elements (ABREs) in target gene promoters, activating stress-responsive genes such as *RD29B* and *RAB18* (Fidler et al., 2022; Lim et al., 2022; Liu et al., 2018; Yao et al., 2020; Khan, 2025).

In the ABA-independent signaling pathway, drought signals are transduced through mitogen-activated protein kinase (MAPK) cascades and calcium ($Ca^{2+}$)-dependent signaling, which contribute to the activation of stress-responsive transcription factors, including dehydration-responsive element-binding (DREB) proteins (Sinha et al., 2011; Yao et al., 2020). DREB transcription factors, particularly DREB2A and DREB2B, bind to dehydration-responsive elements (DREs) in the promoter regions of target genes, thereby regulating their expression in

an ABA-independent manner (Yao et al., 2020). This pathway leads to the activation of several stress-responsive genes, such as *ERD1* and *COR15A* (Wu et al., 2023; Yao et al., 2020).

Understanding the mechanisms plants employ to mitigate drought stress is critical for sustaining plant growth and productivity. Given the accelerating impact of climate change on crop yield, a detailed understanding of drought response pathways is essential for developing sustainable strategies to improve crop resilience.

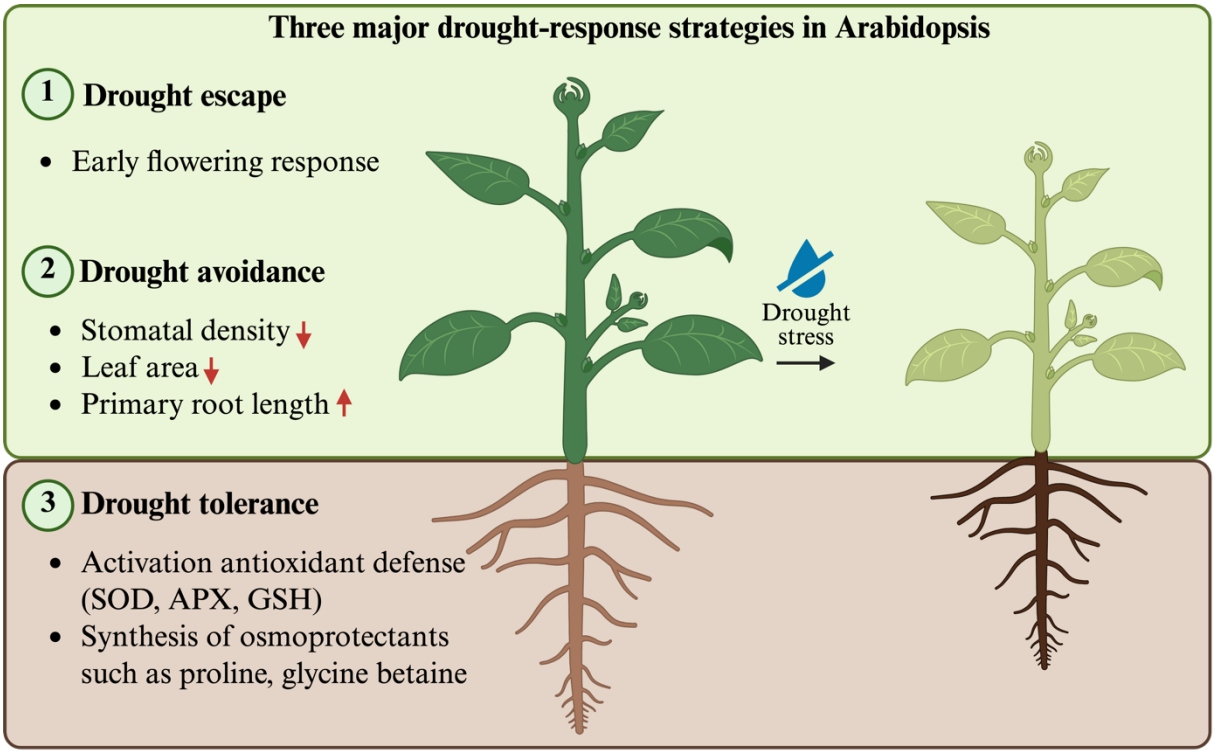



**Figure 1. Major drought response strategies employed by *Arabidopsis thaliana*.** Created with BioRender.

## Plant growth-promoting bacteria as modulators of drought stress tolerance and their underlying mechanisms

Plants exist within a dynamic environment in which their root systems are in constant interaction with a diverse array of soil microorganisms (Bardgett & Van Der Putten, 2014; Bulgarelli et al., 2013; Knights et al., 2021). These interactions range from mutualistic to parasitic depending on the organisms involved (Mendes et al., 2013). Microorganisms that promote plant growth are collectively referred to as plant growth-promoting bacteria (PGPB) (de Zelicourt et al., 2013; Lugtenberg & Kamilova, 2009; Pérez-Montaño et al., 2025). They enhance plant growth and development through diverse mechanisms, including improved nutrient uptake, the regulation of phytohormone production, and the induction of systemic

resistance against pathogens (de Zelicourt et al., 2013; Glick, 2012; Lugtenberg & Kamilova, 2009; Orozco-Mosqueda et al., 2018).

Beyond their role in promoting growth under normal conditions, PGPB have also been shown to significantly improve plant growth under abiotic stress conditions, particularly drought (Jakubowska et al., 2025; Pérez-Montaño et al., 2025). As mentioned in the previous section, plants possess a range of endogenous physiological and molecular mechanisms to mitigate the adverse effects of drought stress (Fang & Xiong, 2015; Kooyers, 2015; Laxa et al., 2019; Sharma et al., 2025; Singh et al., 2015; Zia et al., 2021). Plants can further benefit from their association with PGPB, which enhance drought tolerance in the host through multiple mechanisms, including phytohormone modulation (such as indole-3-acetic acid, IAA), 1-aminocyclopropane-1-carboxylate (ACC) deaminase activity, exopolysaccharide-mediated biofilm formation, osmotic adjustment, and modulation of antioxidant defense systems (Glick, 2012, 2014; Lugtenberg & Kamilova, 2009; Orozco-Mosqueda et al., 2018; Pérez-Montaño et al., 2025) (Figure 2).

Numerous PGPB produce the phytohormone auxin, specifically IAA, which enhances root growth, promotes lateral root formation, and enables roots to explore deeper soil layers (Chieb & Gachomo, 2023; Pérez-Montaño et al., 2025). The secretion of IAA by PGPB is particularly important under drought conditions, as it promotes root system remodeling (Chieb & Gachomo, 2023; Pérez-Montaño et al., 2025). In addition, some PGPB modulate ABA levels in the host, thereby modulating drought stress responses (Cohen et al., 2009; Gupta et al., 2022; Imran et al., 2023). Another important phytohormonal mechanism involves the production of ACC deaminase, which degrades the ethylene precursor ACC (Hewedy et al., 2026; Orozco-Mosqueda et al., 2020). Under drought stress conditions, elevated ethylene levels inhibit root growth (Hewedy et al., 2026; Orozco-Mosqueda et al., 2020). The production of ACC deaminase by PGPB therefore reduces ACC availability, limiting ethylene synthesis and ultimately enhancing drought tolerance in the host (Hewedy et al., 2026; Orozco-Mosqueda et al., 2020).

Another critical mechanism that PGPB deploy to mitigate the negative effects of drought is biofilm formation (Karimi et al., 2022; Pérez-Montaño et al., 2025). Biofilm formation is primarily driven by the production of exopolysaccharides (EPS), such as cellulose, which facilitate bacterial attachment and aggregation on the root surface (Bhattacharyya et al., 2023; Karimi et al., 2022; Lu et al., 2018; Morcillo & Manzanera, 2021). Biofilm development in the

rhizosphere creates a protective microenvironment that retains moisture around the root system, thereby reducing water loss and alleviating drought stress (Bhattacharyya et al., 2023; Morcillo & Manzanera, 2021; Naseem et al., 2018). Through this mechanism, EPS-producing PGPB help maintain high root water potential and support nutrient uptake from the surrounding soil under drought stress conditions (Bhattacharyya et al., 2023; Morcillo & Manzanera, 2021; Naseem et al., 2018). Several studies have highlighted the functional importance of EPS production in drought tolerance (Lu et al., 2018; Wang et al., 2019). Inoculation of tomato plants with biofilm-deficient mutants of *Bacillus amyloliquefaciens* 54 resulted in increased plant susceptibility to drought stress (Wang et al., 2019). On the other hand, inoculation with strong biofilm-forming mutants conferred resistance, as it increased relative water content compared to non-inoculated controls (Wang et al., 2019). In another study, the EPS-producing strain *Bacillus amyloliquefaciens* FZB42 improved plant growth under drought stress, while its EPS-deficient *epsC* mutant showed markedly reduced root colonization and diminished drought tolerance (Lu et al., 2018). As illustrated in these examples, biofilm formation is one of the essential traits of PGPB for enhancing drought tolerance.

Several PGPB induce plant osmolyte accumulation, such as proline, glycine betaine, and trehalose, which contribute to drought tolerance (Eswaran et al., 2024; Pérez-Montaño et al., 2025). The accumulation of these compounds within plant tissues lowers osmotic potential and helps maintain cellular water balance under drought stress conditions (Eswaran et al., 2024; García et al., 2017). Particularly, some PGPB modulate the plant's own osmolyte biosynthesis by upregulating key biosynthetic genes involved in proline synthesis such as $\Delta^1$-pyrroline-5-carboxylate synthetase (*P5CS*) and $\Delta^1$-pyrroline-5-carboxylate reductase (*P5CR*) in the host, thereby enhancing the plant's endogenous osmotic adjustment capacity (Ghosh et al., 2017).

Ultimately, PGPB also modulate the antioxidant defense system of the host plant under drought stress (Chieb & Gachomo, 2023; Pérez-Montaño et al., 2025). Drought stress promotes excessive accumulation of ROS, which cause oxidative damage to cellular components, including lipids, proteins, and nucleic acids (Bali, 2025). In response, plants activate their endogenous antioxidant systems to mitigate ROS-induced damage (Haghpanah et al., 2024; Hasanuzzaman et al., 2020; Laxa et al., 2019). PGPB enhance this response by regulating the activity of key antioxidant enzymes, including SOD, CAT, and APX, thereby reducing oxidative damage and improving plant growth and development under drought stress conditions (Batool et al., 2020; Pérez-Montaño et al., 2025). Several studies have also highlighted the essential role of PGPB in antioxidant mechanisms to enhance drought tolerance (Batool et al., 2020;

Pérez-Montaño et al., 2025; Pishchik et al., 2024). For instance, inoculation with *Bacillus subtilis* significantly enhanced SOD and CAT antioxidant enzyme activities in potato plants, which was associated with improved plant growth under drought stress conditions (Batool et al., 2020).

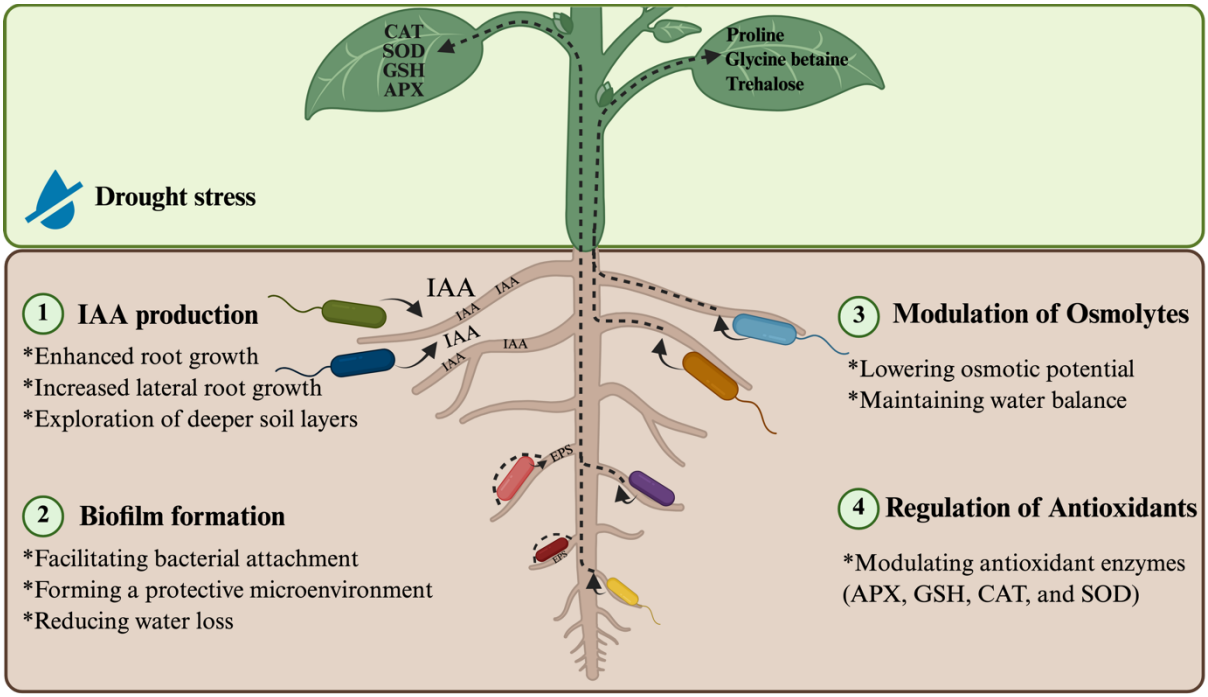



**Figure 2. Drought tolerance mechanisms utilized by plant growth-promoting bacteria (PGPB) under drought stress.** Created with Biorender.

## Sulfur metabolism and its role in plant stress responses

Sulfur (S) is an essential macronutrient required by all living organisms, including plants, humans, and microorganisms (Kopriva et al., 2019; Narayan et al., 2023). It plays fundamental roles in cellular metabolism, contributing to the synthesis of coenzymes and cofactors, and to antioxidant defense systems (Kopriva et al., 2019; Narayan et al., 2023). In particular, sulfur is critical for the synthesis of the amino acids cysteine and methionine, which are crucial for protein synthesis and serve as building blocks for a wide range of sulfur-containing metabolites vital for cellular function (Gigolashvili & Kopriva, 2014; Kopriva et al., 2019; Narayan et al., 2023). In plants, sulfur is predominantly taken up from the soil in the form of sulfate ($SO_4^{2-}$) via specialized sulfate transporters (SULTRs) (Gigolashvili & Kopriva, 2014; Kopriva, 2006). Once inside the plant, sulfate undergoes a series of reduction steps before being assimilated into organic compounds (Gigolashvili & Kopriva, 2014; Kopriva, 2006). This process is catalyzed by key enzymes, including ATP sulfurylase, APS reductase, and sulfite reductase, ultimately

leading to the formation of cysteine (Gigolashvili & Kopriva, 2014; Kopriva, 2006; Koprivova & Kopriva, 2016).

Cysteine represents a central branching point in sulfur metabolism (Kopriva, 2006). It serves as a precursor for the synthesis of methionine and various secondary metabolites, as well as GSH, a major antioxidant involved in maintaining cellular redox homeostasis (Gigolashvili & Kopriva, 2014; Hasanuzzaman et al., 2017; Kopriva, 2006). Through these pathways, sulfur assimilation contributes not only to primary metabolism and growth but also to stress responses and overall plant fitness (Kopriva et al., 2019; Moormann et al., 2025; Narayan et al., 2023).

Among sulfur-containing compounds, GSH is the most abundant low-molecular-weight non-protein thiol in plant cells, functioning as a central component of the cellular antioxidant system (Kopriva et al., 2012, 2019; Koprivova & Kopriva, 2016; Narayan et al., 2023). It is synthesized from the amino acids cysteine, glutamate, and glycine, which together form its tripeptide structure (Hasanuzzaman et al., 2017). GSH plays an essential role in protecting plants against oxidative damage by scavenging ROS, particularly under stress conditions such as drought (Hasanuzzaman et al., 2017). Under normal physiological conditions, GSH is predominantly present in its reduced form (Hasanuzzaman et al., 2017). However, drought stress enhances ROS production as part of the plant defense response (Bali, 2025; Nadarajah, 2020). Although ROS function as signaling molecules at low concentrations, their excessive accumulation leads to oxidative damage to cellular components, including lipids, proteins, and nucleic acids (Bali, 2025; Nadarajah, 2020).

To mitigate the detrimental effects of ROS overaccumulation, plants utilize the ascorbate-glutathione (AsA-GSH) cycle, a major pathway involved in the detoxification of ROS (Hasanuzzaman et al., 2017, 2020; Lou et al., 2018). In this cycle, hydrogen peroxide ($H_2O_2$) is primarily detoxified by APX, which oxidizes ascorbate (AsA) in the process (Chew et al., 2003; Gill & Tuteja, 2010; Lou et al., 2018). The oxidized forms of ascorbate are subsequently regenerated through the coordinated action of enzymes such as monodehydroascorbate reductase (MDHAR) and dehydroascorbate reductase (DHAR) (Chew et al., 2003). MDHAR reduces monodehydroascorbate to AsA using NADPH, whereas DHAR reduces dehydroascorbate to AsA using reduced GSH (Chew et al., 2003). During this process, GSH is oxidized to glutathione disulfide (GSSG) and is subsequently regenerated by glutathione reductase (GR) using NADPH (Bose Mazumdar & Chattopadhyay, 2025; Chew et al., 2003). This continuous cycle maintains cellular redox balance and plays a crucial role in supporting

plant survival and stress acclimation under drought conditions (Bose Mazumdar & Chattopadhyay, 2025; Chew et al., 2003).

Given the central role of the GSH-based antioxidant system in drought stress responses, exogenous application of GSH has been also improved drought tolerance in rice (Sohag et al., 2020). GSH treatment elevates the activity of enzymatic antioxidants, including CAT and POX, and increases the levels of non-enzymatic antioxidants such as AsA, while simultaneously reducing ROS accumulation, collectively contributing to improved oxidative stress tolerance (Sohag et al., 2020). Despite these findings, the molecular mechanisms underlying GSH-mediated drought tolerance remain incompletely understood, highlighting the need for further investigation.

**Bacterial sulfur metabolism and its role in soil sulfur cycling and plant nutrition**

Sulfur metabolism plays an important role in bacteria, supporting key processes such as amino acid biosynthesis and energy production (Carbonero et al., 2012; Kim et al., 2024; Kushkevych et al., 2020). Bacteria utilize sulfur to synthesize amino acids (cysteine and methionine), vitamins, and several enzymatic cofactors (Kim et al., 2024; Kushkevych et al., 2020). In assimilatory sulfate reduction, inorganic $SO_4^{2-}$ is reduced stepwise via adenosine 5′-phosphosulfate (APS) and sulfite ($SO_3^{2-}$) to hydrogen sulfide ($H_2S$), which is subsequently incorporated into cysteine through its reaction with O-acetylserine (OAS), catalyzed by OAS thiol-lyase (Kim et al., 2024; Kumar et al., 2018; Mansilla et al., 2000). In Gram-negative bacteria such as *Escherichia coli*, genes involved in this process are regulated by the transcriptional regulator CysB (Albanesi et al., 2005; Kertesz, 2000; LeBoeuf & Grove, 2025).

Beyond biosynthesis, sulfur metabolism also plays a central role in energy metabolism in specialized bacterial groups, particularly under anaerobic conditions (Chen et al., 2021; Kováč et al., 2018; Kumar et al., 2018; Plugge et al., 2011). For instance, sulfate-reducing bacteria (SRB) use sulfate as a terminal electron acceptor in anaerobic respiration, reducing it to $H_2S$ for energy generation (Kováč et al., 2018; Plugge et al., 2011). In contrast, sulfur-oxidizing bacteria (SOB) oxidize reduced sulfur compounds such as $H_2S$ and elemental sulfur to sulfate, using this process to also generate energy (Chen et al., 2021; Kumar et al., 2018).

Importantly, these microbial processes are closely linked to sulfur availability in soil (Chaudhary et al., 2023; Gahan & Schmalenberger, 2014). As mentioned in the previous section, plants take up sulfate from the soil through their roots to synthesize cysteine and other

essential sulfur-containing compounds (Gigolashvili & Kopriva, 2014; Kopriva et al., 2019; Narayan et al., 2023). However, in soil, sulfur is largely present in organic matter such as sulfate esters and sulfonates (Gahan & Schmalenberger, 2014; Mirleau et al., 2005). Therefore, microbial sulfur cycling processes are critical for increasing sulfate availability for plant uptake (Gahan & Schmalenberger, 2014; Mirleau et al., 2005). In this context, soil bacteria play an essential role in sulfate mineralization by breaking down organic matter using enzymes such as arylsulfatases and sulfonatases, thereby releasing sulfate from organic matter and making it available to plant roots (Gahan & Schmalenberger, 2014; Mirleau et al., 2005).

**Sulfur metabolism in plant-microbe interactions under abiotic stress**

Sulfur metabolism plays a substantial role in plant-microbe interactions under abiotic stress conditions (Kopriva et al., 2019). As sulfur is a key component of the antioxidant defense system, it helps alleviate the detrimental effects of abiotic stresses (Takahashi et al., 2023). Several studies have highlighted the importance of sulfur metabolism and sulfur-containing compounds in mediating plant-microbe interactions under abiotic stress conditions (Andrés-Barrao et al., 2021; Mukherjee et al., 2025; Shekhawat et al., 2024).

For instance, the root endophytic bacterium *Enterobacter* sp. SA187 enhances Arabidopsis growth under salt stress conditions (Andrés-Barrao et al., 2021). The study has shown that sulfur metabolism in both SA187 and Arabidopsis contributes to their beneficial interaction under salt stress conditions (Andrés-Barrao et al., 2021). The integrated regulation of sulfur metabolism in the plant and bacteria supports the overall dynamics of this interaction during salt stress (Andrés-Barrao et al., 2021). It has been demonstrated that SA187 transfers the sulfur-containing molecule 2-keto-4-methylthiobutyric acid (KMBA) to the plant, which acts as a precursor of ethylene (Andrés-Barrao et al., 2021). KMBA is converted into ethylene within the plant, and ethylene signaling subsequently regulates the sulfur regulon (Andrés-Barrao et al., 2021). This modulation of the sulfur regulon not only enhances sulfate uptake and promotes the synthesis of cysteine but also influences key antioxidant molecules such as GSH that scavenge ROS under salt stress (Andrés-Barrao et al., 2021). Furthermore, another study on SA187 revealed that it confers high-light stress protection in Arabidopsis via ethylene-dependent mechanisms (Shekhawat et al., 2024). The study demonstrated that SA187 influences sulfur and iron uptake and activates the glutathione redox system, thereby enhancing plant tolerance to high-light stress (Shekhawat et al., 2024).

In addition, another study demonstrated that extracellular secretion of GSH by an 18-membered bacterial community improves Arabidopsis growth under sulfur-deficient conditions (Mukherjee et al., 2025). The importance of microbial GSH production was further confirmed using a Δ*gshA* mutant derived from wild-type *Pseudomonas* sp. 6A2 (Mukherjee et al., 2025). Application of extracellular secretions from the Δ*gshA* mutant and wild-type *Pseudomonas* sp. 6A2 showed that the mutant reduced Arabidopsis growth, indicating that bacterial glutathione synthesis is essential for its beneficial effects under sulfur-deficient conditions (Mukherjee et al., 2025).

These studies underline the importance of sulfur metabolism in plant-microbe interactions under abiotic stress conditions (Andrés-Barrao et al., 2021; Mukherjee et al., 2025; Shekhawat et al., 2024). To date, the importance of sulfur metabolism in plant-microbe interactions under drought stress remains poorly understood. Understanding these interactions in molecular detail and their underlying mechanisms will not only improve our knowledge but also enhance the potential to develop strategies for improving crop resilience under abiotic stress.

***Pseudomonas argentinensis* SA190 as a model organism**

*Pseudomonas argentinensis* SA190 is a root endophyte isolated from the root nodules of the desert plant *Indigofera argentea* in Saudi Arabia (Alwutayd et al., 2023; Lafi et al., 2016). SA190 treatment enhanced Arabidopsis growth under 25% polyethylene glycol (PEG)-induced drought stress conditions (Alwutayd et al., 2023). The study showed that SA190 improves water use efficiency and regulates stomatal behavior, thereby alleviating drought stress (Alwutayd et al., 2023).

Building on this, transcriptome analysis indicated that SA190 upregulated aquaporin genes, including *TIP1;2, TIP2;1, PIP1;3,* and *PIP1;5*, in roots under 25% PEG-induced drought stress (Alwutayd et al., 2023). The study also highlighted enrichment of histone H3 lysine 4 trimethylation (H3K4me3) at these aquaporin genes, indicating epigenetic regulation (Alwutayd et al., 2023). Furthermore, analysis of the ABA-deficient mutant *aba2-1* and pyrabactin resistance/pyrabactin resistance-like (PYR/PYL) receptor mutants showed reduced SA190-induced expression of aquaporin genes under PEG stress, indicating that the ABA signaling pathway is important for regulating aquaporin gene expression in response to SA190 (Alwutayd et al., 2023).

In addition, SA190 treatment improved biomass production in crops such as alfalfa under drought stress (Alwutayd et al., 2023). However, the key molecules and mechanisms contributing to the beneficial effects of SA190 remain unclear.

**Aim of this study**

Given the importance of plant growth-promoting bacteria (PGPB) in enhancing plant performance under stress, it is essential to identify their key traits and understand the mechanisms underlying their beneficial effects (Pérez-Montaño et al., 2025). In this study, *Pseudomonas argentinensis* SA190 is used as a model PGPB to systematically characterize its physiology and plant growth-promoting properties. To achieve this, a transposon mutant library was generated and screened to identify genes and microbial traits essential for root colonization and plant growth promotion. Drought stress was used as a biologically relevant condition for the functional analysis of PGP traits, since SA190 was isolated from a desert plant adapted to arid environments.

Building on the mutant screen approach, targeted analyses were performed to investigate specific mechanisms contributing to SA190-mediated plant benefits. In particular, biofilm formation was tested as a key trait for root colonization, and sulfur metabolism was studied as a previously uncharacterized component of the Arabidopsis-SA190 interaction. The objectives of this thesis are:

1) To characterize the physiology of SA190 and identify its key PGP traits using a transposon mutant screen

2) To investigate the role of biofilm formation in SA190 root colonization and its contribution to plant growth promotion under PEG-induced drought stress

3) To elucidate the role of sulfur metabolism in the beneficial interaction between SA190 and *Arabidopsis thaliana* under PEG-induced drought stress

To address the first two objectives, a transposon mutant library was generated and screened under 25% PEG-induced drought conditions. Mutants affected in biofilm formation were specifically analyzed to assess their contribution to root colonization and PGP activity. Random amplification of transposon ends (RATE)-PCR was optimized to map insertion sites.

To address the third objective, sulfur metabolism was investigated using Arabidopsis mutants (*sultr1;2*, *apr2*, and *cad2-1*) under PEG-induced drought stress. Redox parameters and GC-MS-based metabolite profiling were analyzed to characterize sulfur-related responses. Additionally, bacterial *gshA* and *gshB* mutants were used to assess the contribution of bacterial GSH biosynthesis to plant growth promotion under PEG stress.

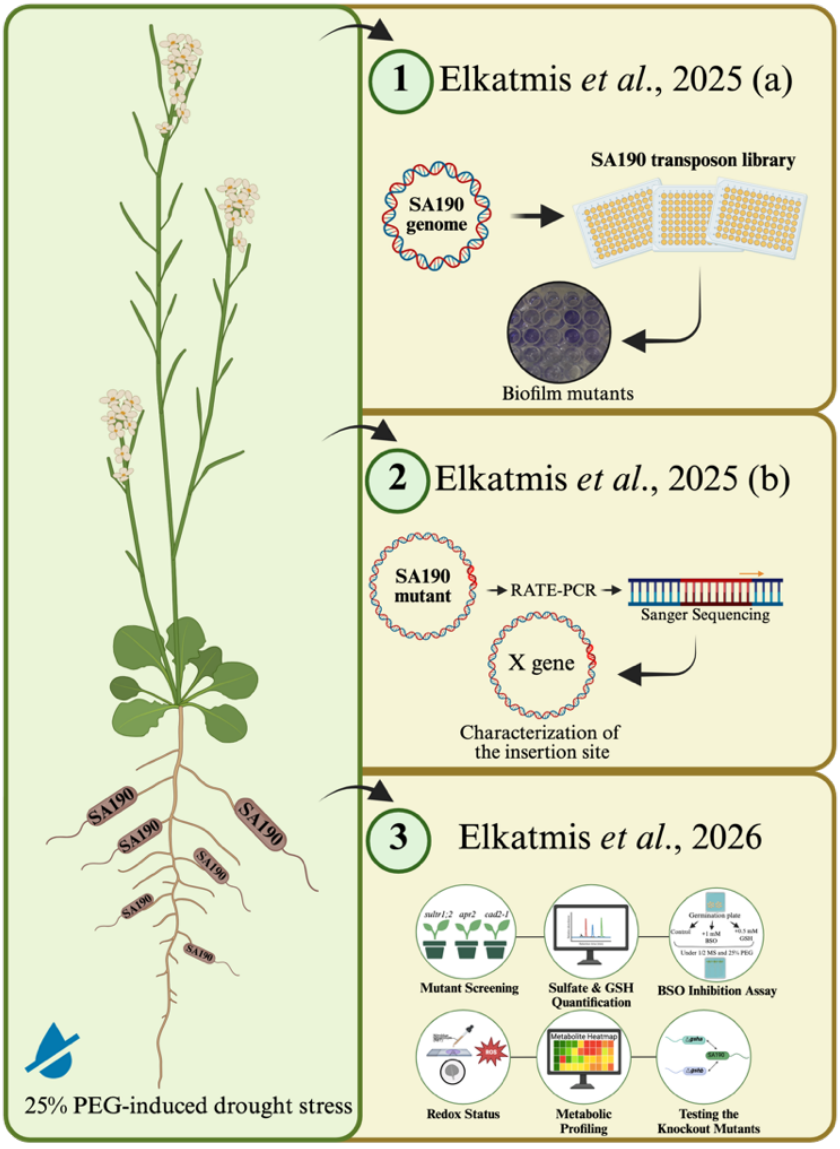



**Figure 3. Representation of the studies carried out in this thesis.** 1) A mutant library of SA190 was generated, and the importance of biofilm-related genes in drought tolerance and root colonization was characterized (Elkatmis, Parween, et al., 2025). 2) Insertion sites in the SA190 transposon library were mapped by optimizing RATE-PCR (Elkatmis, Han, et al., 2025). 3) The role of sulfur metabolism and glutathione (GSH) was investigated in the beneficial interaction between SA190 and Arabidopsis under PEG-induced drought stress (Elkatmis et al., 2026). Created with Biorender.

## Publications included in this thesis

**Elkatmis B**, Parween S, Eida AA, Jalal R, Lafi F, Alam I, Kopriva S, Hirt H, Saad MM. (2025) Integrated genomic and mutagenesis analysis of *Pseudomonas argentinensis* SA190 reveals mechanisms of plant root colonization and stress resilience. BMC Microbiology 25, 785. https://doi.org/10.1186/s12866-025-04495-2

**Elkatmis B**, Han B, Parween S, Kopriva S, Hirt H, Saad MM. (2025) Comprehensive mapping of EZ-Tn5 transposon insertion sites in *Pseudomonas argentinensis* SA190 using RATE-PCR. Bio-protocol 15: e5389. https://doi.org/10.21769/BioProtoc.5389

**Elkatmis B**, Alkhateeb RS, Mannes C, Jalal R, Trapp M, Westhoff P, Ozkan C, Thelen GM, Han B, Saad MM, Kopriva S, Hirt H. (2026) Root endophyte sulfur metabolites enhance redox balance and drought tolerance in Arabidopsis. bioRxiv 2026.06.15.732246. https://doi.org/10.64898/2026.06.15.732246

# Chapter 1

## Integrated genomic and mutagenesis analysis of *Pseudomonas argentinensis* SA190 reveals mechanisms of plant root colonization and stress resilience

**Elkatmis B,** Parween S, Eida AA, Jalal R, Lafi F, Alam I, Kopriva S, Hirt H, Saad MM (2025)

BMC Microbiology 25, 785. https://doi.org/10.1186/s12866-025-04495-2

### Authors contributions

**B.E**.: Data curation, investigation, validation, methodology development, writing—original draft, and writing—review and editing. S.P., A.A.E., R.J., F.L., and I.A.: Methodology refinement and data curation. S.K.: Conceptualization, supervision, and manuscript review and editing. H.H.: Funding acquisition, project supervision, and writing—review and editing. M.M.S.: Project ideation and conceptualization, supervision of experimental design, protocol tuning, validation, and manuscript writing—review and editing.

Elkatmis *et al. BMC Microbiology* (2025) 25:785

BMC Microbiology

https://doi.org/10.1186/s12866-025-04495-2

RESEARCH Open Access

# Integrated genomic and mutagenesis analysis of *Pseudomonas argentinensis* SA190 reveals mechanisms of plant root colonization and stress resilience

Büsra Elkatmis[1,2], Sabiha Parween[1], Abdul Aziz Eida[1], Rewaa Jalal[3], Feras Lafi[4], Intikhab Alam[5], Stanislav Kopriva[2], Heribert Hirt[1,6*] and Maged M. Saad[1*]

**Abstract**

**Background** *Pseudomonas argentinensis* SA190 is a desert-adapted, plant-associated bacterium with demonstrated potential to enhance plant growth under abiotic stress. In this study, we conducted a comprehensive genomic and functional characterization of SA190 to uncover the molecular mechanisms underlying its biofilm formation, root colonization, and plant growth-promoting traits.

**Results** The SA190 genome consists of a single circular chromosome (5.07 Mb, 64% GC) encoding 4561 predicted ORFs. Functional annotation revealed genes related to phosphate solubilization (*pqq* operon), antifungal activity, and stress mitigation, including ACC deaminase. AntiSMASH analysis identified eight biosynthetic gene clusters linked to secondary metabolite production, including siderophores, terpenes, and β-lactones. Metabolic profiling demonstrated selective utilization of root exudate-associated sugars, consistent with rhizosphere adaptation. By a Tn5 transposon mutagenesis approach, we identified key regulators required for biofilm formation. Biofilm mutants deficient in *wspC*, *rpoE*, and *fliD* were differentially compromised in plant colonization and plant growth promotion under ambient and/or drought conditions.

**Conclusion** Our study suggests that SA190 is a metabolically streamlined yet ecologically versatile PGPB and provides functional insights into its potential application as a bioinoculant for sustainable agriculture in arid environments.

**Keywords** Drought tolerance, Transposon mutagenesis, Biofilm formation and sustainable agriculture

*Correspondence:
Heribert Hirt
Heribert.hirt@kaust.edu.sa
Maged M. Saad
Maged.saad@kaust.edu.sa
[1]DARWIN21, Biological and Environmental Science and Engineering Division, King Abdullah University of Science and Technology (KAUST), Thuwal 23955-6900, Saudi Arabia
[2]Institute for Plant Sciences, Cluster of Excellence on Plant Sciences, University of Cologne, Zülpicher Str. 47b, Cologne 50674, Germany
[3]Department of Biological Sciences, College of Sciences, University of Jeddah, Jeddah 21493, Saudi Arabia
[4]College of Natural and Health Sciences, Zayed University, Dubai, United Arab Emirates
[5]Computational Bioscience Research Center, Computer, Electrical and Mathematical Sciences and Engineering Division, King Abdullah University of Science and Technology (KAUST), Thuwal 23955-6900, Kingdom of Saudi Arabia
[6]Max Perutz Laboratories, University of Vienna, Vienna, Austria

© The Author(s) 2025. **Open Access** This article is licensed under a Creative Commons Attribution-NonCommercial-NoDerivatives 4.0 International License, which permits any non-commercial use, sharing, distribution and reproduction in any medium or format, as long as you give appropriate credit to the original author(s) and the source, provide a link to the Creative Commons licence, and indicate if you modified the licensed material. You do not have permission under this licence to share adapted material derived from this article or parts of it. The images or other third party material in this article are included in the article's Creative Commons licence, unless indicated otherwise in a credit line to the material. If material is not included in the article's Creative Commons licence and your intended use is not permitted by statutory regulation or exceeds the permitted use, you will need to obtain permission directly from the copyright holder. To view a copy of this licence, visit http://creativecommons.org/licenses/by-nc-nd/4.0/.

## Introduction

Climate change is a significant global challenge that poses a threat to both ecosystems and human populations by affecting food security, especially in regions predicted to experience extreme weather patterns such as droughts [1]. These environmental changes exert considerable stress on plants, which are inherently sessile organisms. Unlike animals, plants cannot relocate in response to stress, making them particularly vulnerable to both biotic stresses (e.g., pathogens) and abiotic stresses (e.g., drought, salinity, high temperatures) [2, 3]. This vulnerability is likely to lead to significant declines in food production, exacerbating the global food security crisis expected as the world's population approaches 10 billion by 2050 [4, 5]. Therefore, understanding plant responses to these stress factors is crucial to develop solutions that ensure agricultural sustainability under changing environmental conditions.

Soil hosts a great microbial diversity [6–8]. This diversity diminishes from bulk soil to the rhizosphere [9, 10]. The plant creates a nutrient-rich environment in the rhizosphere by secreting a wide range of photosynthetically fixed carbon molecules such as amino acids, sugars, enzymes, vitamins, secondary metabolites, and organic acids [7, 8, 11, 12]. These exudates attract bacteria through chemotaxis, and in addition, flagella and type IV pili systems facilitate bacterial motility towards and colonization of the roots [6, 7, 13]. Once rhizosphere-associated bacteria reach the roots, they strengthen their attachment by secreting exopolysaccharides (EPS) and cell surface polysaccharides, converting weak interactions into irreversible binding [6]. This process often leads to the formation of biofilms, which protect bacterial cells from environmental stresses such as temperature fluctuations, pH shifts, drought, and pathogen attacks in the rhizosphere [6, 14]. While these microbial strategies are common among root-colonizing bacteria, plants also selectively recruit diverse beneficial microbes, including endophytes, to form a healthy root microbiome [15, 16]. Among the beneficial microbes, endophytic plant growth-promoting bacteria (PGPB) play a crucial role in enhancing plant performance through various mechanisms [17]. For example, they improve plant growth by producing phytohormones and increasing nutrient acquisition [18]. Despite the abundance of nutrients in the soil, some may not be bioavailable for plants. PGPB help plants to utilize these unavailable nutrients through siderophore production, phosphate solubilization, and nitrogen fixation [19, 20]. Additionally, PGPB contribute significantly to enhancing plant biomass under stress conditions by releasing antioxidants and improving water use efficiency [21, 22]. Stressed plants produce more reactive oxygen species (ROS) than non-stressed ones [23]. Some PGPB bacteria produce antioxidants that reduce ROS accumulation in stressed plants [24]. For example, bacterial carotenoids contribute to the development of stress tolerance in plants, thereby promoting their growth [24]. Taken together, endophytic PGPB contribute significantly to plant growth and productivity.

Arid and semi-arid environments are ideal for identifying plant growth-promoting bacteria, as they harbour microbes naturally adapted to harsh conditions such as drought, salinity, and heat [25]. In line with this, an endophytic bacterium isolated from the nodule of *Indigofera argentea* in the Jizan region of Saudi Arabia was shown to enhance plant biomass under stress conditions [22, 26]. Draft genome sequence and 16 S rRNA analysis confirmed that SA190 belongs to the *Pseudomonas* genus, characterized by a gram-negative cell wall, rod-shaped morphology, aerobic metabolism, and polar flagellar motility [26, 27]. Biochemical analysis showed that SA190 was capable of phosphate solubilization, indole-3-acetic acid (IAA), and siderophore production [26]. SA190 has been shown to be an alternative biostimulant with its plant growth-promoting traits. The endophyte SA190 increased the biomass of Arabidopsis under drought stress [22]. The transcriptomic study revealed that under drought stress, the expression of aquaporin genes, specifically plasma membrane intrinsic proteins (PIPs) and tonoplast intrinsic proteins (TIPs), in Arabidopsis were induced through histone methylation triggered by SA190 [22]. Despite these findings, the specific genes and mechanisms by which SA190 enhances plant growth under stress remain largely unknown. In this study, we aimed to identify the genetic basis of biofilm formation and root colonization in *Pseudomonas argentinensis* SA190. Using integrated genomic and mutagenesis analyses, we focused on identifying regulators that contribute to its function as a rhizosphere-competent, stress-resilient bioinoculant. By characterizing these genetic components, this research provides a deeper understanding of how microbial interactions can be leveraged to improve crop resilience in the face of climate change.

## Materials and methods

### Growth condition of *Pseudomonas argentinensis* SA190 and mutants

*Pseudomonas argentinensis* SA190 was previously isolated from the root nodules of the *Indigofera argentea*, an indigenous desert plant in the Jizan region (16°56.475'N, 42°36.694'E) of Saudi Arabia [26]. SA190 was grown overnight at 28 °C on Luria-Bertani (LB, Invitrogen) supplemented with 0.9% agar (Sigma-Aldrich). For SA190 mutants, 50 $\mu$g/ml kanamycin (kan) was added to the LB medium.

### Genomic DNA isolation

The genomic DNA of SA190 was extracted from the bacterial culture using a Qiagen DNeasy Blood and Tissue Kit (Qiagen GmbH, Hilden, Germany), following the manufacturer's protocol. The extracted DNA was treated with RNase A (Mo Bio Laboratories, Carlsbad, CA, United States) and then purified using the Mo Bio PowerClean Pro DNA Clean-Up Kit (Mo Bio Laboratories, Carlsbad, CA, United States), again following the manufacturer's protocol. The quantity and quality of the DNA were measured using a NanoDrop 2000 (Thermo Fisher Scientific, Wilmington, DE, United States) and a Qubit 2.0 (Life Technologies, Invitrogen Division, Darmstadt, Germany).

### Whole genome sequencing and function annotation

Whole genome sequencing was performed by DNA Link Korea (Seoul, South Korea) using the PacBio RS II sequencing platform (Pacific Biosciences, Menlo Park, CA, United States). Large-insert libraries were sequenced in single-molecule real-time (SMRT) sequencing cells using P6-C4 chemistry. PacBio reads were assembled into a single contig using the *de novo* Hierarchical Genome Assembly Process (HGAP.2) algorithm with default parameters. Genome annotation was conducted using the in-house Automatic Annotation of Microbial Genomes (AAMG) pipeline [28]. Open reading frames (ORFs) were predicted using FragGeneScan. Functional analysis was performed using the Kyoto Encyclopedia of Genes and Genomes (KEGG) [29]. AntiSMASH (version 8.0.4) was used to identify gene clusters associated with secondary metabolites [30].

### Phylogenomic classification of SA190

The genome sequence of SA190 was uploaded to the Type Strain Genome Server (TYGS) (https://tygs.dsmz.de) to compare it with the genomes available in the TYGS database using the MASH algorithm for a fast approximation of intergenomic relatedness. Ten strains with the smallest MASH distances were selected. These closely related strains were identified based on the 16S rRNA. The data were extracted using RNAmmer [31]. The sequences were then BLASTed against the 16 S rRNA gene sequences of the strains available in the database. This method was utilized to choose the most suitable strains based on their bitscore. The Genome BLAST Distance Phylogeny (GBDP) approach was used to calculate the precise distances using the "coverage" algorithm and distance formula d5 [31]. The closest strain genome to SA190 was determined based on the distance results. For the phylogenomic analysis, pairwise comparisons among the genomes were performed using GBDP. Intergenomic distances were accurately calculated using the "trimming" algorithm with distance formula d5, with 100 replicates generated for each distance measurement. The recommended settings of GGDC 3.0 were used to calculate the DDH values and confidence intervals. FASTME 2.1.6.1 and SPR post-processing were used for intergenomic distances in the phylogenetic tree [32]. The tree was visualized with PhyD3 [33].

### Average Amino Acid Identity (AAI) calculation

Pairwise genomic similarity was assessed using Average Amino Acid Identity (AAI) analysis. Protein-coding sequences were extracted from each genome resulting from ANI analysis, and reciprocal best BLAST hits (RBH) were identified to determine orthologous gene pairs between genomes. For each ortholog pair, amino acid sequences were aligned using BLASTP, and pairwise identity was calculated. The AAI value for each genome pair was computed as the arithmetic mean of amino acid identity across all identified orthologous proteins. The EzAAI software (version 1.2.2) [34] was used with default parameters, employing a minimum alignment length threshold of 70% and a BLASTP e-value cutoff of 1e-5 to ensure robust ortholog identification.

### Biochemical assays

Biochemical analyses were performed to evaluate the plant growth-promoting traits of SA190. Phosphate solubilization was tested on Pikovskaya's (PVK) agar plates (M520, Himedia). Indole-3-acetic acid (IAA) production by SA190 was measured according to Bric et al., 1991 [35] Siderophore production by SA190 was evaluated using the method described by Louden et al., 2011 [36]. Zinc solubilization was tested on modified PVK agar plates supplemented with 3% ZnO and 0.1% ZnCO3, as described by Bapiri et al., 2012 [37]. Tolerance to abiotic stresses was assessed by growing SA190 in LB broth (Lennox L Broth Base, Invitrogen) supplemented with 10% or 20% (w/v) polyethylene glycol (PEG) 8000 for drought stress and 0.1 M, 0.5 M or 1 M NaCl for salt stress. The API 50 CH test kit (Biomerieux, France) was used to test the fermentation of 49 carbohydrates in SA190, following the manufacturer's protocol. The antibiotic sensitivity of SA190 was tested using a clearing test. Antibiotic disks were placed on LB plates, and 100 $\mu$l of SA190 culture was spread onto the plates. Bacterial growth around the disks indicated antibiotic resistance (R), while no growth around the disks demonstrated antibiotic sensitivity (S).

### Tn5 mutagenesis and insertion mapping workflow

**Preparation of competent cells** A single colony of SA190 was cultured in LB broth to mid-log phase ($OD_{600} \approx 0.4$). Cells were chilled, washed twice with ice-cold sterile water, and resuspended in 10% glycerol. Aliquots (100 $\mu$L) were stored at – 80 °C.

### Electroporation with EZ-Tn5™ <KAN-2>

Competent cells were thawed and mixed with 0.5 $\mu$L of EZ-Tn5 transposon DNA (Epicentre). Electroporation was performed using the Bio-Rad MicroPulser (Ec1 program, 1.5 kV). SOC medium (900 $\mu$L) was added immediately post-electroporation, followed by 1.5 h recovery at 28 °C. Transformed cells were plated on LB agar supplemented with kanamycin (50 $\mu$g/mL). Control transformations (no transposon) were included.

### Construction of mutant library

The library was constructed according to Elkatmis et al., 2025 [38]. In brief, individual kanamycin-resistant colonies were transferred to 96-well plates containing $LB_{kan}$ broth. Glycerol stocks were prepared (1:1 with 20% glycerol) and stored at − 80 °C. For screening, mutants were replicated onto $LB_{kan}$ agar using a 96-pin replicator.

### RATE-PCR for insertion site mapping

Insertion sites were mapped using Random Amplification of Transposon Ends (RATE-PCR) following the insertation protocol in Elkatmis et al., 2025 [38]. Boiled cell lysates were used as PCR templates with primers Inv-1 or Inv-2 and Phusion polymerase. Amplification involved a three-phase cycling protocol. Products were purified with ExoSAP-IT and submitted to Sanger sequencing using KAN-2 specific primers. Detailed reagent composition, PCR conditions, and primer sequences are listed in Supplementary Table 1.

### Sequence analysis validation

Insertion sites in the SA190 Tn5 mutants were validated by Sanger and HiSeq sequencing (Supplementary Table 2) [38]. Sequence data were analyzed using SnapGene (Version 6.2.1) and further examined with the NCBI BLASTn program to identify disrupted genes. This process allowed for creating a gene list for the identified SA190 mutants.

### Biofilm formation assay

Biofilm formation was quantitatively assessed using a colorimetric assay [39]. Wild-type SA190 and mutants were grown overnight in LB and $LB_{kan}$ broth, respectively. The overnight cultures were diluted at 1:100 and transferred to a 96-well plate. This plate was incubated at 28 °C overnight. After incubation, the liquid was decanted, and the plate was rinsed with water to remove residual liquid. Next, 125 $\mu$l of 0.1% crystal violet solution was added to each well, and the plate was incubated at room temperature for 15 min. The plate was then rinsed four times with water and allowed to dry for 4 h. To solubilize the crystal violet, 125 $\mu$l of 30% acetic acid was added to each well, and the plate was incubated at room temperature for 15 min. Absorbance was measured at 550 nm using a plate reader (TECAN Infinite).

### Plant drought resistance assays

The plant drought resistance assay was performed as described by Alwutayd et al., 2023 [22], with minor modifications. Arabidopsis seeds were surface sterilized with 70% ethanol + 0.05% SDS for 10 min with shaking at 3000 rpm. The seeds were washed three times with 1 ml of 100% ethanol. SA190 and mutants were streaked onto LB and $LB_{kan}$ plates, respectively. Plates were incubated overnight at 28 °C. A single colony from the plates was transferred to LB broth medium. Fifty $\mu$g/ml kanamycin antibiotic was used in LB broth medium for mutants. Liquid cultures were incubated overnight at 28 °C, 220 rpm. 100 $\mu$l was taken from the overnight culture and transferred to fresh LB and $LB_{kan}$ broth medium. Incubation at 28 °C was followed by centrifugation at 3000 rpm for 15 min. The bacterial culture was washed with ½ MS solution (Murashige and Skoog basal salts, Sigma-Aldrich). The optical density of the bacterial suspension was set to $OD_{600}$ 0.21. 100 $\mu$l of bacterial suspension was added to 50 ml of ½ MS agar and poured into the square Petri plate (120 mm x 120 mm). 100 $\mu$l of ½ MS solution was added to 50 ml of ½ MS agar for the mock treatment. Sterilized seeds were distributed on the plates. The plates were covered with aluminium foil and kept in the dark at 4 °C for two days. They were transferred to the growth chamber under long-day photoperiod conditions (16 h light, 8 h dark). After five days of germination, seedlings with 1.0–1.5 cm root length were transferred to ½ MS and ½ MS + 25% PEG plates. Six seedlings were transferred for each plate. They were placed into the growth chamber under the same conditions. The fresh weight of the seedlings was measured 15 days after the seedlings were transferred to non-stress and stress plates. The colony-forming units (CFU) in the roots were determined by following M. Saad et al., 2018 [40] to compare the colonization efficiency between wild type SA190 and the mutants. To assess the CFU levels of endophytes, roots were surface sterilized with 70% ethanol for 30 s, followed by two rinses with sterile water.

### Statistical analysis

All statistical analyses in this study were conducted using GraphPad Prism (version 10.2.0). Biofilm data were analyzed using Welch's and Brown–Forsythe one-way ANOVA. Post hoc multiple comparisons were performed with Dunnett's T3 test. Results are presented as column graphs, and different letters above the bars indicate statistically significant differences between groups ($p < 0.05$). Colony-forming unit (CFU) data were generated from

four independent biological replicates and $log_{10}$-transformed prior to analysis. The plant assay was performed with three biological replicates and two technical replicates. Data were analyzed using two-way ANOVA, followed by Tukey's post hoc test for multiple comparisons. In the boxplot, whiskers represent the minimum and maximum values, while the horizontal line indicates the median. Different letters indicate statistically significant differences based on two-way ANOVA ($p < 0.05$).

### Data deposition

The genome sequence of SA190 was deposited in NCBI/DDBJ/EMBL database under the accession number CP056087.1 with BioProject no. PRJNA312745.

## Results and discussion

### Genome sequence assembly and general features

To ensure the accuracy and completeness of the SA190 genome assembly, we re-sequenced the strain using PacBio long-read sequencing technology. This approach provided improved coverage of 100x and resolution, confirming the integrity of the genomic assembly and enabling more precise identification of genetic elements. The genome of SA190 consists of a single circular chromosome of 5,076,637 bp with no plasmids (Fig. 1). The GC content of the genome is 64%. A total of 4561 of ORFs (protein coding genes), 90 pseudogenes, 64 transfer RNAs (tRNAs), 12 ribosomal RNAs (rRNAs), and 1 noncoding RNA (ncRNA) (Table 1). A clear GC skew transition was observed at positions 60,912 and 3,147,121 on the chromosome, corresponding to the origin of replication (*oriC*) and replication termination (*terC*) sites, respectively (Fig. 1a). The *oriC* in the SA190 chromosome is confirmed by the conservation of the gene operon SA190PBcda_000000664–669, which encodes *gyrB-recF-dnaN-dnaA-rpmH-rnpA* in that region [41]. In *Pseudomonas* species, the number of tRNAs varies between 60 and 80, while the number of rRNAs ranges from 4 to 7 [42]. High copy number of rRNAs showed the correlation of the high growth rate of the bacteria and adaptation to the environmental responses [43]. For example, *Sphingomonas* sp. strain RB2256 carries a single rRNA operon, exhibits a slow growth rate, and shows limited adaptability to changing environments [43, 44]. In contrast, *Bacillus subtilis*, which harbors 10 rRNA operons, grows rapidly and adapts more readily to environmental fluctuations [43, 45]. Similarly, *Pseudomonas* species with higher numbers of rRNA and tRNA genes tend to grow faster and adapt more effectively to environmental changes [42, 46]. This adaptation allows *Pseudomonas* to gain an advantage in accessing nutrients and competing with other microorganisms [42, 46].

### Genomic Identification of *Pseudomonas argentinensis* SA190 Using ANI and AAI Analyses

To accurately determine the taxonomic position of strain SA190, we performed both Average Nucleotide Identity (ANI) and Average Amino Acid Identity (AAI) analyses on whole genome level. Based on the TYGS genome-to-genome comparison, strain SA190 showed the highest relatedness to *Pseudomonas argentinensis* LMG 22,563, with a digital DNA–DNA hybridization (dDDH) value of 75% (confidence interval 71.0–78.6%), which is well above the accepted species threshold of 70%. The DDH of 75 corresponds to an ANI of about 96–97%, confirming the same species (Fig. 2A) [47, 48]. To further resolve species-level classification, we conducted AAI analysis, which confirmed that SA190 shares 93.5% amino acid identity with *P. argentinensis* LMG 22,563, firmly supporting species-level assignment (Fig. 2B) [49]. Other *Pseudomonas* species showed lower AAI values (84 – 88%), and non-*Pseudomonas* taxa fell below 76%, indicating clear genus- and species-level boundaries (Supplementary Table 4) [50, 51]. SA190's genomic features including a genome size of ~ 5.06 Mb, GC content of ~ 64%, and ~ 4,642 protein-coding genes are consistent with *P. argentinensis* and typical of the *Pseudomonas* genus [52]. These multi-layered genomic comparisons (ANI, AAI, and genome metrics) confirm that SA190 is a bona fide strain of *P. argentinensis*, closely related to the type strain LMG 22,563.

### Biochemical characteristics of SA190

Evaluation of the plant growth-promoting (PGP) traits revealed that *P. argentinensis* SA190 solubilized phosphate and produced indole acetic acid (IAA) and siderophores, but it could not solubilize zinc (Table 2). Siderophore production and phosphate solubilization of SA190 are shown in Supplementary Fig. 1. These results indicate that SA190 exhibits most of the traits associated with PGPB, establishing a beneficial interaction with the host to enhance its biomass. Antibiogram results indicated that SA190 was resistant to penicillin G but sensitive to ampicillin, chloramphenicol, erythromycin, kanamycin, oxytetracycline, streptomycin, tetracycline, and rifampicin (Table 3). SA190 exhibited tolerance under salt stress (up to 1 M NaCl) and drought stress (up to 20% PEG) (Table 4).

The carbon substrate utilization profile of SA190 was assessed using the API 50 CH system, providing insights into the strain's metabolic versatility and ecological adaptation. Out of 49 tested carbon sources, SA190 exhibited a selective pattern of substrate usage, utilizing a total of 11 compounds with a focus on simple sugars and a few derivatives (Supplementary Table 5).

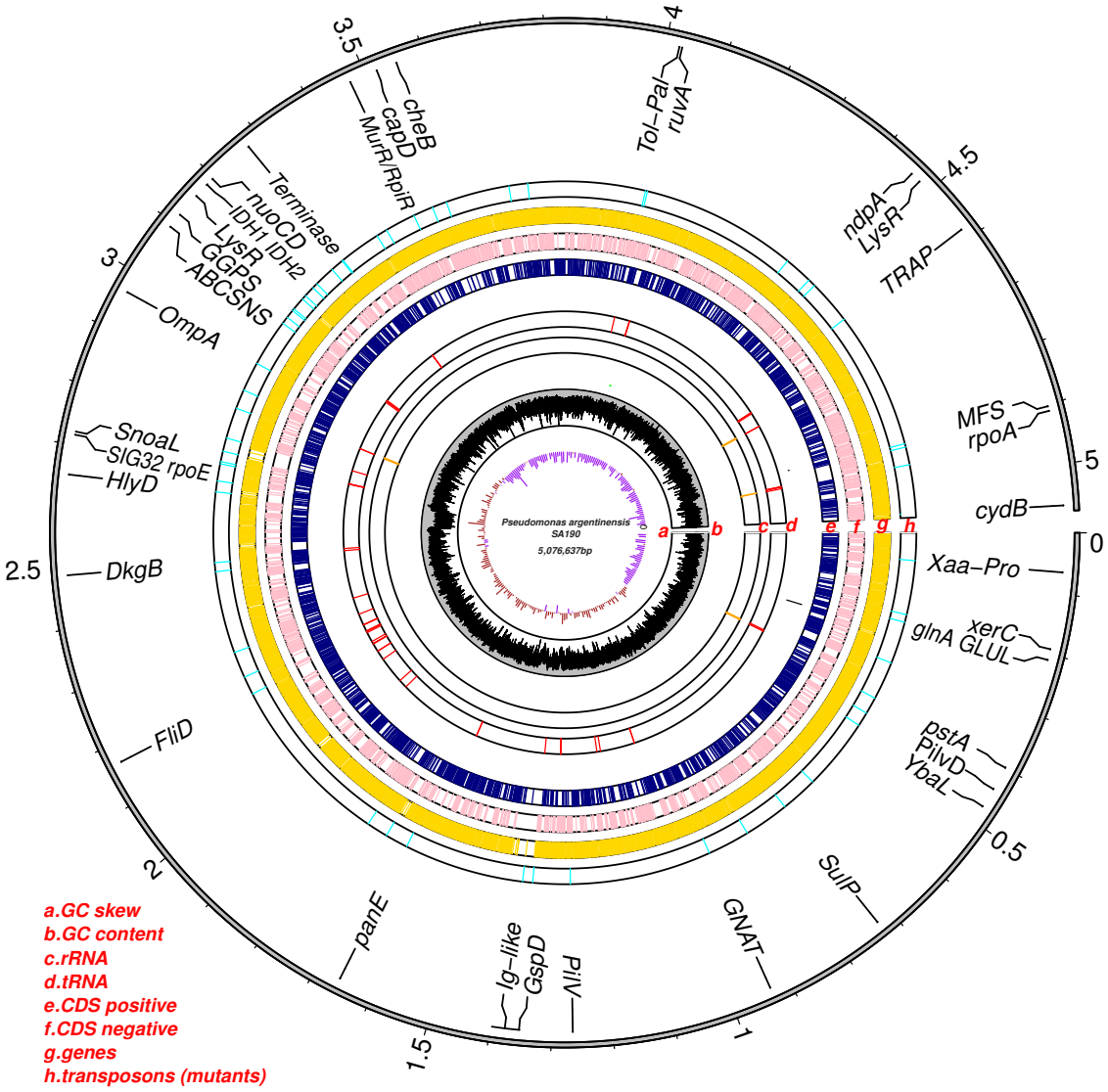



**Fig. 1** Genome map of *Pseudomonas argentinensis* SA190. The singular chromosome consists of 5.0 Mb. Circle **a** indicates the GC skew. Circle **b** shows the GC% content. Circle **c** highlights rRNA-related genes. Circle **d** indicates tRNA-related genes. Circle **e** represents CDS-positive genes. Circle **f** shows CDS-negative genes. Circle **g** indicates genes. Circle **h** marks transposon insertion sites and the names of the disrupted genes

SA190 demonstrated a selective carbohydrate utilization pattern. Among monosaccharides, the strain was able to metabolize D-mannose, L-fucose, and L-rhamnose, while it did not utilize D-glucose, D-fructose, or D-galactose, which is consistent with the atypical carbon preferences reported in several *Pseudomonas* species [53, 54]. The ability to utilize methyl-α-D-mannopyranoside further supports the presence of enzymes capable of processing glycoside-linked sugars, a trait often linked with competitive colonization strategies in beneficial rhizobacteria [19]. Among disaccharides, SA190 metabolized D-lactose, sucrose, and D-trehalose, all of which are not only abundant in root exudates but also have been shown to enhance microbial survival and stress tolerance in the rhizosphere [55, 56]. However, the strain did not utilize D-maltose, D-melibiose, or D-cellobiose, suggesting substrate-specific transport or enzymatic limitations.

For glycosides, the strain was able to process salicin and esculin, indicating β-glucosidase activity. The bacterium also utilizes select polysaccharides, including inulin and

**Table 1.** SA190 genome structure and features

| Feature | Count |
|---|---|
| Genome size (bp) | 5,076,637 |
| Genome Coverage | 100x |
| GC content (%) | 64% |
| CDS (ORFs / protein-coding genes) | 4561 |
| Gene | 4548 |
| Pseudogenes | 90 |
| tRNA | 64 |
| rRNA | 12 |
| riboswitch | 11 |
| region | 1 |
| ncRNA | 1 |
| RNase_P_RNA | 1 |
| SRP_RNA | 1 |
| tmRNA | 1 |

amidon (starch), as well as certain polyols like glycerol, erythritol, and xylitol. Additionally, SA190 could metabolize potassium gluconate, suggesting active periplasmic oxidation pathways [57, 58]. The strain's positive utilization of potassium gluconate is consistent with metabolic features commonly observed in plant-associated *Pseudomonas* species, where gluconate metabolism plays a central role in colonization and carbon flux through the Entner–Doudoroff pathway [2, 3]. These pathways are also implicated in biofilm formation and oxidative stress tolerance, reinforcing previous findings that link SA190's genomic features and biofilm-related genes with plant growth promotion [59]. Collectively, these findings suggest that *P. argentinensis* SA190 employs a specialized metabolic strategy tailored to the rhizosphere environment, efficiently utilizing root-derived carbohydrates while lacking the machinery to process more complex or less abundant carbon sources. This specialization likely contributes to its ecological success and previously reported capabilities in promoting plant growth under abiotic stress conditions [25].

### Genome mining and secondary metabolite biosynthetic potential of *Pseudomonas argentinensis* SA190

Genome mining revealed that SA190 carries stress-tolerance genes that may contribute to enhancing plant growth. A gene cluster responsible for phosphate solubilization, a crucial trait that ensures the plant's access to bioavailable phosphate, was identified. The *pqqEDCBAF* operon consists of six genes involved in synthesizing pyrroloquinoline quinone (PQQ), which belongs to metabolites promoting plant growth [26, 60]. Additionally, genes encoding glucan endo-1,3-beta-D-glucosidase and chitinase, which exhibit antifungal activity, were discovered in SA190 [26]. In this way, SA190 can inhibit the growth of pathogenic fungi and protect plants from fungal infections [61]. The genome of SA190 also contains the *acdS* gene, which is important for plant growth. The *acdS* gene encodes the enzyme 1-aminocyclopropane-1-carboxylic acid deaminase (ACC deaminase), which enhances plant biomass and stress tolerance by lowering excessive ethylene production [62].

To assess the biosynthetic potential of *P. argentinensis* SA190, the genome was analysed using the antiSMASH (version 8.0.4). A total of eight biosynthetic gene clusters (BGCs) were identified, representing a diverse array of secondary metabolite classes, including RiPP-like compounds, redox cofactors, terpene precursors, non-ribosomal peptides (NRPs), β-lactones, terpenes, and NAGGN-type saccharide (Supplementary Fig. 2). Similar known clusters for eight biosynthetic clusters, identified by MIBiG comparison, are shown in Supplementary Figs. 3, 4, and 5. Region 1 (83,002–142,575 bp) was annotated as a hybrid cluster comprising RiPP-like, arylpolyene, and resorcinol biosynthetic elements. This cluster showed a low similarity to the APE Vf cluster, which is known for producing pigments that contribute to oxidative stress resistance in Gram-negative bacteria. Arylpolyenes serve as functional analogs to carotenoids, offering membrane protection and antioxidant functions in biofilms and host-associated environments [63]. Region 2 (870,281–892,428) was annotated as a redox – cofactor biosynthetic cluster. Region 3 (1,315,872–1,336,759) was annotated as a terpene-precursor biosynthetic cluster. Regions 4 and 5, spanning 2.48–2.79 Mb, encoded NRP-metallophore and NRPS hybrid clusters, known for Pyochelin, Coelibactin, Azotobactin D and Cupriachelin clusters, respectively. Coelibactin and Cupriachelin metabolites are typically involved in metal ion acquisition—notably iron and copper—critical for microbial survival in nutrient-limited environments like the rhizosphere. Siderophores and metallophores also contribute to microbial competitiveness and plant-beneficial traits [64]. Region 6 (2.81–2.84 Mb) was predicted to encode a β-lactone biosynthetic cluster. Although β-lactones are relatively underexplored compared to other classes, they are structurally related to β-lactam antibiotics and are increasingly recognized for their roles in antimicrobial defense and inter-microbial competition [65]. Region 7 (3.10–3.12 Mb) displayed a terpene biosynthetic cluster with high similarity to a carotenoid-producing cluster. Terpenes and carotenoids are associated with a broad range of functions, including light protection, membrane stabilization, and plant-microbe signalling, and are known to enhance rhizobacterial survival under abiotic stress conditions [66]. Region 8 (3.50–3.52 Mb) was identified as an NAGGN-type saccharide cluster, resembling O-antigen biosynthesis systems. These gene clusters are typically involved in lipopolysaccharide (LPS) assembly, which plays key roles in bacterial adhesion, immune modulation, and biofilm development, thus contributing to colonization efficiency and plant-microbe interaction dynamics.

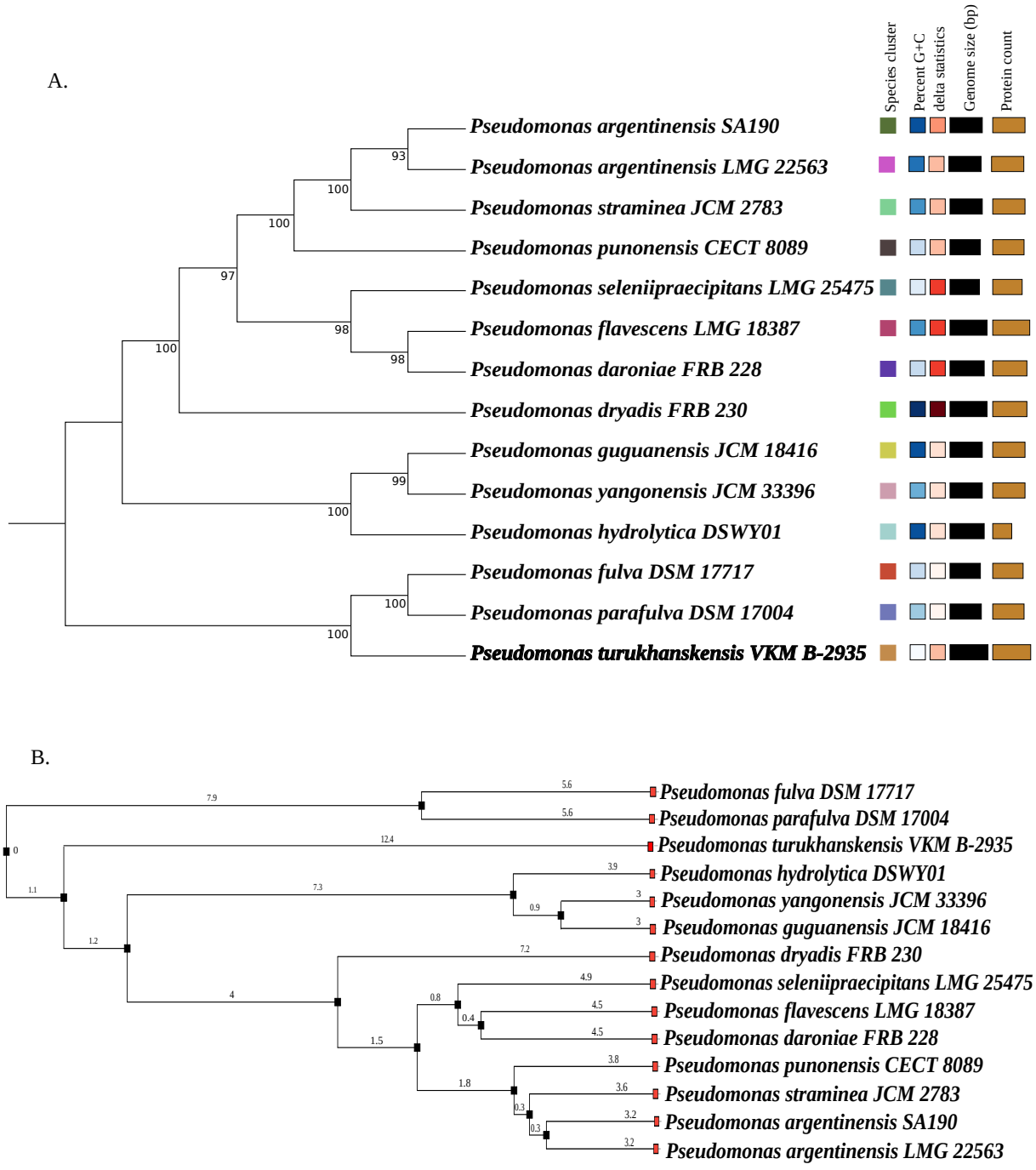



**Fig. 2** Phylogenomic analysis of *Pseudomonas argentinensis* SA190**.** (**A**) 16 S rRNA phylogeny tree based on 16 S rRNA sequence. The analysis was conducted using Genome Basic Local Alignment Search Tool (BLAST) distance phylogenies (GBDP) on the Type Strain Genome Server (TYGS) platform. (**B**) Average Amino Acid Identity (AAI) with identity greater than 70% and e-value of < = 1e-5. The branch legth of each orthologous pair has been highlighted

The diversity of BGCs identified in SA190 indicates a robust capacity to synthesize structurally diverse and functionally significant secondary metabolites. These include compounds with potential roles in rhizosphere colonization, plant protection, and environmental resilience. The presence of siderophore-like NRPs, oxidative stress-related arylpolyenes, and LPS-modifying saccharides aligns with previously described phenotypes of PGPB bacteria,

**Table 2.** Biochemical characteristics of SA190

| **Plant growth-promoting traits** | |
|---|---|
| Phosphate solubilization | + |
| Zinc solubilization | - |
| Siderophore production | + |
| Indole-3-acetic acid (IAA) production | + |

**Table 3.** Antibiotic resistance profile of SA190

| **Antibiotic resistance markers** | |
|---|---|
| Ampicillin | S |
| Chloramphenicol | S |
| Erythromycin | S |
| Kanamycin | S |
| Oxytetracycline | S |
| Penicillin G | R |
| Streptomycin | S |
| Tetracycline | S |
| Rifampicin | S |

**Table 4.** Abiotic stress resistance of SA190

| **Resistance to abiotic stresses** | |
|---|---|
| Salt stress | |
| Growth LB | + |
| Growth LB + 0.1 M NaCI | + |
| Growth LB + 0.5 M NaCI | + |
| Growth LB + 1 M NaCI | - |
| Osmotic stress | |
| Growth in 10% PEG 8000 | + |
| Growth in 20% PEG 8000 | + |

such as biofilm formation, stress tolerance, and plant growth promotion in arid environments [67]. The genomic potential observed here reinforces the ecological versatility and translational potential of *P. argentinensis* SA190 as a bioinoculant candidate for sustainable agriculture.

### Chemotaxis and colonization

The chemotaxis ability of bacteria is crucial for their survival, adaptation, and colonization [68]. Bacteria detect environmental signals and initiate a response through a two-component regulatory system [69]. In SA190, 119 genes are associated with the two-component system. Key genes involved in the chemotaxis of SA190 include two copies of *cheA* (SA190PBcda_000004008, SA190PBcda_000000517), *cheB* (SA190PBcda_000001286, SA190PBcda_000000523), and *cheY* (SA190PBcda_000004010, SA190PBcda_000000515), as well as three copies of *cheR* (SA190PBcda_000001285, SA190PBcda_000002421, SA190PBcda_000000521) and *cheV* (SA190PBcda_000002420, SA190PBcda_000002652, SA190PBcda_000004099). These genes, functioning as histidine kinases and response regulators, play a significant role in processing environmental signals, thus facilitating bacterial movement [70]. SA190 also has four copies of the *cheW* gene (SA190PBcda_000000518, SA190PBcda_ 000000520, SA190PBcda_000003996, SA190PBcda_000003997), which is crucial for establishing the link between methylaccepting chemotaxis proteins (MCPs) and *cheA* by synthesizing coupling proteins [71].

Flagella, essential for bacterial motility, directly contributes to the chemotaxis of bacteria [72]. The flagellar filament comprises the flagellin protein and a filament cap protein [72]. SA190 possesses the flagellin protein FliC (encoded by *fliC*, SA190PBcda_000002443) and a filament cap composed of the FliD protein (SA190PBcda_000002445). The *fliG* (SA190PBcda_000004032), *fliM* (SA190PBcda_000004022), and *fliN* (SA190PBcda_000004021) genes encode the cytoplasmic ring elements necessary for generating the torque required for flagellar movement, thereby significantly enhancing SA190's motility [72]. Additionally, the genome of SA190 contains two flagellar motor proteins, MotA and MotB, which are integral to the operation of the flagella and, thus, to the overall chemotactic process [73].

Bacteria move into the rhizosphere through chemotaxis and produce exopolysaccharides (EPS) to adhere to plant roots [6]. At this stage, biofilm formation and quorum sensing are crucial for successful colonization. The ability of SA190 to colonize plant roots greatly contributes to its beneficial effects on plant growth [22]. In SA190, the Wsp regulatory system is hypothesized to govern biofilm formation and surface-related characteristics [74]. Key genes in this system, including *wspA* (SA190PBcda_000005030), *wspB* (SA190PBcda_000005029), *wspD* (SA190PBcda_000005027), *wspR* (SA190PBcda_000005024), *wspF* (SA190PBcda_000005025), and *wspC* (SA190PBcda_000005028), play essential roles in biofilm formation in response to environmental signals.

Quorum sensing, a bacterial communication mechanism, directly interacts with biofilm formation and regulates EPS production in response to varying environmental conditions [75]. This mechanism allows bacteria to form more robust biofilms, which protect them from abiotic stresses such as drought. The EPS matrix can absorb and retain water, thereby protecting the bacteria from the adverse effects of drought [76]. Consequently, the formation of biofilms on plant roots enhances the plant's uptake and improves its resilience to drought stress, significantly contributing to plant-microbe interactions [76].

SA190 contains nine genes encoding LuxR family transcriptional regulators. Among these, *luxR* (SA190PBcda_000004790) represents the canonical quorum-sensing regulator. Two genes act as metabolic LuxR-like regulators, including SA190PBcda_000004434 (*malT*) and SA190PBcda_000003557 (amino acid transport). Five genes are annotated as two-component response regulators with LuxR domains (SA190PBcda_000003314,

SA190PBcda_000003452, SA190PBcda_000005291, SA190PBcda_000005781, and SA190PBcda_000005817). Additionally, SA190PBcda_000000956 encodes a dual-function protein that contains both a LuxR family transcriptional regulator domain and a serine/threonine kinase domain. These LuxR family regulators may play a central role in coordinating quorum-sensing–mediated regulation of metabolism and signalling in SA190.

### Characterization of biofilm genes in *Pseudomonas argentinensis* SA190 by Tn5 transposon library

To investigate the role of biofilm formation in plant-bacteria interaction in *P. argentinensis* SA190, we utilized a Tn5 transposon-induced mutation library. The Tn5 transposon system was employed to generate a transposon library containing 3,742 mutants of *P. argentinensis* SA190, resulting from 13 independent transformations. Since *P. argentinensis* SA190 contains only chromosomal DNA and lacks plasmids, all Tn5 insertions occurred within the chromosomal genes of SA190. To identify the insertion sites in the SA190 mutants, we used Random Amplification of Transposon Ends (RATE-PCR) followed by Sanger sequencing [32]. The distribution of Tn5 insertions across the genome of SA190 is illustrated in (Fig. 1h). Importantly, no significant accumulation of Tn5 insertions was observed in any specific region of the SA190 genome, indicating an even distribution of insertions. This even distribution of Tn5 insertions across the genome allows us to focus on bacterial traits that could play a role in successful root colonization. Biofilm formation is one of the crucial bacterial traits for root colonization. To investigate the role of biofilm formation in root colonization and plant growth promotion by SA190, we screened 1,000 transposon mutants using a crystal violet biofilm formation assay. Wild-type SA190 exhibited a biofilm formation value of approximately 1.5 ($OD_{550}$), which was used as a reference (Fig. 3). Among the 1,000 mutants, 21 showed a noticeable reduction in biofilm formation compared to the wild type. From these, we selected three mutants—*wspC*::Tn5, *rpoE*::Tn5, and *fliD*::Tn5—with biofilm values below 0.25 for further analysis, applying this stringent threshold to identify mutants with severely impaired biofilm production (Fig. 3). This $OD_{550}$ cut-off was chosen to classify mutants with low biofilm formation, ensuring that our analysis specifically addressed the impact of reduced biofilm capacity on root colonization and plant growth.

To investigate the functional role of *wspC*, *rpoE* and *fliD* in *P. argentinensis* SA190, we evaluated the colonization capacity of the mutants in *Arabidopsis thaliana* under non-stress and 25% PEG-induced drought stress conditions. After 15 days of plant growth, colonization levels of the mutants under non-stress conditions were similar to the wild-type SA190 (Fig. 4A). However, under 25% PEG-induced drought stress, the mutants exhibited a significant reduction in colonization compared to the wild type, indicating a stress-specific colonization defect. We next investigated the bacterial fitness in *wspC*::Tn5, *rpoE*::Tn5, and *fliD*::Tn5 mutants, they exhibited growth comparable to the wild-type SA190, indicating that the transposon insertions did not impair bacterial fitness (Supplementary Fig. 6). Then, we introduced a root surface sterilization step to remove epiphytic cells, allowing us to distinguish between loosely and stably associated bacteria. This approach enabled us to assess the effect of biofilm-related mutants on the stable colonization of SA190 on the root surface. Colonization of the mutants was significantly reduced under 25% PEG-induced drought stress

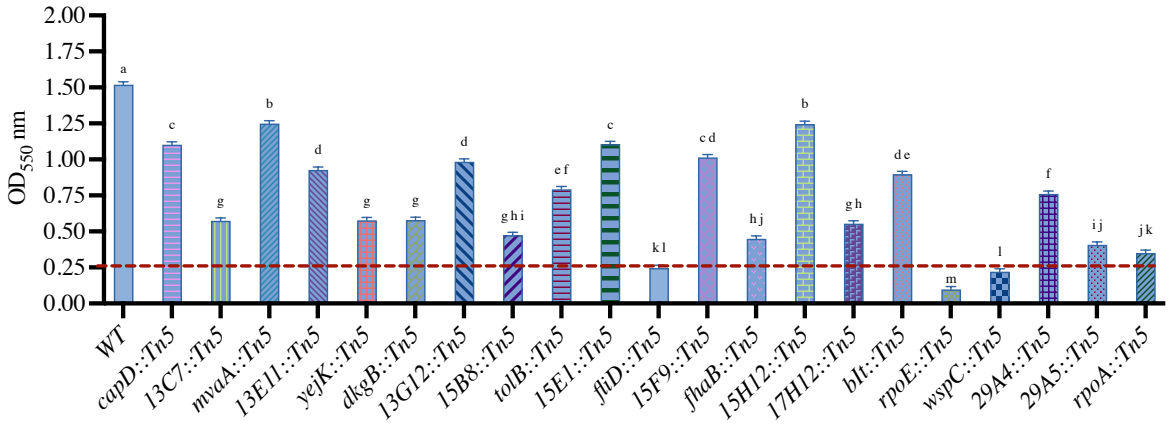



**Fig. 3** Biofilm formation of SA190 and Tn5 mutants determined by crystal violet staining. Biofilm formation was analysed on the 96-well plate surface after 24 h of incubation at 28 °C. The absorbance value of 0.25 was used as a stringent cut-off to capture mutants with severely impaired biofilm production. Bars represent the mean values, with error bars representing SD. Different letters indicate statistically significant differences based on the Welch and Brown-Forsythe versions of one-way ANOVA

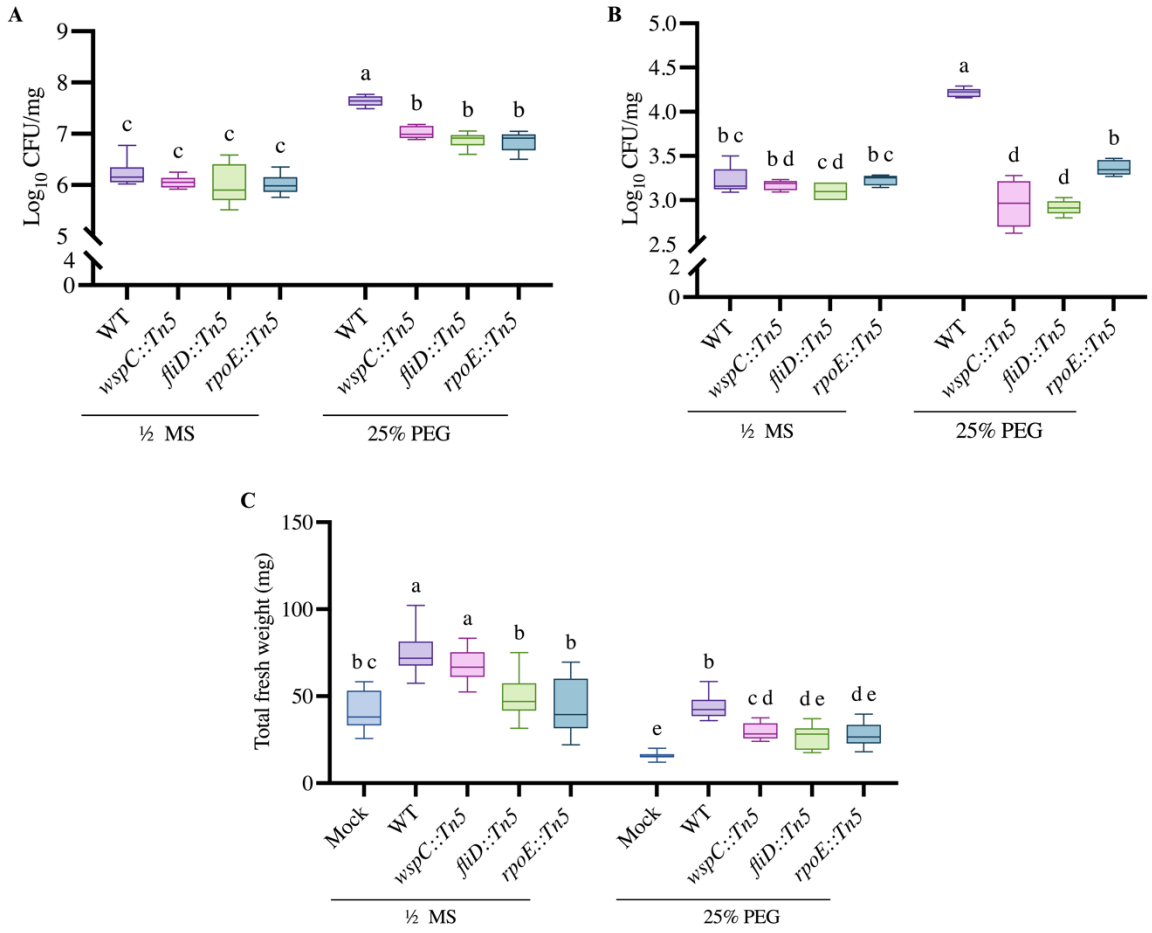



**Fig. 4** Analysing the impact of biofilm-related mutants on bacterial root colonization. Total bacterial titres of WT and mutants in Arabidopsis roots grown on ½ MS (non-stress) and 25% PEG-induced drought stress conditions (**A**). Endophytic bacterial titres of WT and mutants in Arabidopsis roots grown on ½ MS (non-stress) and 25% PEG-induced drought stress after root surface sterilization (**B**). The total fresh weight of non-colonized (mock) plants and plants colonized with SA190 or *wspC*::Tn5, *rpoE*::Tn5, and *fliD*::Tn5 mutants was measured after 15 days of growth on ½ MS and 25% PEG-induced drought stress (**C**). A ½ MS solution was used for the mock treatment. The boxplots show colony-forming unit (CFU) data from four independent biological replicates. The plant assay was performed with three biological replicates and two technical replicates ($n$ = 36). In the boxplots, whiskers represent the minimum and maximum values, while the horizontal line indicates the median. Different letters indicate statistically significant differences based on two-way ANOVA

after surface sterilization step (Fig. 4B). It suggests impaired stable root attachment in the mutants. This result supports the notion that *wspC*, *rpoE*, and *fliD* genes are particularly important for persistence on the root surface under drought stress conditions. To determine whether reduced colonization translates into a diminished growth-promoting effect, we assessed total plant fresh weight. Under non-stress conditions, plants colonized by the *wspC*::Tn5 mutant exhibited biomass levels comparable to those inoculated with wild-type SA190, whereas plants treated with the *rpoE*::Tn5 and *fliD*::Tn5 mutants showed a significant reduction in biomass (Fig. 4C). However, under 25% PEG-induced drought conditions, Arabidopsis plants inoculated with the mutants significantly decreased biomass compared to wild-type SA190 (Fig. 4C). This reduction in plant growth promotion results from the mutant's compromised biofilm formation and root colonization capacity.

To contextualize our findings, we reviewed previous studies on the roles of *wspC*, *rpoE*, and *fliD* in biofilm formation and bacterial colonization. The *wspC* gene encodes a methyltransferase that modifies the WspA receptor, playing a central role in chemotaxis and regulation of the Wsp chemosensory pathway, which enhances both biofilm formation and motility [77, 78]. Given this regulatory function, *wspC* is important for bacterial colonization and adaptation to environmental stress. Chemotaxis and biofilm-related genes have been shown to

play similar roles in other bacterial strains. For example, in *Pseudomonas aeruginosa*, the Wsp (wrinkly spreader phenotype) chemosensory system—which includes *wspC*—functions analogously to chemotaxis pathways and is involved in sensing environmental cues and envelope stress [77]. This system regulates intracellular levels of cyclic-di-GMP, a second messenger that governs the transition between motile and sessile (biofilm) lifestyles [77]. Activation of the Wsp pathway in response to surface contact or envelope perturbations leads to enhanced biofilm formation, enabling bacteria to adhere more effectively to surfaces, including plant roots [77]. Similarly, in *Bacillus subtilis*, disruption of the chemotaxis gene *cheV* resulted in a significant decline—over 15%—in the bacterium's ability to colonize tomato roots [79]. The *cheV* gene was shown to play a crucial role in signal transduction during chemotaxis and biofilm, enabling bacteria to move toward favourable environments such as plant root exudates [79]. Loss of this function compromises the bacterium's motility and capacity to establish stable associations with the host plant [79]. Consistently, the disruption of the *wspC* gene reduces biofilm formation in SA190, negatively affecting its stable attachment to the root. As a result, SA190 was unable to fully exert its beneficial effects on the plant. Moreover, our findings suggest that the *wspC* gene contributes to stable root colonization by SA190 and may play a role in establishing plant-microbe interactions.

The *rpoE* gene encodes an alternative sigma factor critical for the extracytoplasmic stress response in Gram-negative bacteria, playing a vital role in maintaining cell envelope integrity and responding to environmental stress [80]. Despite its recognized importance in bacterial physiology, the specific role of *rpoE* in biofilm formation and root colonization by SA190 has not been fully elucidated. In a study involving Crohn's disease-associated adherent-invasive *Escherichia coli* (AIEC), inhibition of the *RpoE* sigma factor led to a significant reduction in biofilm formation and bacterial adhesion to intestinal epithelial cells, impairing colonization and persistence within the host [81]. Similarly, in *Salmonella enterica*, *rpoE* mutants exhibited increased sensitivity to extracytoplasmic stress, resulting in compromised biofilm development and a diminished ability to colonize host tissues [82]. In *E. coli*, the RpoE controls the expression of genes involved in maintaining the integrity of the outer membrane and the envelope stress response [83, 84]. Loss of RpoE function disrupts proper outer membrane protein folding, leading to defects in biofilm formation and reduced surface attachment [83, 84]. This stress response is crucial for bacterial survival under stressful conditions and for the maturation of biofilms on various surfaces [83, 84]. Similarly, the *rpoE* gene plays a crucial role in SA190's biofilm formation, root colonization, and the resulting beneficial effects on plant growth under drought stress conditions.

*fliD* encodes a structural component of the bacterial flagellum essential for motility and many studies have emphasized the importance of the *fliD* gene in various bacterial systems [72]. For instance, in *Helicobacter pylori*, the *fliD* mutant showed delayed biofilm initiation and surface attachment [85]. Similarly, a study on *Clostridioides difficile* demonstrated that mutants lacking key flagellar components (*fliC*, *fliD*, and *flgE*) showed reduced colonization and adherence to the intestinal epithelium during infection [86]. These studies support the idea that flagellar components are essential for motility, surface attachment, and stable host interaction [86]. In parallel with the findings of these studies, our data demonstrate that the *fliD* gene in SA190 contributes to biofilm formation, stable root colonization, and the beneficial effects of SA190 on the plant.

Taken together, these results suggest that biofilm-related genes (*wspC*, *rpoE*, and *fliD*) contribute to stable root colonization and influence plant growth under 25% PEG-induced drought stress. Disruption of these genes reduces bacterial persistence on roots, limiting SA190's beneficial effects and highlighting the role of biofilm formation in plant-microbe interactions. We note that complementation of the *wspC*, *rpoE*, and *fliD* mutants was not performed, which is a limitation of the Tn5 transposon library due to the potential disruption of large genomic regions. The mechanistic basis by which *wspC*, *rpoE*, and *fliD* influence biofilm formation remains to be elucidated. In *Pseudomonas*, biofilm development is regulated through the coordinated action of multiple pathways [87–89]. For example, the Gac/Rsm system controls biofilm matrix production [89], cyclic-di-GMP (c-di-GMP) metabolism promotes biofilm formation [90], quorum sensing (QS) regulates the population density of biofilm-forming cells [88], and exopolysaccharide (EPS) biosynthesis contributes directly to the establishment of the biofilm matrix [87]. The interplay among these systems ensures the initiation, maturation, and stability of biofilms [87]. The *wsp* operon has been associated with the modulation of c-di-GMP levels, thereby influencing surface attachment and biofilm stability [77, 78]. *rpoE* encodes an extracytoplasmic sigma factor involved in envelope stress responses, which can indirectly modulate biofilm-associated gene expression and EPS production [80, 82]. *fliD* encodes the flagellar cap protein, and mutations that impair flagellar function often reduce surface attachment and the initiation of biofilm formation [85]. Although our study identifies these genes as candidate contributors to biofilm formation in SA190, further studies are needed to determine how they integrate into the canonical regulatory networks described in other *Pseudomonas* species.

## Conclusion

*Pseudomonas argentinensis* SA190 represents a metabolically streamlined yet functionally diverse PGPB with strong ecological adaptability. Its genetic potential for metabolite biosynthesis, stress resilience, and efficient root colonization underscores its value as a bioinoculant in sustainable agriculture. Notably, Tn5 transposon mutagenesis identified *wspC*, *rpoE*, and *fliD* as candidate genes potentially involved in biofilm formation and colonization. Disruption of these genes impaired biofilm integrity and reduced the bacterium's ability to promote plant growth under drought stress, highlighting its role of biofilm-mediated attachment in rhizosphere competence. These insights demonstrate the power of functional genomics in unravelling the mechanisms underlying beneficial plant-microbe interactions. Collectively, this work provides a robust foundation for the translational deployment of SA190 to enhance plant resilience and productivity, particularly in arid and saline environments.

**Abbreviations**

| | |
|---|---|
| ORFs | Open reading frames |
| EPS | Exopolysaccharides |
| PGPB | Growth-promoting bacteria |
| ROS | Reactive oxygen species |
| IAA | Indole-3-acetic acid |
| SMRT | Single-molecule real-time |
| HGAP | Hierarchical Genome Assembly Process |
| KEGG | Kyoto Encyclopedia of Genes and Genomes |
| TYGS | Type Strain Genome Server |
| GBDP | Genome BLAST Distance Phylogeny |
| RATE-PCR | The random amplification of transposon ends |
| CFU | Colony-forming units |
| ANI | Average Nucleotide Identity |
| AAI | Average Amino Acid Identity |

## Supplementary Information

The online version contains supplementary material available at https://doi.org/10.1186/s12866-025-04495-2.

Supplementary Material 1

**Acknowledgements**
The authors would thank all members of Hirt lab, the BESE management team, and the Bioscience Core Labs in KAUST for the technical assistance and their help in many aspects of this work. The work was funded by KAUST fund BAS/1/1062-01-01 to HH as part of the DARWIN21 desert initiative (http://www.darwin21.org/). SK and BE are supported by the Deutsche Forschungsgemeinschaft (DFG) under Germany´s Excellence Strategy – EXC 2048/1 – project 390686111 and under Priority Programme "2125 Deconstruction and Reconstruction of Plant Microbiota (DECRyPT)", project 401836049.

**Authors' contributions**
B.E.: Data curation, investigation, validation, methodology development, writing—original draft, and writing—review and editing. S.P., A.A.E., R.J., F.L., and I.A.: Methodology refinement and data curation. S.K.: Conceptualization, supervision, and manuscript review and editing. H.H.: Funding acquisition, project supervision, and writing—review and editing. M.M.S.: Project ideation and conceptualization, supervision of experimental design, protocol tuning, validation, and manuscript writing—review and editing.

**Data availability**
"The genome sequence of SA190 was deposited in NCBI/DDBJ/EMBL database under the accession number CP056087.1 with BioProject no. PRJNA312745".

## Declarations

**Ethics approval and consent to participate**

Not applicable.

**Consent for publication**

There is no conflict to consent for publication.

**Competing interests**

The authors declare that the research was conducted in the absence of any commercial or financial relationships that could be construed as a potential conflict of interest.

Received: 8 July 2025 / Accepted: 21 October 2025
Published online: 27 November 2025

**References**

1. Duchenne-Moutien RA, Neetoo H. Climate change and emerging food safety issues: a review. J Food Prot. 2021;84:1884–97. https://doi.org/10.4315/JFP-2 1-141.
2. Verma V, Ravindran P, Kumar PP. Plant hormone-mediated regulation of stress responses. BMC Plant Biol. 2016. https://doi.org/10.1186/s12870-016-0771-y.
3. Zhang H, Zhu J, Gong Z, Zhu JK. Abiotic stress responses in plants. Nat Rev Genet. 2022;23:104–19. https://doi.org/10.1038/s41576-021-00413-0.
4. van Dijk M, Morley T, Rau ML, Saghai Y. A meta-analysis of projected global food demand and population at risk of hunger for the period 2010–2050. Nat Food. 2021;2:494–501. https://doi.org/10.1038/s43016-021-00322-9.
5. Tigchelaar M, Battisti DS, Naylor RL, Ray DK. Future warming increases probability of globally synchronized maize production shocks. Proc Natl Acad Sci U S A. 2018;115:6644–9. https://doi.org/10.1073/pnas.1718031115.
6. Knights HE, Jorrin B, Haskett TL, Poole PS. Deciphering bacterial mechanisms of root colonization. Environ Microbiol Rep. 2021;13:428–44. https://doi.org/1 0.1111/1758-2229.12934.
7. Bulgarelli D, Schlaeppi K, Spaepen S, Van Themaat EVL, Schulze-Lefert P. Structure and functions of the bacterial microbiota of plants. Annu Rev Plant Biol. 2013;64:807–38. https://doi.org/10.1146/annurev-arplant-050312-120106.
8. Bardgett RD, Van Der Putten WH. Belowground biodiversity and ecosystem functioning. Nature. 2014;515:505–11. https://doi.org/10.1038/nature13855.
9. Saghaï A, Wittorf L, Philippot L, Hallin S. Loss in soil microbial diversity constrains microbiome selection and alters the abundance of N-cycling guilds in barley rhizosphere. Appl Soil Ecol. 2022. https://doi.org/10.1016/j.apsoil.2021. 104224.
10. Berg G, Smalla K. Plant species and soil type cooperatively shape the structure and function of microbial communities in the rhizosphere. FEMS Microbiol Ecol. 2009;68:1–13. https://doi.org/10.1111/j.1574-6941.2009.00654.x.
11. Ma W, Tang S, Dengzeng Z, Zhang D, Zhang T, Ma X. Root exudates contribute to belowground ecosystem hotspots: a review. Front Microbiol. 2022. https://doi.org/10.3389/fmicb.2022.937940.
12. Vives-Peris V, de Ollas C, Gómez-Cadenas A, Pérez-Clemente RM. Root exudates: from plant to rhizosphere and beyond. Plant Cell Rep. 2020;39:3–17. https://doi.org/10.1007/s00299-019-02447-5.
13. Xu Z, Liu Y, Zhang N, Xun W, Feng H, Miao Y, et al. Chemical communication in plant–microbe beneficial interactions: a toolbox for precise management of beneficial microbes. Curr Opin Microbiol. 2023;72:102269. https://doi.org/1 0.1016/j.mib.2023.102269.
14. Yin W, Wang Y, Liu L, He J. Biofilms. The microbial protective clothing in extreme environments. Int J Mol Sci. 2019. https://doi.org/10.3390/ijms20143423.
15. Vismans G, van Bentum S, Spooren J, Song Y, Goossens P, Valls J, et al. Coumarin biosynthesis genes are required after foliar pathogen infection for the creation of a microbial soil-borne legacy that primes plants for SA-dependent defenses. Sci Rep. 2022;12:22473. https://doi.org/10.1038/s41598-022-26551-x.

16. Berendsen RL, Pieterse CMJ, Bakker PAHM. The rhizosphere microbiome and plant health. Trends Plant Sci. 2012;17:478–86. https://doi.org/10.1016/j.tplant s.2012.04.001.
17. de Zelicourt A, Al-Yousif M, Hirt H. Rhizosphere microbes as essential partners for plant stress tolerance. Mol Plant. 2013;6:242–5. https://doi.org/10.1093/m p/sst028.
18. Glick BR. Plant growth-promoting bacteria: mechanisms and applications. Scientifica. 2012;2012:963401. https://doi.org/10.6064/2012/963401.
19. Lugtenberg B, Kamilova F. Plant-growth-promoting rhizobacteria. Annu Rev Microbiol. 2009;63:541–56. https://doi.org/10.1146/annurev.micro.62.081307.162918
20. Orozco-Mosqueda M, del Rocha-Granados C, del Glick M, Santoyo BR. Microbiome engineering to improve biocontrol and plant growth-promoting mechanisms. Microbiol Res. 2018;208:25–31. https://doi.org/10.1016/j.micres. 2018.01.005.
21. Wang H, Liu R, You MP, Barbetti MJ, Chen Y. Pathogen biocontrol using plant growth-promoting bacteria (PGPR): role of bacterial diversity. Microorganisms. 2021. https://doi.org/10.3390/microorganisms9091988.
22. Alwutayd KM, Rawat AA, Sheikh AH, Almeida-Trapp M, Veluchamy A, Jalal R, et al. Microbe-induced drought tolerance by ABA-mediated root architecture and epigenetic reprogramming. EMBO Rep. 2023. https://doi.org/10.15252/e mbr.202256754.
23. Nadarajah KK. Ros homeostasis in abiotic stress tolerance in plants. Int J Mol Sci. 2020;21:1–29. https://doi.org/10.3390/ijms21155208.
24. Chieb M, Gachomo EW. The role of plant growth promoting rhizobacteria in plant drought stress responses. BMC Plant Biol. 2023. https://doi.org/10.1186/ s12870-023-04403-8.
25. de Zélicourt A, Synek L, Saad MM, Alzubaidy H, Jalal R, Xie Y, et al. Ethylene induced plant stress tolerance by *Enterobacter* sp. SA187 is mediated by 2-keto-4-methylthiobutyric acid production. PLoS Genet. 2018. https://doi.or g/10.1371/journal.pgen.1007273.
26. Lafi FF, Alam I, Geurts R, Bisseling T, Bajic VB, Hirt H, et al. Draft genome sequence of the phosphate-solubilizing bacterium *Pseudomonas argentinensis* strain SA190 isolated from the desert plant *Indigofera argentea*. Genome Announc. 2016. https://doi.org/10.1128/genomeA.01431-16.
27. Stanier RY, Palleroni NJ, Doudoroff M. The aerobic pseudomonads: a taxonomic study. J Gen Microbiol. 1966;43:159–271. https://doi.org/10.1099/0022 1287-43-2-159.
28. Alam I, Antunes A, Kamau AA, Alawi WB, Kalkatawi M, Stingl U, et al. Indigo- integrated data warehouse of microbial genomes with examples from the red sea extremophiles. PLoS ONE. 2013. https://doi.org/10.1371/journal.pone. 0082210.
29. Kanehisa M, Goto S, Kawashima S, Okuno Y, Hattori M. The KEGG resource for Deciphering the genome. Nucleic Acids Res. 2004. https://doi.org/10.1093/n ar/gkh063. 32 DATABASE ISS.
30. Blin K, Shaw S, Kloosterman AM, Charlop-Powers Z, Van Wezel GP, Medema MH, et al. AntiSMASH 6.0: improving cluster detection and comparison capabilities. Nucleic Acids Res. 2021;49:W29–35. https://doi.org/10.1093/nar/ gkab335.
31. Lagesen K, Hallin P, Rødland EA, Staerfeldt H-H, Rognes T, Ussery DW. RNAm-mer: consistent and rapid annotation of ribosomal RNA genes. Nucleic Acids Res. 2007;35:3100–8. https://doi.org/10.1093/nar/gkm160.
32. Lefort V, Desper R, Gascuel O. FastME 2.0: A Comprehensive, Accurate, and fast Distance-Based phylogeny inference program. Mol Biol Evol. 2015;32:2798–800. https://doi.org/10.1093/molbev/msv150.
33. Kreft L, Botzki A, Coppens F, Vandepoele K, Van Bel M. PhyD3: a phylogenetic tree viewer with extended phyloxml support for functional genomics data visualization. Bioinformatics. 2017;33:2946–7. https://doi.org/10.1093/bioinfor matics/btx324.
34. Kim D, Park S, Chun J. Introducing ezaai: a pipeline for high throughput calcu-lations of prokaryotic average amino acid identity. J Microbiol. 2021;59:476–80. https://doi.org/10.1007/s12275-021-1154-0.
35. Bric JM, Bostock RM, Silverstone SE. Rapid in situ assay for indoleacetic acid production by bacteria immobilized on a nitrocellulose membrane. Appl Environ Microbiol. 1991;57:535–8. https://doi.org/10.1128/aem.57.2.535-538.1 991.
36. Louden BC, Haarmann D, Lynne AM. Use of blue agar CAS assay for sidero-phore detection. J Microbiol Biol Educ. 2011;12:51–3. https://doi.org/10.1128/ jmbe.v12i1.249.
37. Bapiri A, Asgharzadeh A, Mujallali H, Khavazi K, Pazira E. Evaluation of zinc solubilization potential by different strains of fluorescent pseudomonads. J Appl Sci Environ Manage. 2012;16:295–8.
38. Karlyshev AV, Pallen MJ, Wren BW. Single-primer PCR procedure for rapid identification of transposon insertion sites. Biotechniques. 2000;28:1078–82. https://doi.org/10.2144/00286bm05.
39. Elkatmis B, Han B, Parween S, Kopriva S, Hirt H, Saad MM. Comprehensive mapping of EZ-Tn5 transposon insertion sites in *PseudomonasArgentinensis* SA190 using RATE-PCR. BIO-PROTOCOL. 2025;15:e5389. https://doi.org/10.21769/BioProtoc.5389.
40. O'Toole GA. Microtiter dish biofilm formation assay. J Visualized Experiments. 2010. https://doi.org/10.3791/2437.
41. Saad M, de Zelicourt A, Rolli E, Synek L, Hirt H. Quantification of root colonizing bacteria. Bio Protoc. 2018;8. https://doi.org/10.21769/bioprotoc.2927.
42. Ogasawara N, Moriya S, von Meyenburg K, Hansen FG, Yoshikawa H. Conservation of genes and their organization in the chromosomal replication origin region of *Bacillus subtilis* and *Escherichia coli*. EMBO J. 1985;4:3345–50. https:// doi.org/10.1002/j.1460-2075.1985.tb04087.x.
43. Loper JE, Hassan KA, Mavrodi DV, Davis EW, Lim CK, Shaffer BT, et al. Comparative genomics of plant-associated *Pseudomonas* spp.: insights into diversity and inheritance of traits involved in multitrophic interactions. PLoS Genet. 2012. https://doi.org/10.1371/journal.pgen.1002784.
44. Stevenson BS, Schmidt TM. Life history implications of rRNA gene copy number in *Escherichia coli*. Appl Environ Microbiol. 2004;70:6670–7. https://do i.org/10.1128/AEM.70.11.6670-6677.2004.
45. Fegatella F, Lim J, Kjelleberg S, Cavicchioli R. Implications of rRNA operon copy number and ribosome content in the marine oligotrophic Ultrami-crobacterium *sphingomonas* sp. strain RB2256. Appl Environ Microbiol. 1998;64:4433–8. https://doi.org/10.1128/AEM.64.11.4433-4438.1998.
46. Kunst F, Ogasawara N, Moszer I, Albertini AM, Alloni G, Azevedo V, et al. The complete genome sequence of the gram-positive bacterium *Bacillus subtilis*. Nature. 1997;390:249–56. https://doi.org/10.1038/36786.
47. Winsor GL, Lam DKW, Fleming L, Lo R, Whiteside MD, Yu NY, et al. Pseudomonas genome database: improved comparative analysis and population genomics capability for Pseudomonas genomes. Nucleic Acids Res. 2011. https://doi.org/10.1093/nar/gkq869.
48. Auch AF, von Jan M, Klenk H-P, Göker M. Digital DNA-DNA hybridization for microbial species delineation by means of genome-to-genome sequence comparison. Stand Genomic Sci. 2010;2:117–34. https://doi.org/10.4056/sigs. 531120.
49. Richter M, Rosselló-Móra R. Shifting the genomic gold standard for the prokaryotic species definition. Proc Natl Acad Sci U S A. 2009;106:19126–31. https://doi.org/10.1073/pnas.0906412106.
50. Meier-Kolthoff JP, Auch AF, Klenk H-P, Göker M. Genome sequence-based species delimitation with confidence intervals and improved distance func-tions. BMC Bioinformatics. 2013;14:60. https://doi.org/10.1186/1471-2105-1 4-60.
51. Konstantinidis R-RLM. Bypassing cultivation to identify bacterial species. Microbe. 2014;9:111–8. https://doi.org/10.1128/microbe.9.111.1.
52. Konstantinidis KT, Tiedje JM. Genomic insights that advance the species definition for prokaryotes. Proc Natl Acad Sci U S A. 2005;102(7):2567–72. https://doi.org/10.1073/pnas.0409727102.
53. Silby MW, Winstanley C, Godfrey SAC, Levy SB, Jackson RW. *Pseudomonas* genomes: diverse and adaptable. FEMS Microbiol Rev. 2011;35:652–80. https://doi.org/10.1111/j.1574-6976.2011.00269.x.
54. Badri DV, Vivanco JM. Regulation and function of root exudates. Plant Cell Environ. 2009;32:666–81. https://doi.org/10.1111/j.1365-3040.2009.01926.x.
55. Bais HP, Weir TL, Perry LG, Gilroy S, Vivanco JM. The role of root exudates in rhizosphere interactions with plants and other organisms. Annu Rev Plant Biol. 2006;57:233–66. https://doi.org/10.1146/annurev.arplant.57.032905.105159.
56. Compant S, Clément C, Sessitsch A. Plant growth-promoting bacteria in the rhizo- and endosphere of plants: their role, colonization, mechanisms involved and prospects for utilization. Soil Biol Biochem. 2010;42:669–78. https://doi.org/10.1016/j.soilbio.2009.11.024.
57. Walker TS, Bais HP, Grotewold E, Vivanco JM. Root exudation and rhizosphere biology. Plant Physiol. 2003;132:44–51. https://doi.org/10.1104/pp.102.019661.
58. Kraffczyk I, Trolldenier G, Beringer H. Soluble root exudates of maize: influence of potassium supply and rhizosphere microorganisms. Soil Biol Biochem. 1984;16:315–22. https://doi.org/10.1016/0038-0717(84)90025-7.
59. Molina-Santiago C, Pearson JR, Navarro Y, Berlanga-Clavero MV, Caraballo-Rodriguez AM, Petras D, et al. The extracellular matrix protects *Bacillus subtilis* colonies from *Pseudomonas* invasion and modulates plant co-colonization. Nat Commun. 2019. https://doi.org/10.1038/s41467-019-09944-x.
60. Andrés-Barrao C, Lafi FF, Alam I, de Zélicourt A, Eida AA, Bokhari A, et al. Complete genome sequence analysis of *Enterobacter* sp. SA187, a plant

multi-stress tolerance promoting endophytic bacterium. Front Microbiol. 2017. https://doi.org/10.3389/fmicb.2017.02023.
61. Choi O, Kim J, Kim JG, Jeong Y, Jae SM, Chang SP, et al. Pyrroloquinoline Quinone is a plant growth promotion factor produced by Pseudomonas fluorescens B16. Plant Physiol. 2008;146:657–68. https://doi.org/10.1104/pp.107.1 12748.
62. Kebede A, Kebede M. In silico analysis of promoter region and regulatory elements of glucan endo-1,3-beta-glucosidase encoding genes in *solanum tuberosum*: cultivar DM 1–3 516 R44. J Genet Eng Biotechnol. 2021. https://do i.org/10.1186/s43141-021-00240-0.
63. Herpell JB, Alickovic A, Diallo B, Schindler F, Weckwerth W. Phyllosphere symbiont promotes plant growth through ACC deaminase production. ISME J. 2023;17:1267–77. https://doi.org/10.1038/s41396-023-01428-7.
64. Johnston I, Osborn LJ, Markley RL, McManus EA, Kadam A, Schultz KB, et al. Identification of essential genes for *Escherichia coli* aryl polyene biosynthesis and function in biofilm formation. NPJ Biofilms Microbiomes. 2021. https://do i.org/10.1038/s41522-021-00226-3.
65. Miethke M, Marahiel MA. Siderophore-based iron acquisition and pathogen control. Microbiol Mol Biol Rev. 2007;71:413–51. https://doi.org/10.1128/MMB R.00012-07.
66. Koglin A, Walsh CT. Structural insights into nonribosomal peptide enzymatic assembly lines. Nat Prod Rep. 2009;26:987–1000. https://doi.org/10.1039/b90 4543k.
67. Yuan JS, Himanen SJ, Holopainen JK, Chen F, Stewart CN. Smelling global climate change: mitigation of function for plant volatile organic compounds. Trends Ecol Evol. 2009;24:323–31. https://doi.org/10.1016/j.tree.2009.01.012.
68. Saad MM, Eida AA, Hirt H, Doerner P. Tailoring plant-associated microbial inoculants in agriculture: A roadmap for successful application. J Exp Bot. 2020;71:3878–901. https://doi.org/10.1093/jxb/eraa111.
69. Mattingly AE, Weaver AA, Dimkovikj A, Shrout JD. Assessing travel conditions: environmental and host influences on bacterial surface motility. J Bacteriol. 2018;200:e00014. https://doi.org/10.1128/JB.00014-18.
70. Liu C, Sun D, Zhu J, Liu W. Two-component signal transduction systems: a major strategy for connecting input stimuli to biofilm formation. Front Micro-biol. 2019. https://doi.org/10.3389/fmicb.2018.03279.
71. Mascher T, Helmann JD, Unden G. Stimulus perception in bacterial signal-transducing histidine kinases. Microbiol Mol Biol Rev. 2006;70:910–38. https:// doi.org/10.1128/MMBR.00020-06.
72. Huang Z, Pan X, Xu N, Guo M. Bacterial chemotaxis coupling protein: struc-ture, function and diversity. Microbiol Res. 2019;219:40–8. https://doi.org/10.1 016/j.micres.2018.11.001.
73. Nedeljković M, Sastre DE, Sundberg EJ. Bacterial flagellar filament: a supramo-lecular multifunctional nanostructure. Int J Mol Sci. 2021. https://doi.org/10.3 390/ijms22147521.
74. Doyle TB, Hawkins AC, McCarter LL. The complex flagellar torque generator of *Pseudomonas aeruginosa*. J Bacteriol. 2004;186(19):6341–50. https://doi.org/1 0.1128/JB.186.19.6341-6350.2004.
75. Hickman JW, Tifrea DF, Harwood CS. A chemosensory system that regulates biofilm formation through modulation of Cyclic diguanylate levels. Proc Natl Acad Sci U S A. 2005;102:14422–7. https://doi.org/10.1073/pnas.0507170102.
76. Zeng X, Zou Y, Zheng J, Qiu S, Liu L, Wei C. Quorum sensing-mediated micro-bial interactions: mechanisms, applications, challenges and perspectives. Microbiol Res. 2023. https://doi.org/10.1016/j.micres.2023.127414.
77. Li Y, Narayanan M, Shi X, Chen X, Li Z, Ma Y. Biofilms formation in plant growth-promoting bacteria for alleviating agro-environmental stress. Sci Total Environ. 2024;907:167774. https://doi.org/10.1016/j.scitotenv.2023.167774.
78. O'Neal L, Baraquet C, Suo Z, Dreifus JE, Peng Y, Raivio TL, et al. The Wsp system of *Pseudomonas aeruginosa* links surface sensing and cell envelope stress. Proc Natl Acad Sci U S A. 2022;119:e2117633119. https://doi.org/10.1073/pna s.2117633119.
79. Güvener ZT, Harwood CS. Subcellular location characteristics of the *Pseudo-monas aeruginosa* GGDEF protein, WspR, indicate that it produces cyclic-di-GMP in response to growth on surfaces. Mol Microbiol. 2007;66:1459–73. https://doi.org/10.1111/j.1365-2958.2007.06008.x.
80. Gao S, Wu H, Yu X, Qian L, Gao X. Swarming motility plays the major role in migration during tomato root colonization by *Bacillus subtilis* SWR01. Biol Control. 2016;98:11–7. https://doi.org/10.1016/j.biocontrol.2016.03.011.
81. Hayden JD, Ades SE. The extracytoplasmic stress factor, σE, is required to maintain cell envelope integrity in *Escherichia coli*. PLoS ONE. 2008. https://do i.org/10.1371/journal.pone.0001573.
82. Chassaing B, Darfeuille-Michaud A. The σE pathway is involved in biofilm formation by Crohn's disease-associated adherent-invasive *Escherichia coli*. J Bacteriol. 2013;195:76–84. https://doi.org/10.1128/JB.01079-12.
83. Rowley G, Spector M, Kormanec J, Roberts M. Pushing the envelope: extracytoplasmic stress responses in bacterial pathogens. Nat Rev Microbiol. 2006;4:383–94. https://doi.org/10.1038/nrmicro1394.
84. De Las Peñas A, Connolly L, Gross CA. The SigmaE-mediated response to extracytoplasmic stress in Escherichia coli is transduced by RseA and RseB, two negative regulators of SigmaE. Mol Microbiol. 1997;24:373–85. https://do i.org/10.1046/j.1365-2958.1997.3611718.x.
85. Rhodius VA, Suh WC, Nonaka G, West J, Gross CA. Conserved and variable functions of the SigmaE stress response in related genomes. PLoS Biol. 2006;4:e2. https://doi.org/10.1371/journal.pbio.0040002.
86. Ratthawongjirakul P, Thongkerd V, Chaicumpa W. The impacts of a FliD mutation on the biofilm formation of *Helicobacter pylori*. Asian Pac J Trop Biomed. 2016;6:1008–14. https://doi.org/10.1016/j.apjtb.2016.10.005.
87. Baban ST, Kuehne SA, Barketi-Klai A, Cartman ST, Kelly ML, Hardie KR, et al. The role of flagella in *clostridium difficile* pathogenesis: comparison between a non-epidemic and an epidemic strain. PLoS ONE. 2013. https://doi.org/10.13 71/journal.pone.0073026.
88. Lichtenberg M, Kragh KN, Fritz B, Kirkegaard JB, Tolker-Nielsen T, Bjarnsholt T. Cyclic-di-GMP signaling controls metabolic activity in *Pseudomonas aerugi-nosa*. Cell Rep. 2022;41:111515. https://doi.org/10.1016/j.celrep.2022.111515.
89. Hemmati J, Nazari M, Abolhasani FS, Ahmadi A, Asghari B. In vitro investigation of relationship between quorum-sensing system genes, biofilm forming ability, and drug resistance in clinical isolates of *Pseudomonas aeruginosa*. BMC Microbiol. 2024;24:99. https://doi.org/10.1186/s12866-024-03249-w.
90. Anderson AJ, Kang BR, Kim YC. The Gac/Rsm signaling pathway of a bio-control bacterium, *Pseudomonas chlororaphis* O6. Research in Plant Disease. 2017;23:212–27. https://doi.org/10.5423/rpd.2017.23.3.212.

**Publisher's Note**
Springer Nature remains neutral with regard to jurisdictional claims in published maps and institutional affiliations.

# Chapter 2

## Comprehensive mapping of EZ-Tn5 transposon insertion sites in *Pseudomonas argentinensis* SA190 using RATE-PCR

**Elkatmis B**, Han B, Parween S, Kopriva S, Hirt H, Saad MM (2025)

Bio-protocol 15: e5389. https://doi.org/10.21769/BioProtoc.5389

### Authors contributions

**B.E.** data curation, investigation, validation, methodology, writing—original draft, and writing—review and editing; B.H. methodology, data curation, S.P. methodology, data curation; S.K. conceptualization, supervision and review and editing. H.H. funding acquisition, supervision, and writing—review and editing; M.M.S. methodology establishment, conceptualization, supervision, validation, and writing—review and editing.

bio-protocol

Open Access

**Published: Jul 20, 2025**

# Comprehensive Mapping of EZ-Tn5 Transposon Insertion Sites in *Pseudomonas argentinensis* SA190 Using RATE-PCR

Büsra Elkatmis[1, 2], Baoda Han[1], Sabiha Parween[1], Stanislav Kopriva[2], Heribert Hirt[1, 3, *] and Maged M. Saad[1, *]

[1]DARWIN21, Biological and Environmental Science and Engineering Division, King Abdullah University of Science and Technology (KAUST), Thuwal, Saudi Arabia
[2]Institute for Plant Sciences, Cluster of Excellence on Plant Sciences (CEPLAS), University of Cologne, Cologne, Germany [3]Max Perutz Laboratories, University of Vienna, Vienna, Austria
*For correspondence: maged.saad@kaust.edu.sa; heribert.hirt@kaust.edu.sa

## Abstract

Transposon mutagenesis is a powerful tool for investigating gene function in bacteria, particularly in newly discovered species. In this study, we applied the hyperactive EZ-Tn5 transposase system to *Pseudomonas argentinensis* SA190, an endophytic bacterium known for enhancing plant resilience under drought stress. By leveraging the random amplification of transposon ends (RATE)-PCR method, we successfully mapped the insertion sites of the transposon within the SA190 genome. This approach enabled the precise identification of disrupted genes, offering insights into their roles in bacterial function and interaction with host plants. Our comprehensive protocol, including competent cell preparation, transformation, and insertion site mapping, provides a reliable framework for future studies aiming to explore gene function through mutagenesis.

## Key features

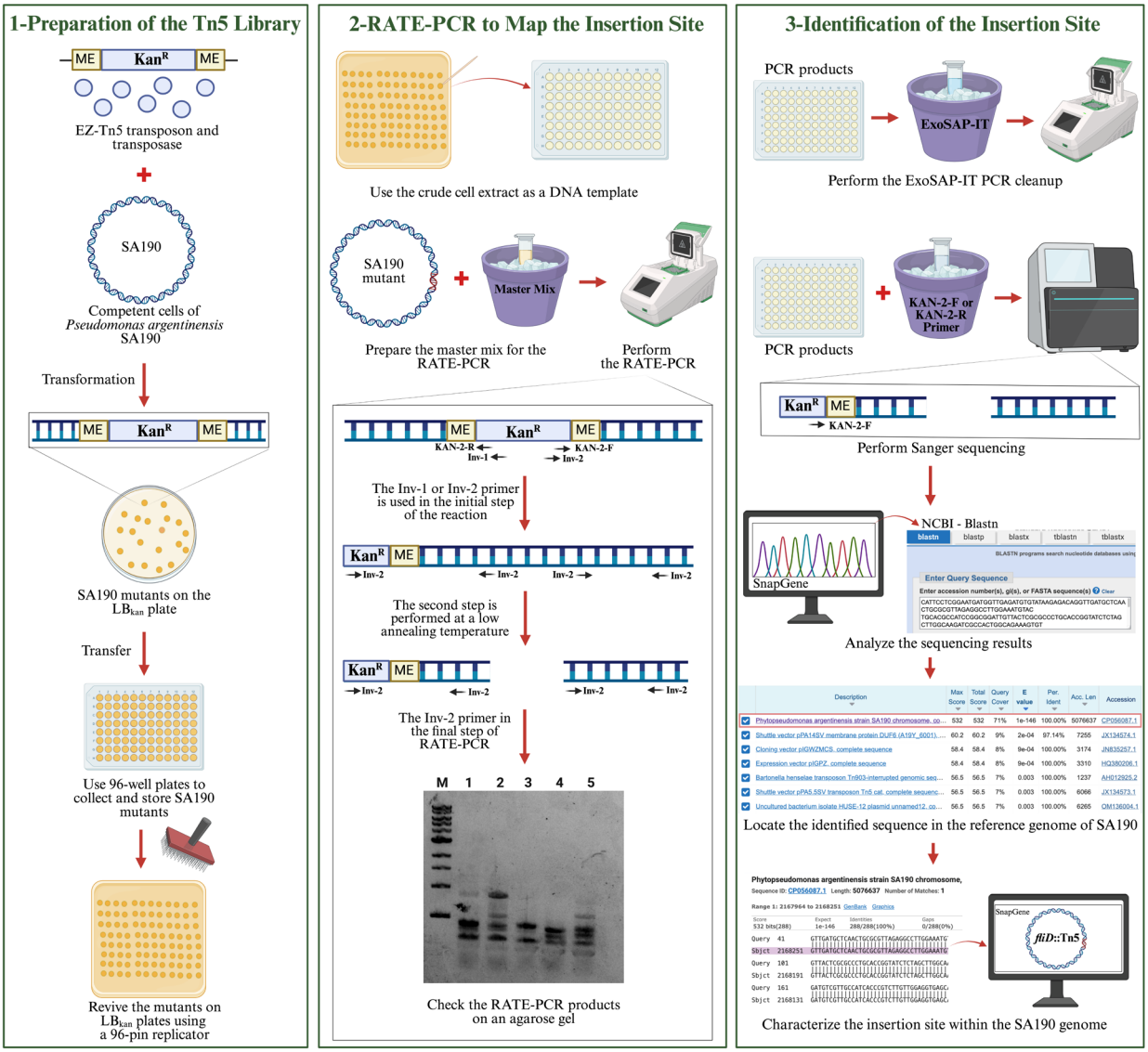
- The use of the hyperactive EZ-Tn5 transposase system ensures efficient and detectable random mutagenesis across the *Pseudomonas argentinensis* SA190 genome, facilitating comprehensive gene disruption studies.
- The technique is employed to identify and map the transposon insertion sites, allowing for precise determination of gene function and its impact on bacterial phenotypes.
- This method enables the exploration of a broad range of gene functions within SA190, particularly those involved in plant growth promotion and stress tolerance.
- This method can be readily adapted to generate mutant libraries in other bacterial species, emphasizing its transferability.

**Keywords:** Transposon mutagenesis, Gene disruption, Gene mapping, *Pseudomonas argentinensis* SA190, Tn5 insertion site, Sanger sequencing

**Cite as: Elkatmis, B. et al. (2025). Comprehensive Mapping of EZ-Tn5 Transposon Insertion Sites in *Pseudomonas argentinensis* SA190 Using RATE-PCR. Bio-protocol 15(14): e5389. DOI: 10.21769/BioProtoc.5389**

Copyright: © 2025 The Authors; exclusive licensee Bio-protocol LLC.
This is an open access article under the CC BY-NC license (https://creativecommons.org/licenses/by-nc/4.0/).

## Graphical overview




**Workflow for characterizing the Tn5 insertion site in the *Pseudomonas argentinensis* SA190 genome using RATEPCR**

## Background

Identification of essential genes by bacterial genomic studies helps to understand the functions of biological processes in bacteria [1–4]. One of the indispensable tools for studying genes in bacteria is mutagenesis, e.g., transposons insertion [1,5]. It allows us to establish a link between gene disruption and phenotypic traits. Tn5 is one of the most common transposases used to generate random mutations in the bacterial genome [6]. However, random mutagenesis methods vary in precision and efficiency, with chemical and UV mutagenesis often causing multiple mutations [7], while conventional transposons frequently exhibit lower insertion efficiency and can result in multiple insertions per genome [8]. The EZ-Tn5 transposome system addresses these limitations by incorporating a hyperactive Tn5 transposase and a kanamycin resistance cassette, allowing high-frequency, single-copy insertions that simplify mutant analysis [4,8]. Its broad host range and proven reliability across diverse bacterial species make EZ-Tn5 the preferred tool for generating effective mutant libraries in this study [8].

Mechanistically, the EZ-Tn5 transposome system, developed from the native Tn5 structure, consists of hyperactive Tn5 transposase and a kanamycin antibiotic cassette [6,9]. In the EZ-Tn5 system, the hyperactive transposase binds to the mosaic ends at the ends of the kanamycin cassette and facilitates random transposition in the genome [6,9]. The presence

of the kanamycin cassette facilitates the selection of bacteria in which transposition occurs. After transposition takes place in the bacterial genome, the transposase decays [9]. In this way, transposition occurs only once in the genome.
In this work, the EZ-Tn5 transposon system was applied on the bacteria *Pseudomonas argentinensis* SA190, an endophytic plant growth-promoting bacteria that enhances plant performance under drought stress [10]. As SA190 is a newly discovered bacterium, it is crucial to understand its essential genes. Elucidating the role of genes in SA190 will contribute to understanding the beneficial interaction between SA190 and plants. SA190 should first be prepared as competent cells to receive the transposon DNA for transposon mutagenesis. The transposon is transferred to recipient-competent cells by transformation. Since EZ-Tn5 performs random mutagenesis in the bacterial genome, identifying the mutated gene is vital in establishing a significant relationship between the gene and its function. To achieve this, we employed the random amplification of transposon ends (RATE)-PCR method, a fast and effective approach for identifying disrupted genes in the genome [11,12]. Specific primers designed for the transposon ends were used to amplify one of the transposon-end regions. RATE-PCR involves three stages, utilizing a combination of high-stringency and low-stringency temperatures to produce both specific and nonspecific PCR products of various sizes on agarose gels. These products were then subjected to Sanger sequencing using either the forward or reverse primers of the EZ-Tn5 transposon. The resulting sequences were compared against the SA190 reference genome to precisely characterize the disrupted genes.

## Materials and reagents

### Biological materials

1. *Pseudomonas argentinensis* SA190 (isolated from surface-sterilized root nodules of the plant *Indigofera argentea* in the Jizan area (16°56.475′N, 42°36.694′E) of Saudi Arabia [13], kindly provided by Heribert Hirt Lab at King Abdullah University of Science and Technology (KAUST), Jeddah, Saudi Arabia).

### Reagents

1. Kanamycin sulfate (Fisher Bioreagents, catalog number: 25389-94-0)
2. Bacto™ tryptone (Gibco, catalog number: 211705)
3. Sodium chloride (NaCl) (Merck, catalog number: 1064049025)
4. Bacto™ yeast extract (Gibco, catalog number: 212750)
5. Sodium hydroxide (NaOH) (Merck, catalog number: 71687-500G)
6. LB broth with agar (Sigma-Aldrich, catalog number: L2897-250G)
7. Potassium chloride (KCI) (Merck, catalog number: P9541-500G)
8. Magnesium chloride ($MgCI_2$) (Merck, catalog number: 208337-100G)
9. Magnesium sulfate ($MgSO_4$) (Merck, catalog number: M7506-500G)
10. Glucose (Merck, catalog number: G8270-100G)
11. Absolute glycerol (Sigma-Aldrich, catalog number: G5516)
12. Nuclease-free water (New England Biolabs, catalog number: B1500S)
13. Phusion® High-Fidelity DNA polymerase (New England Biolabs, catalog number: M0530L)
14. ExoSAP-IT PCR product cleanup reagent (Thermo Fisher Scientific, catalog number: 78-201-1ML)
15. 10 mM dNTPs (Thermo Fisher Scientific, catalog number: 18427089)

### Solutions

1. Luria-Bertani (LB) agar (see Recipes)
2. Luria-Bertani (LB) media (see Recipes)
3. Super optimal broth with catabolite repression (SOC) media (see Recipes)
4. Kanamycin sulfate stock solution (50 mg/mL) (see Recipes)

## Recipes

### 1. Luria-Bertani (LB) agar

| Reagent | Final concentration | Quantity |
|---|---|---|
| Tryptone | 1% (w/v) | 10 g |
| Yeast extract | 0.5% (w/v) | 5 g |
| NaCl | 1% (w/v) | 10 g |
| Agar | 0.9% | 9 g |
| Milli-Q $H_2O$ | variable | Fill to 1 L |
| Total | n/a | 1 L |

a. Adjust pH to 7.0 using 5 M NaOH
b. Autoclave (121 °C, 15 min, 100.8 kPa).

### 2. Luria-Bertani (LB) media

| Reagent | Final concentration | Quantity |
|---|---|---|
| Tryptone | 1% (w/v) | 10 g |
| Yeast extract | 0.5% (w/v) | 5 g |
| NaCl | 1% (w/v) | 10 g |
| Milli-Q $H_2O$ | variable | Fill to 1 L |
| Total (optional) | n/a | 1 L |

a. Adjust pH to 7.0 using 5 M NaOH
b. Autoclave (121 °C, 15 min, 100.8 kPa).

### 3. Super optimal broth with catabolite repression (SOC) media

| Reagent | Final concentration | Quantity |
|---|---|---|
| Tryptone | 2% (w/v) | 20 g |
| Yeast extract | 0.5% (w/v) | 5 g |
| NaCl | 10 mM | 2 mL |
| KCl | 2.5 mM | 2.5 mL |
| $MgCl_2$ | 10 mM | 10 mL |
| $MgSO_4$ | 10 mM | 10 mL |
| Milli-Q $H_2O$ | variable | Fill to 980 mL |
| Total | n/a | 980 mL |

a. Autoclave (121 °C, 15 min, 100.8 kPa).
b. After autoclaving, add 20 mL of filter-sterilized 1 M glucose.

### 4. Kanamycin sulfate stock solution (50 mg/mL)

| Reagent | Final concentration | Quantity |
|---|---|---|
| Kanamycin sulfate | 50 mg/mL | 0.5 g |
| Milli-Q $H_2O$ | variable | 10 mL |
| Total | n/a | 10 mL |

a. Filter sterilize the solution using a 0.2 µm filter and 10 mL syringe.
b. Aliquot 500 µL stocks and store at -20 °C.

## Laboratory supplies

1. 1.5 mL Eppendorf tubes (Thermo Fisher Scientific, catalog number: AM12450)
2. 2 mL Eppendorf tubes (Thermo Fisher Scientific, catalog number: AM12475)

3. Nunc™ Petri dishes (Thermo Fisher Scientific, catalog number: 263991)
4. Nunc™ square BioAssay dishes (Thermo Fisher Scientific, catalog number: 240845)
5. Inoculating loop (VWR®, catalog number: 612-7277)
6. L-shaped spreader (VWR®, catalog number: 612-1561)
7. 50 mL conical tubes (Thermo Fisher Scientific, catalog number: AM12502)
8. 0.1 cm electroporation cuvette (Thermo Fisher Scientific, catalog number: P41050)
9. Nalgene™ polycarbonate Erlenmeyer flask (Thermo Fisher Scientific, catalog number: 4103-0250PK)
10. Serological pipette (Thermo Fisher Scientific, catalog number: 170358T)
11. EZ-Tn5™ <KAN-2> Insertion kit (Epicentre, catalog number: EZ1921K)

*Note: This product is no longer available; as an alternative, we suggest using EZ-Tn5 Transposase (LGC Biosearch Technologies, catalog number: TNP92110)*

12. Corning™ Costar™ 96-well plate, sterile (Fisher Scientific, catalog number: 10695951)
13. PCR tubes (Thermo Fisher Scientific, catalog number: AB0490)
14. 0.2 µm Fisherbrand™ syringe filters, sterile (Thermo Fisher Scientific, catalog number: 09-719C)
15. 10 mL BD Luer-Lok™ disposable syringes without needles (Thermo Fisher Scientific, catalog number: 14-823-2A)
16. Toothpick (local purchase)

## Equipment

1. MicroPulser Electroporator (Bio-Rad Laboratories, catalog number: 1652100)
2. Centrifuge 5430 (Eppendorf, catalog number: 5427000610)
3. New Brunswick Innova® 40/40R Benchtop Orbital Shaker (Eppendorf, catalog number: M1299-0090)
4. Heratherm™ General Protocol Microbiological Incubator (Thermo Fisher Scientific, catalog number: 51028063)
5. SimpliAmp™ Thermal Cycler (Thermo Fisher Scientific, catalog number: A24811)
6. 96-Pin Microplate Replicator (Boekel Scientific, catalog number: 140500)
7. Eppendorf™ Research™ plus, mechanical single-channel pipettes multipacks (Thermo Fisher Scientific, catalog number: 13-684-250)
8. Autoclave (any manufacturer)
9. Thermo Scientific™ Revco™ ExF -86 °C upright ultra-low temperature freezer (Thermo Fisher Scientific, catalog number: EXF24086A)
10. Liquid nitrogen (N2) tank (any manufacturer)

## Software and datasets

1. SnapGene® (SnapGene, Version 6.2.1, https://www.snapgene.com/)
2. NCBI Blastn program, free use, web-based platform (https://blast.ncbi.nlm.nih.gov/Blast.cgi)

## Procedure

### A. Preparation of competent cells of *Pseudomonas argentinensis* SA190

1. Freshly streak the glycerol stock of *Pseudomonas argentinensis* SA190 onto an LB agar plate (Recipe 1) using a loop and incubate at 28 °C for overnight (16 h) incubation.

*Note: The genome size of SA190 is 5,076,637 bp, and approximately 20,000 bacterial colonies are required to achieve 4× full genome coverage.*

2. The next day, select a single colony from the plate and transfer to a flask containing 40 mL of LB media (Recipe 2).
3. Incubate the flask at 28 °C and 220 rpm.

4. Transfer 100 µL from the overnight culture to a new flask containing 40 mL of LB broth media.
5. Incubate at 28 °C and 220 rpm until the $OD_{600}$ reaches 0.4.

*Note: The doubling time of SA190 is approximately 60 min at 28 °C in LB broth media.*

6. Grow the bacterial culture to an $OD_{600}$ of 0.4, evenly transfer into two 50 mL tubes, and place on ice.
7. Centrifuge the 50 mL tubes at 5,660× *g* for 5 min at 4 °C.
8. Discard the supernatant from the 50 mL tubes.
9. Resuspend the pellet in 20 mL of ice-cold $H_2O$ by gently shaking the 50 mL tubes.
10. Centrifuge at 5,660× *g* for 5 min at 4 °C.
11. Discard the supernatant from the 50 mL tubes.
12. Resuspend the pellet in 2 mL of 10% glycerol by gently shaking the 50 mL tubes.
13. Aliquot the sample into 1.5 mL Eppendorf tubes by transferring 100 µL to each.
14. Transfer the 1.5 mL Eppendorf tubes from ice to liquid nitrogen.
15. For long-term storage, store the tubes at -80 °C.

*Note: Electrocompetent cells can be stored at -80 °C for up to 6 months without a significant loss of efficiency.*

## B. Transformation

1. Place two tubes of competent cells from -80 °C on ice.
2. Put electroporation cuvettes and 2 mL Eppendorf tubes on ice.
3. Thaw EZ-Tn5 transposon DNA and competent cells on ice for 15 min.
4. Transfer 100 µL of the competent cells to a 0.1 cm electroporation cuvette® as a control.
5. Wipe around the cuvette with tissue paper to prevent arcing.
6. Use the Ec1 program (V = 1.8 kV, 2.5 ms) for electroporation.
7. Insert the cuvette into the electroporation device and press the button to apply the pulse.
8. Immediately add 900 µL of prewarmed SOC media (room temperature or 28 °C; Recipe 3) to the cuvette.
9. Transfer all the liquid from the electroporation cuvette to a 2 mL Eppendorf tube and place it on ice.
10. Add 0.5 µL of EZ-Tn5 transposon DNA to the second tube of competent cells.

*Note: EZ-Tn5 DNA is diluted in sterile water, and typically 0.5–1.0 µg is used per electroporation.*

11. Incubate on ice for approximately 10 min.
12. Transfer 100 µL of the competent cells containing EZ-Tn5 transposon DNA to an electroporation cuvette.
13. Wipe around the cuvette with tissue paper to prevent arcing.
14. Use the Ec1 program for electroporation.
15. Insert the cuvette into the electroporation device and press the button to apply the pulse.
16. Immediately add 900 µL of SOC media to the cuvette.
17. Transfer all the liquid from the electroporation cuvette to a 2 mL Eppendorf tube.
18. Place both 2 mL Eppendorf tubes in the incubator at 28 °C and 220 rpm for 1.5 h.
19. Remove the Eppendorf tubes from the incubator and work on a clean bench.
20. Prepare $LB_{kan}$ plates using the kanamycin sulfate stock (50 mg/mL) (Recipe 4).
21. Using an L-shaped loop, plate 100 µL from each tube onto an $LB_{kan}$ plate (final concentration: 50 µg/mL kanamycin).
22. Centrifuge the remaining culture in the tube at 5,660× *g* for 3 min.
23. Discard the supernatant.
24. Resuspend the pellet in 200 µL of SOC media.
25. Spread 50 µL of the suspension on $LB_{kan}$ plates (50 µg/mL).
26. Incubate the plates at 28 °C for 1.5 days.
27. Following incubation on $LB_{kan}$ plates, transformants appear as distinct colonies.

*Note: Typically, 300–500 colonies are obtained per electroporation, but this number may vary depending on the bacterial species. PCR screening or sequencing confirms that 100% of the colonies contain unique insertions.*

## C. Preparation of the EZ-Tn5 transposon library

1. Check the control and sample plates in the incubator.
2. Take a 96-well plate.
3. Pour $LB_{kan}$ (50 µg/mL) into a reservoir.
4. Transfer 200 µL of $LB_{kan}$ to each well of the 96-well plate using a multichannel pipette.

5. Pick a bacterial colony from the sample plate with a sterile toothpick.
*Note: The toothpick is sterilized using an autoclave.*
6. Place the colony into a well of the 96-well plate. After finishing each row, remove the toothpicks and continue with the next row.
7. Complete filling the whole plate and cover it.
8. Place the plate in a 28 °C incubator overnight without shaking.
9. The next day, take a new 96-well plate.
10. Add 75 µL of 20% glycerol to each well of the new 96-well plate using a multichannel pipette.
11. Remove the overnight 96-well plate from the incubator and transfer 75 µL from each well to the new plate for preparing glycerol stock.
12. Cover the new plate and store it at -80 °C.

## D. Reviving the transposon library

1. Prepare $LB_{kan}$ agar plates in square BioAssay plates (final concentration on the plate: 50 µg/mL kanamycin).
2. Remove the 96-well plate from -80 °C and place it on ice.
3. Revive the bacterial cells from the glycerol stock by placing them on the $LB_{kan}$ agar plate using a 96-pin microplate replicator.
*Note: The 96-pin replicator is sterilized by dipping it in 70% ethanol and flaming.*
4. Incubate at 28 °C overnight.

## E. Preparation of bacterial mutants for RATE-PCR

1. Prepare autoclaved Milli-Q water, toothpicks, and sterile PCR tubes.
2. Label the PCR tubes according to the position of the bacterial colonies on the 96-well plate.
3. Add 50 µL of autoclaved Milli-Q water to the sterile PCR tubes.
4. Take a small colony from the $LB_{kan}$ plate, starting from position $A_1$ to $H_{12}$, and transferring it to the PCR tubes using a toothpick.
5. Heat the samples at 95 °C for 10 min using a thermocycler.
6. Use the crude cell extract as a DNA template for the RATE-PCR protocol.

## F. RATE-PCR to map the insertion site

1. Prepare the master mix for the RATE-PCR reaction (per sample: 1 µL of DNA, 0.2 µL of Phusion polymerase, 4 µL of 5× HF reaction buffer, 1 µL of 10 µM Inv1 or Inv2 primer (Table 1), 0.4 µL of 10 mM dNTPs, and 13.4 µL of nuclease-free water).

**Table 1. Primers used for the RATE-PCR reaction**

| Primer name | Sequence (5′ to 3′) |
|---|---|
| Inv-1 | ATGGCTCATAACACCCCTTGTATTA |
| Inv-2 | GAACTTTTGCTGAGTTGAAGGATCA |

2. Set the thermocycler for the RATE-PCR conditions: Initial denaturation at 94 °C for 1 min, 20 cycles of 30 s at 94 °C, 30 s at 55 °C, 3 min at 72 °C, 30 cycles of 30 s at 94 °C, 30 s at 30 °C, 2 min at 72 °C, 30 cycles of 30 s at 94 °C, 30 s at 55 °C, 2 min at 72 °C, final extension at 72 °C for 5 min, and hold at 4 °C.

## G. Preparation of RATE-PCR products for sequencing

1. Take 5 µL of RATE-PCR products and place them in a 96-well microplate using a multichannel pipette.
2. Add 2 µL of ExoSap-IT to the PCR products and put the 96-well microplate on ice.
3. Incubate at 37 °C for 15 min using the thermocycler.
4. Incubate at 80 °C for 15 min using the thermocycler.
5. Put the 96-well microplate on ice.

6. Add 5 µL of 10 µM KAN-2 forward or reverse primer (Table 2).
7. Add 3 µL of nuclease-free water.
8. Cover the 96-well microplate and send for Sanger sequencing.

**Table 2. Primers used for Sanger sequencing**

| Primer name | Sequence (5′ to 3′) |
|---|---|
| KAN-2-F | ACCTACAACAAAGCTCTCATCAACC |
| KAN-2-R | GCAATGTAACATCAGAGATTTTGAG |

## Data analysis

RATE-PCR generates specific and nonspecific PCR products using Inv-1 or Inv-2 primers, resulting in multiple bands on an agarose gel. The Sanger sequencing primer (Kan-2-R or Kan-2-F) was selected based on the inverse primer (Inv-1 or Inv-2) used in the RATE-PCR. The Kan-2 primer specifically binds to the end of the kanamycin resistance cassette in the RATE-PCR product. It is used in Sanger sequencing to read the genomic region adjacent to the transposon insertion site.

The Sanger sequencing data were analyzed using the NCBI BLASTN tool, which compares the query sequence against entries in the nucleotide database to identify regions of similarity. The SA190 (CP056087.1) genome appeared at the top of the BLASTN results, indicating a high-confidence match. By examining the alignment between the query sequence and the SA190 genome, the exact gene or intergenic region disrupted by the transposon can be identified. The aligned sequence is then mapped onto the SA190 reference genome using the SnapGene program (Version 6.2.1), allowing for precise characterization of the insertion site and detailed annotation of the affected gene or genomic region.

## Validation of protocol

Insertion site validation was primarily conducted using Sanger sequencing, which remains the standard for confirming the precise genomic location of transposon insertions amplified via RATE-PCR (Table 3). To further assess the robustness and accuracy of the protocol, a subset of mutants was additionally analyzed using Illumina HiSeq sequencing (Table 4). The concordance between both approaches confirmed the reliability of the RATE-PCR method for mapping EZ-Tn5 insertion sites. Detailed insertion site data, including genomic coordinates, gene annotations, and sequencing confirmation methods, are presented in Tables 3 and 4.

**Table 3. Identification of the SA190 mutants by Sanger sequencing**

| Mutant ID | Insertion Site (bp) | Strand | Disrupted gene | Gene function (NCBI annotation) | Flanking genomic sequence (5'–3') | Confirmation method |
|---|---|---|---|---|---|---|
| BET15-E8 | 2,168,204 | – | SA190_FliD | Flagellar filament capping protein | …GCTCA**[Tn5]**TGGCG… | Sanger sequencing |
| BET18-H5 | 2,717,175 | – | SA190_RpoE | RNA polymerase sigma factor | …CGTGC**[Tn5]**GCGGC… | Sanger sequencing |
| BET13-G8 | 4,458,951 | + | SA190_YejK | Nucleoid-associated protein | …GTCGT**[Tn5]**ATGTA… | Sanger sequencing |
| BET2-A1 | 2,965,440 | + | SA190_OmpA | TCOOP OmpA-OmpF porin OOP family protein | …TTCCG**[Tn5]**GTGAC… | Sanger sequencing |

Table 3 summarizes the identification of insertion sites in individual SA190 mutants through Sanger sequencing of RATEPCR amplicons. The table includes the Sanger read identifier, corresponding gene name or intergenic region, nucleotide match identity, alignment length, and insertion coordinates on the SA190 genome. All insertions were confirmed by 100% identity to the reference genome (GenBank: GCA_001044605.1), validating the protocol's ability to reliably localize EZTn5 transposon insertions at single-nucleotide resolution.

**Table 4. Validation of insertion sites in SA190 mutants by HiSeq Sequencing technology**

| Sample ID | Mutant1 | Mutant 2 | Mutant 3 | Mutant 4 | Mutant 5 |
|---|---|---|---|---|---|
| **qseqid** | Tn5 | Tn5 | Tn5 | Tn5 | Tn5 |
| **sseqid** | NODE_1_length_680816_cov_194.442609 | NODE_1_length_497665_cov_196.568265 | NODE_19_length_79072_cov_140.973758 | NODE_20_length_79072_cov_144.562517 | NODE_2_length_497665_cov_160.085036 |
| **Percentage of identical matches** | 100 | 100 | 100 | 100 | 100 |
| **Alignment length** | 108 | 108 | 108 | 108 | 108 |
| **Mismatch** | 0 | 0 | 0 | 0 | 0 |
| **gapopen** | 0 | 0 | 0 | 0 | 0 |
| **qstart** | 1 | 1 | 1 | 1 | 1 |
| **qend** | 108 | 108 | 108 | 108 | 108 |
| **sstart** | 214682 | 317444 | 18276 | 60797 | 34962 |
| **send** | 214575 | 317551 | 18383 | 60690 | 349728 |
| **evalue** | 9.2E-52 | 9.2E-52 | 9.2E-52 | 9.2E-52 | 9.2E-52 |
| **bitscore** | 200 | 200 | 200 | 200 | 200 |

Table 4 summarizes the alignment results of Tn5 insertion site flanking sequences from five representative mutants mapped against the SA190 genome. For each sample, query and subject sequence identifiers (qseqid and sseqid), alignment statistics (percentage identity, alignment length, mismatches, gaps), and mapping coordinates (start and end positions) are shown. All insertions displayed 100% identity with the reference genome, confirming the accuracy of the RATE-PCR amplification and insertion mapping. The e-value and bit score further confirm the significance of each alignment. Sequencing was performed using Illumina HiSeq technology.

# General notes and troubleshooting

## General notes

1. Sterility: Throughout the entire procedure, ensure that all materials and work surfaces are sterile to prevent contamination. Use aseptic techniques, including working near a flame or in a biosafety cabinet, where applicable.
2. Competent cells: Handle competent cells with care, as they are highly sensitive to temperature changes. Always keep them on ice except during electroporation. Avoid repeated freeze-thaw cycles to maintain cell competency.
3. Electroporation: Ensure that the electroporation cuvettes are dry on the outside before use to prevent arcing, which can lead to the loss of your sample or damage to the electroporator.
4. Incubation: During all incubation steps, maintain consistent temperature and shaking conditions as specified. Variations in these parameters can significantly affect bacterial growth and transformation efficiency.
5. SOC media: SOC media is critical for the recovery of cells post-electroporation. Ensure that the media is prewarmed and that you add it immediately after electroporation to maximize recovery rates.
6. Plating: When plating transformed cells, ensure even spreading of the culture on the agar surface for consistent colony growth. Use freshly prepared $LB_{kan}$ plates to ensure proper antibiotic selection.
7. Glycerol stocks: When preparing glycerol stocks, ensure that the glycerol is thoroughly mixed with the bacterial culture to prevent cell damage during freezing. Store the glycerol stocks promptly at -80 °C to preserve viability.
8. Labeling: Properly label all tubes, plates, and 96-well plates throughout the procedure. Mislabeling can lead to confusion and loss of valuable data, especially when dealing with large numbers of samples.

9. RATE-PCR preparation: When preparing the RATE-PCR master mix, ensure accurate pipetting of all reagents to maintain the correct concentrations. Use nuclease-free water and freshly prepared dNTPs to avoid degradation of the PCR reaction components.
10. PCR cycling conditions: Double-check the thermocycler settings before starting the PCR run. The specific cycling conditions are crucial for the success of the RATE-PCR, particularly the multiple cycling steps and temperature variations.
11. Product handling: After PCR amplification, handle the PCR products carefully to avoid contamination or loss. When using ExoSap-IT for cleanup, ensure that the incubation times and temperatures are precisely followed for optimal results.
12. Sequencing preparation: Properly prepare the samples for sequencing by ensuring accurate addition of primers and water. Seal the 96-well plate securely before sending it to the core lab to prevent any contamination or evaporation during transport.

## Troubleshooting

**Problem 1**: No colony growth on plates.
Possible cause: Inefficient electroporation or damaged competent cells.
Solution: Verify that the electroporation conditions (voltage, pulse length) are optimal and that cuvettes are clean and dry. Ensure competent cells were handled properly and remain on ice.

**Problem 2**: Low transformation efficiency.
Possible cause: Suboptimal cell concentration or incorrect handling during electroporation.
Solution: Ensure that the $OD_{600}$ of the bacterial culture is correctly measured and falls within the range of 0.4–0.6 before proceeding with electroporation. Confirm that the DNA concentration and quality are adequate.

**Problem 3**: Arcing during electroporation.
Possible cause: Residual moisture on the outside of the cuvette or high salt concentration in the sample.
Solution: Thoroughly dry the outside of the cuvette before electroporation. Check the composition of the sample and buffer to ensure low ionic strength.

**Problem 4**: Inconsistent colony growth.
Possible cause: Uneven spreading of bacteria on agar plates or inconsistency in antibiotic concentration.
Solution: Use sterile technique to evenly spread the bacterial culture. Prepare fresh $LB_{kan}$ plates with the correct antibiotic concentration and ensure they are evenly poured.

**Problem 5**: Contamination.
Possible cause: Non-sterile equipment or materials.
Solution: Double-check the sterility of all materials and equipment. Always use sterile pipette tips, and work in a clean environment. Consider using a biosafety cabinet if contamination persists.

**Problem 6**: Poor glycerol stock viability.
Possible cause: Inadequate mixing of glycerol or improper freezing.
Solution: Ensure that the glycerol is thoroughly mixed with the culture before aliquoting. Immediately transfer the aliquots to -80 °C after preparation.

**Problem 7**: Difficulty in colony picking.
Possible cause: Dense or small colonies on the agar plate.
Solution: Adjust the plating density to prevent overcrowding. If colonies are too small, consider extending the incubation time to allow for better growth.

**Problem 8**: Failed or low-yield RATE-PCR.
Possible cause: Incorrect PCR setup or degraded reagents.
Solution: Ensure that all PCR components are fresh and properly stored. Double-check the accuracy of pipetting and the thermocycler settings.

**Problem 9**: ExoSap-IT cleanup issues.
Possible cause: Incorrect incubation times or temperatures.
Solution: Follow the exact protocol for ExoSap-IT cleanup. Ensure that the incubator or thermocycler is properly calibrated.

**Problem 10**: Sequencing problems.
Possible cause: Incorrect primer or low DNA concentration.
Solution: Verify the primer sequences and concentrations before adding them to the PCR products. Ensure that the PCR products are at an appropriate concentration for sequencing.

## Acknowledgments

The authors would like to thank all members of Hirt lab, the CDA management team, and the Bioscience Core Labs in KAUST for the technical assistance and their help in many aspects of this work. The work was funded by KAUST fund BAS/1/1062-01-01 to H.H. as part of the DARWIN21 desert initiative (http://www.darwin21.org/). S.K. and B.E. are supported by the Deutsche Forschungsgemeinschaft (DFG) under Germany's Excellence Strategy – EXC 2048/1 – project 390686111 and under Priority Programme "2125 Deconstruction and Reconstruction of Plant Microbiota (DECRyPT)," project 401836049.
Graphical overview was created with BioRender.com: Elkatmis, B. (2025) https://BioRender.com/3a2mg1e

### Author contributions

B.E. data curation, investigation, validation, methodology, writing—original draft, and writing—review and editing; B.H. methodology, data curation, S.P. methodology, data curation; S.K. conceptualization, supervision and review and editing. H.H. funding acquisition, supervision, and writing—review and editing; M.M.S. methodology establishment, conceptualization, supervision, validation, and writing—review and editing.

## Competing interests

The authors declare that they have no conflicts of interest.

Received: April 09, 2025; Accepted: June 19, 2025; Available online: July 09, 2025; Published: July 20, 2025

# References

1. Freed, N. E. (2017). Creation of a Dense Transposon Insertion Library Using Bacterial Conjugation in Enterobacterial Strains Such As *Escherichia Coli* or *Shigella flexneri*. *J Visualized Exp.* e3791/56216. https://doi.org/10.3791/56216
2. Hayes, F. (2003). Transposon-Based Strategies for Microbial Functional Genomics and Proteomics. *Annu Rev Genet.* 37(1): 3–29. https://doi.org/10.1146/annurev.genet.37.110801.142807
3. Naorem, S. S., Han, J., Zhang, S. Y., Zhang, J., Graham, L. B., Song, A., Smith, C. V., Rashid, F. and Guo, H. (2018). Efficient transposon mutagenesis mediated by an IPTG-controlled conditional suicide plasmid. *BMC Microbiol.* 18(1): e1186/s12866–018–1319–0. https://doi.org/10.1186/s12866-018-1319-0
4. Nlebedim, V. U., Chaudhuri, R. R. and Walters, K. (2021). Probabilistic identification of bacterial essential genes via insertion density using TraDIS data with Tn5 libraries. *Bioinformatics.* 37(23): 4343–4349. https://doi.org/10.1093/bioinformatics/btab508
5. Filloux, A., Ramos, J. L. (2014). Preface. Pseudomonas methods and protocols. *Methods Mol Biol.* 1149:v. https://doi.org/10.1007/978-1-4939-0473-0
6. Capadona, J. and Jarvis, B. *Kits and Reagents for Nucleic Acid Extraction and Purification Research*. https://www.genetargetsolutions.com.au/wp-content/uploads/2014/06/Epicentre-Mutagenesis-Tn5-Transposomics.pdf
7. Xu, T., Bharucha, N. and Kumar, A. (2011). Genome-Wide Transposon Mutagenesis in Saccharomyces cerevisiae and Candida albicans. *Methods Mol Biol.*: 207–224. https://doi.org/10.1007/978-1-61779-197-0_13

8. Vidal, J. E., Chen, J., Li, J. and McClane, B. A. (2009). Use of an EZ-Tn5-Based Random Mutagenesis System to Identify a Novel Toxin Regulatory Locus in Clostridium perfringens Strain 13. *PLoS One.* 4(7): e6232. https://doi.org/10.1371/journal.pone.0006232
9. Epicentre Biotechnologies EZ-Tn5™ Insertion Kit. *Cold Spring Harb Protoc.* 2006(17): pdb.kit13–pdb.kit13. https://www.yumpu.com/en/document/view/37026513/protocol-for-ez-tn5tm-insertion-kit
10. Alwutayd, K. M., Rawat, A. A., Sheikh, A. H., Almeida-Trapp, M., Veluchamy, A., Jalal, R., Karampelias, M., Froehlich, K., Alzaed, W., Tabassum, N., et al. (2023). Microbe-induced drought tolerance by ABA-mediated root architecture and epigenetic reprogramming. *EMBO Rep.* 24(8): e202256754. https://doi.org/10.15252/embr.202256754
11. Karlyshev, A. V., Pallen, M. J. and Wren, B. W. (2000). Single-Primer PCR Procedure for Rapid Identification of Transposon Insertion Sites. *Biotechniques.* 28(6): 1078–1082. https://doi.org/10.2144/00286bm05
12. Ribot, E. M., Quinn, F. D., Bai, X. and Murtagh, J. J. (1998). Rapid Amplification of Transposon Ends for the Isolation, Cloning and Sequencing of Transposon-Disrupted Chromosomal Genes. *Biotechniques.* 24(1): 16–22. https://doi.org/10.2144/98241bm01
13. Lafi, F. F., Alam, I., Geurts, R., Bisseling, T., Bajic, V. B., Hirt, H. and Saad, M. M. (2016). Draft Genome Sequence of the Phosphate-Solubilizing Bacterium Pseudomonas argentinensis Strain SA190 Isolated from the Desert Plant *Indigofera argentea Genome Announc.* 4(6): e01431–16. https://doi.org/10.1128/genomea.01431-16

# Chapter 3

## Root endophyte sulfur metabolites enhance redox balance and drought tolerance in Arabidopsis

**Elkatmis B**, Alkhateeb RS, Mannes C, Jalal R, Trapp M, Westhoff P, Ozkan C, Thelen GM, Han B, Saad MM, Kopriva S, Hirt H (2026)

bioRxiv 2026.06.15.732246. https://doi.org/10.64898/2026.06.15.732246

### Authors contributions

M.M.S., S.K., and H.H., supervised the project; **B.E.**, S.K., and H.H. conceptualized the project; **B.E.**, S.K., and H.H. designed experiments; Experimental works were mainly carried out by **B.E.** with help of R.S.A, C.M., R.J., C.O., and G.M.T.; **B.E.** analyzed the data and generated figures; M.T. performed the HPLC-MS/MS; P.W. performed GC-MS and analyzed metabolite profiles; **B.E.** and B.H. generated the mutants; **B.E.** and R.S.A. drafted the manuscript, all authors read, edited, and aproved the final manuscript.

bioRxiv preprint doi: https://doi.org/10.64898/2026.06.15.732246; this version posted June 15, 2026. The copyright holder for this preprint (which was not certified by peer review) is the author/funder, who has granted bioRxiv a license to display the preprint in perpetuity. It is made available under a CC-BY-NC-ND 4.0 International license.

# *Root endophyte sulfur metabolites enhance redox balance and drought tolerance in Arabidopsis*

Büsra Elkatmis[1,2,3], Rabeaa S. Alkhateeb[3], Catherine Mannes[1], Rewaa Jalal[4], Marilia Trapp[3], Philipp Westhoff[2,5], Ceyda Ozkan[1], Giulia Marie Thelen[1,2], Baoda Han[3], Maged M. Saad[3], Stanislav Kopriva[1,2,*], Heribert Hirt[3,6,*]

[1]Institute for Plant Sciences, University of Cologne, 50674, Cologne, Germany

[2]Cluster of Excellence on Plant Sciences (CEPLAS), 50674, Cologne, Germany

[3]DARWIN21, Biological and Environmental Science and Engineering Division, King Abdullah University of Science and Technology (KAUST), 23955-6900 Thuwal, Saudi Arabia

[4]Department of Biological Sciences, College of Sciences, University of Jeddah, Jeddah 21493, Saudi Arabia

[5]Heinrich Heine University Düsseldorf, Institute for Plant Biochemistry, 40225, Düsseldorf, Germany

[6]Max Perutz Laboratories, University of Vienna, Vienna, Austria

***Corresponding Authors**: Stanislav Kopriva, Heribert Hirt

**Email:** skopriva@uni-koeln.de; heribert.hirt@kaust.edu.sa

**Author Contributions:** M.M.S., S.K., and H.H., supervised the project; B.E., S.K., and H.H. conceptualized the project; B.E., S.K., and H.H. designed experiments; Experimental works were mainly carried out by B.E. with help of R.S.A, C.M., R.J., C.O., and G.M.T.; B.E. analyzed the data and generated figures; M.T. performed the HPLC–MS/MS; P.W. performed GC–MS and analyzed metabolite profiles; B.E. and B.H. generated the mutants; B.E. and R.S.A. drafted the manuscript, all authors read, edited, and aproved the final manuscript.

**Competing Interest Statement:** The authors have no competing interests to disclose.

## Abstract

Drought is a major consequence of climate change and significantly limits crop productivity. Plant growth-promoting bacteria offer a promising solution to mitigate drought stress. The root endophyte *Pseudomonas argentinensis* SA190 has been shown to enhance plant

bioRxiv preprint doi: https://doi.org/10.64898/2026.06.15.732246; this version posted June 15, 2026. The copyright holder for this preprint (which was not certified by peer review) is the author/funder, who has granted bioRxiv a license to display the preprint in perpetuity. It is made available under a CC-BY-NC-ND 4.0 International license.

performance under drought stress conditions, but the mechanistic basis of SA190's beneficial effects remained unclear. Given the pivotal role of sulfur-containing compounds in abiotic stress responses, we investigated multiple sulfur-related Arabidopsis mutants under drought stress. We found that SA190 enhances sulfate uptake and promotes glutathione (GSH) accumulation in shoots under stress conditions. SA190 treatment improved the GSH/GSSG ratio, indicating an enhanced redox balance under drought. Selective inhibition of Arabidopsis GSH biosynthesis using buthionine sulfoximine (BSO) confirmed the essential contribution of bacterial GSH to drought stress. In addition, by generation and use of bacterial mutants deficient in the GSH synthesis pathway, we show that the bacteria directly provide Arabidopsis with either GSH or it's precursor γ-EC. In summary, SA190 promotes drought tolerance by supplying the host plant with additional GSH thereby maintaining cellular redox homeostasis and enhancing drought stress resilience.

**Keywords:** *Pseudomonas argentinensis* SA190, Sulfur, Glutathione, Drought stress, Redox homeostasis.

## Introduction

Drought is one of the most severe abiotic stresses limiting plant growth and agricultural productivity worldwide (1, 2). It reduces water availability, impairs photosynthesis, nutrient uptake, and cellular metabolism, and leads to the accumulation of reactive oxygen species (ROS) (3, 4). Excessive ROS disrupt membrane integrity, damage proteins, and impair essential cellular functions, ultimately resulting in reduced biomass and yield (5). To counteract drought-induced oxidative damage, plants activate a range of defense mechanisms, including enzymatic antioxidants such as catalase (CAT), superoxide dismutase (SOD), glutathione reductase (GR), and glutathione S-transferase (GST), along with non-enzymatic osmolytes and/or antioxidants like proline, glycine betaine, carotenoids, and glutathione (GSH) (6, 7). Among these, sulfur and sulfur-containing compounds play a pivotal role in abiotic stress tolerance (8, 9). In particular, GSH, a central sulfur-containing tripeptide, is essential for ROS detoxification, redox homeostasis, and cellular adaptation under stress conditions (10). Multiple studies demonstrated the importance of GSH in protection against oxidative stress across diverse species (11, 12). For instance, exogenous GSH treatment mitigated oxidative stress in wheat seedlings exposed to heat and drought, enhancing shoot growth traits, such as plant height and branch number (11). Similarly, in tomato, GSH application reduced $H_2O_2$ accumulation under salt stress, increased the

bioRxiv preprint doi: https://doi.org/10.64898/2026.06.15.732246; this version posted June 15, 2026. The copyright holder for this preprint (which was not certified by peer review) is the author/funder, who has granted bioRxiv a license to display the preprint in perpetuity. It is made available under a CC-BY-NC-ND 4.0 International license.

GSH/GSSG ratio, and enhanced activities of antioxidant enzymes such as SOD and CAT, thereby improving redox balance (12).

In addition to intrinsic antioxidant defenses, plants can benefit from interactions with beneficial microbes to enhance stress tolerance. Plant growth-promoting bacteria (PGPB) play a key role in improving plant performance under stress by modulating key physiological processes, including phytohormone regulation, nutrient acquisition, and hydrolytic enzyme production (13, 14). For example, *Piriformospora indica* colonization improves drought tolerance in maize by enhancing root architecture, activating antioxidant pathways, and reprogramming gene expression, especially in sulfur and carbon metabolism (15). Similarly, *Enterobacter* sp. SA187 enhances growth in *Arabidopsis thaliana* under salt stress by supplying 2-keto-4-methylthiobutyric acid (KMBA), a sulfur-containing ethylene precursor that contributes to stress mitigation (16). In addition to these, *Pseudomonas argentinensis* SA190, a desert adapted bacterium, has been shown to enhance plant biomass and drought resilience in Arabidopsis (17, 18). However, the mechanistic basis of this beneficial interaction, particularly its connection to sulfur metabolism and redox regulation, remains poorly understood.

Here, we investigate how SA190 modulates host sulfur metabolism under 25% polyethylene glycol (PEG)-induced drought stress. We show that SA190 enhances GSH accumulation even when the plant's own biosynthetic capacity is impaired, indicating that the bacteria may contribute to the plant's GSH pool or by modulating the plant's pathways. SA190 also enhances redox balance, reduces superoxide accumulation, and activates metabolites involved in GSH biosynthesis. Moreover, we demonstrate that bacterial glutathione biosynthesis, specifically through the *gshA* gene, is critical for root colonization and bacterial fitness. These findings reveal a previously uncharacterized role for microbial sulfur metabolism in promoting plant drought tolerance and position SA190 as a promising candidate for improving crop resilience under drought stress conditions.

## Results

### SA190 Enhances Biomass of Sulfur Mutants, Sulfate Uptake, and Glutathione Levels in Arabidopsis

To assess the role of sulfur metabolism in the SA190-mediated protection against PEG-induced drought stress, we evaluated the *sultr1;2, apr2*, and *cad2-1* mutants. Under control conditions, *sultr1;2* and *cad2-1* mutants exhibited slightly reduced biomass relative to *Arabidopsis thaliana* Col-0 (Figure 1A), reflecting impairments in sulfate uptake (*sultr1;2*) (19–21) and glutathione biosynthesis (*cad2-1*) (22). Under PEG-induced drought stress,

bioRxiv preprint doi: https://doi.org/10.64898/2026.06.15.732246; this version posted June 15, 2026. The copyright holder for this preprint (which was not certified by peer review) is the author/funder, who has granted bioRxiv a license to display the preprint in perpetuity. It is made available under a CC-BY-NC-ND 4.0 International license.

both *sultr1;2* and *cad2-1* mutants displayed heightened drought sensitivity, with pronounced reductions in biomass (Figure 1B). The *apr2* mutant, defective in sulfate reduction (23), also showed reduced biomass under 25% PEG-induced drought stress. The phenotypes of the mutants were consistent with the biomass results (Supplementary Figure 1 and 2). Treatment with SA190 significantly enhanced biomass in all three mutants, particularly under PEG-induced drought stress. In *sultr1;2*, SA190 led to a 3-fold increase in biomass under control conditions and 35-fold increase under PEG-induced stress compared to mock treatment. Similarly, under PEG-induced drought stress SA190 promoted a 5-fold and 25-fold increase in biomass in the *apr2* and the *cad2-1* mutants, respectively. These findings show that glutathione, and possibly other sulfur containing compounds, are crucial for the response of Arabidopsis to PEG-induced drought stress. They also suggest that SA190 may support plant survival under these conditions by promoting uptake or biosynthesis of sulfur-containing compounds.

To determine whether SA190 influences the accumulation of sulfur-containing compounds in plants, we measured sulfate and glutathione (GSH) levels in *Arabidopsis thaliana* Col-0 under control and 25% PEG-induced drought stress conditions. Sulfate and GSH levels were significantly elevated in both shoot and root under PEG-induced drought stress compared to control condition, highlighting the potential role of sulfur metabolism in the drought response (Figure 1). While under control condition, SA190 treatment did not affect sulfate concentration, under PEG-induced drought stress sulfate levels were significantly increased in the shoot of SA190 treated plants relative to mock (Figure 1C). In contrast, sulfate levels in the root of PEG treated plants were significantly reduced with SA190 treatment (Figure 1D), suggesting enhanced translocation of sulfate from the root to the shoot potentially to support increased sulfur demand in aerial tissues.

Sulfate levels in shoots of the sulfur-related mutants (*sultr1;2, apr2, cad2-1*) showed that *sultr1;2* had reduced sulfate levels compared to Col-0 under control and PEG stress conditions, and SA190 did not restore its accumulation in *sultr1;2* (Supplementary Figure 3A and B). Although SA190 rescued the *sultr1;2* growth phenotype under PEG stress, sulfate levels in shoots remained low. A similar pattern was also observed in roots (Supplementary Figure 3C and D). The *apr2* mutant had higher shoot sulfate accumulation than Col-0 under control and PEG stress conditions due to lower rate of sulfate reduction, and SA190 further increased it. In contrast, *cad2-1* showed reduced shoot sulfate compared to Col-0 under control and PEG stress, however, SA190 enhanced the sulfate level in *cad2-1*. Analysis of sulfate levels in the mutants suggests that SA190 may provide a sulfur-containing compound functioning downstream of the sulfur assimilation pathway.

bioRxiv preprint doi: https://doi.org/10.64898/2026.06.15.732246; this version posted June 15, 2026. The copyright holder for this preprint (which was not certified by peer review) is the author/funder, who has granted bioRxiv a license to display the preprint in perpetuity. It is made available under a CC-BY-NC-ND 4.0 International license.

Consistently, in the wild type, SA190 significantly increased GSH levels in the shoot compared to mock under both control and stress conditions (Figure 1E), whereas, GSH in the root remained unchanged (Figure 1F). These results suggest that to mitigate drought-induced oxidative stress, SA190 promotes shoot-specific GSH accumulation, potentially through enhanced sulfate uptake and transport in the root, followed by preferential GSH synthesis in the shoot. Alternatively, SA190 might provide GSH to the plants directly.

**SA190 Enhances GSH Accumulation in Plants Deficient in Glutathione Biosynthesis**

In order to test whether SA190 contributes directly to the GSH pool in plants, we first assessed if SA190 might compensate a buthionine sulfoximine (BSO) inhibition of GSH synthesis in Arabidopsis. BSO is a specific inhibitor of γ-glutamylcysteine synthetase (γ-ECS), the rate limiting enzyme in GSH biosynthesis, and thereby suppresses endogenous GSH production in plants (24). Treatment with 1 mM BSO markedly inhibited Arabidopsis growth under both control and 25% PEG-induced drought stress conditions, resulting in visible phenotypic alterations (Supplementary Figures 4 and 5). Primary root length was significantly reduced in BSO-treated plants compared to control plants under both conditions (Figure 2A and B), which has in turn contributed to a significant reduction in plant biomass (Figure 2C and D). On the other hand, BSO did not affect growth of SA190 (Supplementary Figure 6). The exogenous application of 0.5 mM GSH (Figure 2C and D) enhanced Arabidopsis survival under 25% PEG induced drougt stress, but had no effect under control conditions, indicating that GSH alone can improve plant survival under stress.

Inoculation with SA190 alleviated the negative effects of BSO treatment. Compared to mock, plants inoculated with SA190 showed increased primary root length and higher biomass accumulation on BSO containing agar plates under both control and stress conditions. Exogenous GSH supplementation coupled with SA190 treatment resulted in an additive beneficial effect, as the plants treated with both, GSH and SA190, showed the highest biomass accumulation under stress (Figure 2D). Improved plant growth therefore suggests a synergistic effect between bacterial presence and GSH supplementation.

We then quantified cysteine and GSH in the presence and absence of SA190. In control plants, colonization with SA190 under control as well PEG-induced drought stress conditions did not affect cysteine levels (Figure 2E and F). However, GSH levels were significantly enhanced by the colonization with the bacteria (Figure 2G and H), indicating that SA190 affects GSH synthesis in the host plant. Under BSO treatment, non-colonized shoot samples accumulated cysteine under control conditions (Figure 2E) and exhibited highly diminished GSH levels (Figure 2G and H) compared to control. These observations confirmed the effective inhibition of GSH biosynthesis upon BSO treatment. SA190 inoculation further

bioRxiv preprint doi: https://doi.org/10.64898/2026.06.15.732246; this version posted June 15, 2026. The copyright holder for this preprint (which was not certified by peer review) is the author/funder, who has granted bioRxiv a license to display the preprint in perpetuity. It is made available under a CC-BY-NC-ND 4.0 International license.

increased cysteine levels in BSO-treated plants under both conditions (Figure 2E and F). Importantly, under both non-stressed and stressed conditions, SA190 treated plants showed increased GSH levels compared to non-colonized shoot samples (Figure 2G and H). Exogenous GSH supplementation restored shoot GSH content under both control and PEG-induced drought stress conditions irrespective of SA190 presence (Figure 2G and H). These results suggest that SA190 may contribute to GSH accumulation under PEG-induced drought stress, by supplying GSH to the plant.

To further examine whether SA190 may supply glutathione to the host plant, we analyzed the Arabidopsis glutathione-deficient mutant *cad2-1* in the presence of SA190. Under PEG-induced drought stress, *cad2-1* mutants exhibited a marked reduction in GSH levels compared to Col-0, confirming their compromised glutathione biosynthetic capacity. Notably, SA190 treatment significantly increased GSH levels in *cad2-1* under PEG-induced drought stress conditions (Supplementary Figure 7). These findings suggest that SA190 may contribute to the host glutathione pool, supporting the hypothesis that the bacteria may supply glutathione to the plant.

Altogether, these findings demonstrate a central role for SA190 in enhancing sulfur assimilation and promoting glutathione accumulation under 25% PEG-induced drought stress. In particular, the ability of SA190 to enhance GSH accumulation even when GSH biosynthesis is compromised supports a mode of beneficial interaction in which the bacteria facilitate sulfur metabolism and contribute to improved drought tolerance in Arabidopsis.

## SA190 Enhances Redox Homeostasis and Reduces Superoxide Accumulation Under Drought Stress

Glutathione (GSH) is a major antioxidant that plays a vital role in maintaining cellular redox homeostasis (25). Alongside its reduced form (GSH), the oxidized form, glutathione disulfide (GSSG), contributes as well to redox regulation (25, 26). Lower GSH/GSSG ratios serve as a key indicator of oxidative stress and redox imbalance in plants (26).

In order to assess the impact of SA190 on redox status within the plant, we quantified GSSG levels and calculated the GSH/GSSG ratio in Arabidopsis in response to SA190 treatment. Under 25% PEG-induced drought stress, GSSG levels significantly increased in the plant shoots compared to control conditions (Figure 3A), indicating the presence of oxidative stress. SA190 treatment markedly reduced GSSG levels in the shoot under PEG-induced drought stress, suggesting a mitigation of oxidative damage (Figure 3A). Consistently, SA190 significantly enhanced the GSH/GSSG ratio in the shoot under PEG-induced drought stress conditions, indicating improved antioxidant capacity and restored redox homeostasis

bioRxiv preprint doi: https://doi.org/10.64898/2026.06.15.732246; this version posted June 15, 2026. The copyright holder for this preprint (which was not certified by peer review) is the author/funder, who has granted bioRxiv a license to display the preprint in perpetuity. It is made available under a CC-BY-NC-ND 4.0 International license.

(Figure 3B). In contrast, the GSSG level and the GSH/GSSG ratio in roots remained largely unchanged by SA190 (Figure 3C and 3D), potentially reflecting lower oxidative pressure or tissue-specific differences in glutathione metabolism.

To further evaluate the impact of SA190 on reactive oxygen species (ROS) levels, we performed nitroblue tetrazolium (NBT) staining in SA190-colonized and non-colonized seedlings (Figure 3E). Strong superoxide accumulation marked by the extent of purple stained area was evident in the shoots of non-colonized seedlings under PEG-induced drought stress. In contrast, SA190 visibly reduced superoxide levels, demonstrating that SA190 attenuates ROS accumulation and alleviates oxidative stress in seedlings under PEG-induced drought stress. On the other hand, no differences were observed between the treatments under control conditions (Figure 3E).

**SA190 Activates the Host Metabolism Involved in Glutathione (GSH) Biosynthesis**

To investigate the impact of SA190 on the sulfur metabolism and glutathione (GSH) biosynthesis of the host, we performed metabolic profiling of colonized Arabidopsis shoot and root tissues under control and 25% PEG-induced drought stress conditions. In the absence of SA190, plants subject to drought stress showed a distinct change in metabolic profiles compared to non-stressed plants (Figure 4A and B). As illustrated in the heatmaps, under 25% PEG-induced stress, the levels of myo-inositol, 5-oxoproline, aspartate, proline, and glycine were significantly elevated in root and shoot samples compared with control conditions (Figure 4A and B). These metabolites are associated with osmoprotection, nitrogen storage, and redox buffering (27–30), thus their presence is attributed to the physiological response during adaptation to the negative effects of drought. Notably, treatment with SA190 suppressed the accumulation of aspartate, proline, and glycine in shoot tissues under PEG-induced drought stress condition, suggesting that the presence of SA190 may modulate plant stress metabolism. On the other hand, SA190 treatment significantly increased the abundance of serine, methionine, asparagine, glutamine, and glutamate under PEG-induced drought stress compared to mock treatment (Figure 4A). Metabolites involved in plant sulfur metabolism and glutathione (GSH) biosynthesis are shown in Figure 4C. Among the up-regulated metabolites was glutamate, which plays a central role as an intermediate in amino acids biosynthetic pathways by serving as a precursor for the biosynthesis of glutamine, proline, methionine, and aspartate (31). Another up-regulated metabolite was serine which indirectly contributes to GSH biosynthesis by supplying O-acetylserine (OAS), an intermediate to cysteine biosynthesis (32). These coordinated metabolic changes indicate that SA190 may enhance GSH biosynthesis by promoting both sulfur and nitrogen assimilation. Together, our findings suggest that SA190-

bioRxiv preprint doi: https://doi.org/10.64898/2026.06.15.732246; this version posted June 15, 2026. The copyright holder for this preprint (which was not certified by peer review) is the author/funder, who has granted bioRxiv a license to display the preprint in perpetuity. It is made available under a CC-BY-NC-ND 4.0 International license.

induced metabolic reprogramming under PEG-induced drought stress enhances the plant's antioxidant capacity and stress resilience through targeted regulation of GSH-associated pathways.

**Microbial gshA involved in Glutathione Biosynthesis Plays a Critical Role in Plant Survival under Drought Stress**

The effects of SA190 on Arabidopsis GSH levels can be explained by either stimulation of sulfate assimilation and GSH synthesis, or by providing GSH or its precursors directly to the plants. To test if bacterial GSH might be taken up by Arabidopsis to mitigate PEG-induced drought stress, we generated knockout mutants of the microbial GSH biosynthetic genes *gshA* and *gshB*. GSH measurements in both Δ*gshA* and Δ*gshB* mutants revealed a clear reduction in intracellular glutathione levels compared to wild-type SA190 (Figure 5A), with a more pronounced decrease observed in *gshA*. This is consistent with *gshA* catalyzing the rate limiting step in GSH biosynthesis (33). Measurement of oxidized glutathione (GSSG) showed comparable levels in the mutants and wild-type SA190, indicating that the impairment of biosynthesis did not affect GSSG levels (Figure 5B). The GSH/GSSG ratios were significantly lowered in both mutants (Figure 5C), indicating an impaired redox homeostasis and potentially a compromised capacity to detoxify reactive oxygen species (ROS).

To evaluate the effects of the gene deletions on bacterial fitness, we analyzed the growth curves of both mutant strains as well as SA190 wild-type in LB medium. *gshA* showed a significant growth reduction indicating a vital role of *gshA* in bacterial fitness (Figure 5D). To assess how the deletions of *gshA* and *gshB* affect SA190's plant growth-promoting ability, we performed plant growth assays under control and PEG-induced drought stress conditions. Under control conditions, seedlings colonized with the Δ*gshA* and Δ*gshB* mutants had biomass levels comparable to seedlings treated with wild-type SA190 (Figure 5E). However, under 25% PEG stress, Δ*gshA* only partially rescued the plant phenotype under PEG-induced drought stress as the plants showed a significantly reduced biomass compared to plants colonized with either SA190 or Δ*gshB*.

Next, plant colonization by the two mutants and wild-type SA190 was compared (Figure 5F). While loss of *gshB* did not affect roots colonization (based on CFU/mg) compared to wild-type SA190, the Δ*gshA* mutant revealed a reduced number of bacteria associated with the root, as indicated by lower CFU/mg values. However, that reduction of bacterial levels does not seem to negatively impact the increased colonization due to PEG-induced stress, as the

bioRxiv preprint doi: https://doi.org/10.64898/2026.06.15.732246; this version posted June 15, 2026. The copyright holder for this preprint (which was not certified by peer review) is the author/funder, who has granted bioRxiv a license to display the preprint in perpetuity. It is made available under a CC-BY-NC-ND 4.0 International license.

CFU levels of Δ*gshA* mutant increased (Figure 5F). Together, these findings suggest that *gshA* but not *gshB* is critical for drought stress mitigation effect conferred by SA190.

To further dissect the contribution of bacterial *gshA* and *gshB* and their products to improvement of plant growth under PEG stress, we assessed the interaction of Δ*gshA* and Δ*gshB* mutants with the *cad2-1* mutant. Under control conditions, no obvious differences in phenotypes of *cad2-1* inoculated with the two mutants and wild-type SA190 were observed (Supplementary Figure 8). In contrast, under PEG-induced drought stress, Δ*gshA* was clearly less efficient to rescue the growth inhibition by PEG compared with SA190, whereas Δ*gshB* maintained a phenotype similar to wild-type SA190 (Supplementary Figure 9).

Fresh weight measurements further confirmed these observations. The deletion of *gshA* significantly decreased the ability to increase *cad2-1* biomass under control and PEG stress conditions (Figure 6A and B). In contrast, treatment with Δ*gshB* maintained biomass levels comparable to SA190. Since *cad2-1* has a substantially lower capacity to synthesize GSH, the ability of the Δ*gshB* mutant, which produces γ-glutamylcysteine (γ-EC) but cannot convert it to GSH, to partially restore biomass is notable. This result suggests that γ-EC may be the key bacterial metabolite supporting plant growth under PEG stress. Accordingly, Δ*gshA*, which cannot synthesize γ-EC, failed to enhance growth and biomass accumulation.

GSH quantification from the same samples further supported our conclusion. Under control conditions, inoculation with none of the three strains significantly altered GSH levels in *cad2-1*, while all three promoted GSH accumulation in the wild-type Col-0 (Figure 6C). However, under PEG stress, Δ*gshA* treatment failed to increase GSH accumulation compared with SA190, whereas Δ*gshB* increased GSH levels similar to SA190 (Figure 6D). To verify whether thiols are synthesized in sufficient quantities by the bacteria, we measured cysteine, γglutamylcysteine (γ-EC), and GSH levels in wild-type, Δ*gshA*, and Δ*gshB* (Figure 6E). Cysteine levels were comparable in the wild type and the mutants. In contrast, γ-EC levels were significantly elevated in the Δ*gshB* mutant relative to the wild type and Δ*gshA*, consistent with disruption of *gshB* leading to γ-EC accumulation. Both Δ*gshA* and Δ*gshB* mutants exhibited markedly reduced GSH levels compared to the wild type (Figure 6E). These results indicate that SA190-derived γ-EC may contribute to GSH accumulation and biomass enhancement in *cad2-1* under PEG-induced drought stress.

Taken together, these results indicate that bacterial γ-EC and GSH biosynthesis in SA190 is essential for the enhancement of Arabidopsis performance under PEG-induced drought stress. SA190-associated changes in plant sulfur-related metabolites and redox homeostasis further suggest direct contribution of bacterial sulfur metabolites in modulating host responses to PEG stress.

bioRxiv preprint doi: https://doi.org/10.64898/2026.06.15.732246; this version posted June 15, 2026. The copyright holder for this preprint (which was not certified by peer review) is the author/funder, who has granted bioRxiv a license to display the preprint in perpetuity. It is made available under a CC-BY-NC-ND 4.0 International license.

## Discussion

The role of sulfur metabolism in plant adaptation to abiotic stress is increasingly being recognized (34, 35). Numerous studies have demonstrated that plants exhibit an elevated demand for reduced sulfur under stress conditions (35, 36). Reduced sulfur is required for the biosynthesis of cysteine, methionine, and the antioxidant glutathione (GSH), which play central roles in plant defense, redox signaling, and detoxification of reactive oxygen species (ROS) (26).

In this study, we demonstrate that the beneficial endophyte *Pseudomonas argentinensis* SA190 enhances plant drought tolerance through a mechanism involving sulfur metabolism. Measurements of sulfate and GSH levels in plants colonized with SA190 revealed that SA190 significantly increased the abundance of both metabolites in Arabidopsis under PEG-induced drought stress. Consistent with these findings, previous studies have shown that cysteine and GSH levels increased threefold in *Brassica napus* (37), while GSH and ROS detoxifying enzymes, such as glutathione peroxidase, were elevated in *Moringa oleifera* Lam. under salt stress (38). Together, these observations indicate a clear involvement of sulfur-related metabolites in the mitigation of abiotic stress response in plants.

The importance of sulfur metabolism in SA190-mediated stress tolerance was also confirmed that, under PEG-induced drought stress condition, SA190 rescued the severe growth phenotypes of the mutants *sultr1;2*, *apr2*, and *cad2-1*, which are impaired in sulfate uptake, sulfate assimilation, and glutathione biosynthesis, respectively. These data demonstrate that PGPB can influence plant sulfur metabolism, potentially through the supply of sulfur-containing compounds or by modulating the host's endogenous biosynthetic machinery. Additional experiments revealed that SA190 may directly supply sulfur-containing metabolites to host plant undergoing PEG-induced drought stress. Notably, SA190 treatment markedly increased GSH levels in Arabidopsis exposed to PEG-induced drought stress even when plant GSH biosynthesis was compromised either chemically through BSO or genetically in the *cad2-1* mutant, further supporting this hypothesis.

A growing body of literature indicates that several PGPB improve plant survival under abiotic stress by enhancing sulfur solubility (39), recycling (40), or by modulating the expression of sulfur transport and biosynthesis genes in the host. However, evidence for a direct supply of bacterial sulfur-containing metabolites to plants remains limited. A notable exception is the PGPB strain SA187, which supplies 2-keto-4-methylthiobutyric acid (KMBA) to the plant, leading to increased sulfur content in roots and enhanced survival under salt stress (18).

bioRxiv preprint doi: https://doi.org/10.64898/2026.06.15.732246; this version posted June 15, 2026. The copyright holder for this preprint (which was not certified by peer review) is the author/funder, who has granted bioRxiv a license to display the preprint in perpetuity. It is made available under a CC-BY-NC-ND 4.0 International license.

The elevated GSH levels observed in plants treated with SA190 in this study effectively alleviated oxidative stress and helped maintain cellular redox balance under PEG-induced drought stress conditions. Previous studies have established GSH/GSSG ratios as a reliable indicator of cellular redox status and oxidative stress (41, 42). Measurements of the GSH/GSSG ratios in Arabidopsis colonized with SA190 under PEG-induced drought stress showed a significant increase in reduced GSH relative to the oxidized pool. Consistently, SA190 colonized plants exhibited decreased superoxide accumulation and oxidative damage when exposed to PEG-induced drought stress, further supporting the notion that SA190 may contribute GSH to the plant to maintain redox homeostasis under stress conditions.

SA190 treatment affects plants similarly to exogenous GSH application, which has been shown to alleviate water deficit stress in *Phaseolus vulgaris* plants grown in saline soil (43). Similarly, exogenous GSH application in mung bean (*Vigna radiata* L. cv. Binamoog-1) resulted in enhanced activity of antioxidant and glyoxalase systems and improved GSH/GSSG ratios that were otherwise reduced under PEG-induced drought stress conditions (44). Metabolic profiling further revealed that SA190 treatment significantly increased glutamate and serine levels in Arabidopsis shoots under PEG-induced drought stress. The biosynthetic pathways of these amino acids contribute directly to GSH biosynthesis, thereby linking nitrogen and sulfur metabolism within the plant. These data indicate a coordinated metabolic adjustment mediated by SA190 and suggest an additional route through which SA190 contributes to host metabolic reprogramming by increasing the availability of precursors required for efficient antioxidant production. Taken together, these findings support a model in which SA190 orchestrates a metabolic response that strengthens redox homeostasis in Arabidopsis under PEG-induced drought stress.

Microbial GSH biosynthesis occurs through two ATP-dependent reactions catalysed by the enzymes encoded by the *gshA* and *gshB* genes (45). These genes are essential for maintaining cellular redox balance and are directly implicated in bacterial stress tolerance and virulence (46, 47). In SA190, deletion of *gshA* but not *gshB* inhibited growth, consistent with *gshA* encoding the enzyme responsible for the rate-limiting step of GSH biosynthesis (45). This is similar to plants, where a full knock-out of γ-ECS is embryo lethal while loss of GSH synthetase allows production of viable seeds, although seedlings do not reach maturity (48, 49). Loss of *gshA* and *gshB* not only reduced intracellular GSH levels but also impaired the strain's ability to alleviate drought stress of inoculated Arabidopsis. These results indicate that SA190-mediated drought tolerance depends on bacterial GSH biosynthesis and supports the hypothesis that SA190 promotes plant stress resilience by reinforcing antioxidant defences.

bioRxiv preprint doi: https://doi.org/10.64898/2026.06.15.732246; this version posted June 15, 2026. The copyright holder for this preprint (which was not certified by peer review) is the author/funder, who has granted bioRxiv a license to display the preprint in perpetuity. It is made available under a CC-BY-NC-ND 4.0 International license.

While all results with the wild type plants or the *sultr1;2* and *apr2* mutants could be explained by SA190 stimulating sulfate uptake and metabolism, the results of the combined analysis of bacterial GSH biosynthesis mutants and the plant *cad2-1* mutant can only be explained by a direct supply of GSH and/or related compounds from the bacteria to the plant host. While neither Δ*gshA* nor Δ*gshB* are disturbed in GSH synthesis, Δ*gshB* is able to produce γ-EC. Since GSH synthetase is intact in *cad2-1* mutant, the PGP effect of Δ*gshB* under PEG-induced stress can be explained by delivery of γ-EC to the plants. Whether γ-EC is the sole metabolite transferred from the bacteria to plants, or whether in wild type situation it is GSH, still needs to be elucidated.

Our findings provide evidence for a potential supply of microbial sulfur metabolites to host plants during plant-microbe interactions. Supporting literature remains limited, although several studies have suggested that soil microbes alleviate drought stress by influencing plant sulfur assimilation or by transforming sulfur into bioavailable forms (50). For example, *Pseudomonas putida* S-313, a strain deficient in sulfonate desulfurization, failed to stimulate tomato growth compared with the wild-type strain (50). Similarly, the Δ*gshA* mutant of *Pseudomonas* sp. 6A2 exhibited reduced biomass under sulfur-deficient conditions (51). Importantly, this study demonstrated that extracellularly secreted GSH from rhizosphere bacteria enhanced plant tolerance to sulfur deficiency (51). Together, these findings underscore a conserved link between microbial sulfur metabolism and plant growth promotion.

In conclusion, our results demonstrate that SA190's ability to synthesize GSH is critical not only for its own survival and colonization but also for promoting plant drought tolerance. These findings highlight a microbial contribution to plant sulfur metabolism and redox homeostasis during stress. Future studies should investigate whether similar mechanisms operate in crop species under drought conditions. A deeper understanding of plant-microbe interactions in sulfur metabolism may ultimately facilitate the development of innovative strategies to engineer stress-tolerant crops.

## Materials and Methods

### Bacterial Strains and Growth Conditions

*Pseudomonas argentinensis* SA190 (17), *ΔgshA*, and *ΔgshB* mutants were grown overnight at 28 °C on Luria-Bertani (LB, Invitrogen) supplemented with 0.9% agar (Sigma-Aldrich).

bioRxiv preprint doi: https://doi.org/10.64898/2026.06.15.732246; this version posted June 15, 2026. The copyright holder for this preprint (which was not certified by peer review) is the author/funder, who has granted bioRxiv a license to display the preprint in perpetuity. It is made available under a CC-BY-NC-ND 4.0 International license.

### Plant Assays

Plant assays were conducted as previously described by Alwutayd et., 2023 (18) with minor modifications. *Arabidopsis thaliana* ecotype Columbia-0 (Col-0) and the mutant lines *sultr1;2* (19–21), *cad2-1* (22), and *apr2 (23)* were used in this study. Seeds were surface sterilized with 70% ethanol + 0.05% SDS for 10 min with shaking at 3000 rpm. The seeds were washed three times with 1 mL of 100% ethanol. SA190 and mutants were streaked onto LB plates. Plates were incubated overnight at 28 °C. A single colony from the plates was transferred to LB broth medium. Liquid cultures were incubated overnight at 28 °C, 220 rpm. 100 µL was taken from the overnight culture and transferred to fresh LB broth medium. Incubation at 28 °C was followed by centrifugation at 3000 rpm for 15 min. The bacterial culture was washed with ½ MS solution (Murashige and Skoog basal salts, Sigma-Aldrich). The optical density of the bacterial suspension was set to $OD_{600}$ 0.21. 100 µL of bacterial suspension was added to 50 mL of ½ MS agar and poured into the square Petri plate (120 mm x 120 mm). 100 µL of ½ MS solution was added to 50 mL of ½ MS agar for the mock treatment. Sterilized seeds were distributed on the plates. The plates were covered with aluminum foil and kept in the dark at 4 °C for two days. They were transferred to the growth chamber under long-day photoperiod conditions (16 h light, 8 h dark). After five days of germination, seedlings with 1.0–1.5 cm root length were transferred to ½ MS (non-stress) and ½ MS + 25% PEG plates. Six seedlings were transferred for each plate. They were placed into the growth chamber under the same conditions. The fresh weight of the seedlings was measured 15 days after the seedlings were transferred to ½ MS (nonstress) and ½ MS + 25% PEG plates (PEG-induced drought stress) plates. Primary root length was measured using ImageJ software (Version 1.53t). Root colonization levels were quantified according to the method described by Saad et al. (2018) (52).

### Buthionine Sulfoximine (BSO) Inhibition Assay

Five-day-old non-colonized and SA190-colonized *Arabidopsis thaliana* Col-0 seedlings were transferred to treatment plates containing control, 1 mM buthionine sulfoximine (BSO), or 0.5 mM reduced glutathione (GSH). For the BSO and GSH treatments, stock solutions were added to both the ½ MS agar and the 25% PEG solution to achieve final concentrations of 1 mM BSO and 0.5 mM GSH. As GSH lowers the pH of the media, the pH of both the ½ MS and the PEG solutions was measured after GSH addition and adjusted to 5.7 using sterile 1 M KOH or 1 M HCl. Plates were kept in a growth chamber at 22 °C under long-day conditions (16 h light / 8 h dark). After 12 days of treatment, plants were harvested for fresh weight and thiol quantification.

bioRxiv preprint doi: https://doi.org/10.64898/2026.06.15.732246; this version posted June 15, 2026. The copyright holder for this preprint (which was not certified by peer review) is the author/funder, who has granted bioRxiv a license to display the preprint in perpetuity. It is made available under a CC-BY-NC-ND 4.0 International license.

### Sulfate Measurement

Sulfate quantification was performed as described by Dietzen et al. (2020) (53) with minor modifications. Shoot and root samples (20 mg) were extracted with 1 mL of sterile water, shaken at 4 °C for 1 h, incubated at 95 °C for 15 min, and centrifuged at 4 °C for 45 min. The resulting supernatant was diluted with sterile water and transferred to ion chromatography vials. Standard curves were prepared using 2 mM $K_2SO_4$. Inorganic anions were analyzed using a Dionex ICS-1100 ion chromatography system equipped with a Dionex IonPac AS22 RFIC 4 × 250 mm analytical column (Thermo Scientific). An eluent containing 4.5 mM $Na_2CO_3$ and 1.4 mM $NaHCO_3$ was used as the running buffer.

### Quantification of Cysteine and Reduced Glutathione

For the quantification of cysteine and glutathione, 25 mg of shoot and 10 mg of root tissue were extracted in 0.1 M HCl at a 1:10 (w/v) ratio. After centrifugation at 15,000 rpm for 10 min at 4 °C, 60 µL of the supernatant was mixed with 100 µL of 0.25 M CHES-NaOH buffer (pH 9.4) and 35 µL of 10 mM dithiothreitol (DTT), and incubated at room temperature for 40 min. Subsequently, 5 µL of 25 mM monobromobimane (mBBr) was added for thiol derivatization. After 15 min incubation in the dark, 110 µL of 100 mM methanesulfonic acid was added to terminate the reaction. Samples were centrifuged again at 4 °C for 20 min, and 150 µL of the supernatant was transferred to HPLC vials. Standard curves were prepared using serial dilutions (0–100 mM) of 2 mM L-cysteine and 2 mM reduced glutathione. Thiol derivatives were separated by reverse-phase HPLC using a Eurospher 100-3 C18 column (150 × 4 mm, Knauer) with fluorescence detection (excitation: 380 nm; emission: 470 nm). Two buffers were prepared for the analysis: Buffer C (10% [v/v] methanol and 0.25% acetic acid, pH 3.9) and Buffer D (90% [v/v] methanol and 0.25% acetic acid, pH 3.9), at a constant flow rate of 1 mL $min^{-1}$. Peaks corresponding to cysteine and GSH were identified and quantified based on retention times and standard curves.

### Bacterial Growth Assay

Single colonies of SA190, *ΔgshA*, and *ΔgshB* were inoculated into 50 mL LB broth in Erlenmeyer flasks and incubated overnight at 28 °C with shaking at 200 rpm. Overnight cultures were refreshed, and the initial $OD_{600}$ was adjusted to 0.01. Cultures were then transferred to 48-well plates (Greiner Bio-One, Germany), and different concentrations of buthionine sulfoximine (BSO) were tested to assess its effect on SA190's growth. Final BSO concentrations in the wells were 0.2 mM, 0.5 mM, 1 mM, and 5 mM. Control wells contained no BSO. $OD_{600}$ values were recorded every 10 minutes using a TECAN plate reader (Infinite M200 pro). Growth curves were generated based on time-course $OD_{600}$ measurements.

bioRxiv preprint doi: https://doi.org/10.64898/2026.06.15.732246; this version posted June 15, 2026. The copyright holder for this preprint (which was not certified by peer review) is the author/funder, who has granted bioRxiv a license to display the preprint in perpetuity. It is made available under a CC-BY-NC-ND 4.0 International license.

**Quantification of Reduced and Oxidized Glutathione by HPLC–MS/MS**

For plant samples, approximately 80 mg of shoot tissue and 50 mg of root tissue were homogenized using a tissue lyser. One milliliter of extraction solution was added to each sample, followed by shaking at 700 rpm for 30 minutes at 4 °C. For bacterial samples, overnight cultures of SA190, *ΔgshA*, and *ΔgshB* were grown in 50 mL LB broth at 28 °C with shaking at 200 rpm. The following day, 5 mL of each culture was transferred into fresh LB medium and incubated until reaching an optical density at 600 nm ($OD_{600}$) of 0.4. Cultures were centrifuged at 5,000 rpm for 10 minutes at 4 °C, and the supernatants were discarded. Pellets were resuspended in 1 mL of extraction solution and shaken at 700 rpm for 30 minutes at 4 °C. After extraction, all samples were centrifuged at 16,000 × g for 10 minutes at 4 °C. The supernatants were collected and transferred to HPLC vials. Six biological replicates were used for both plant and bacterial samples.

Reduced (GSH) and oxidized (GSSG) glutathione were quantified using high-performance liquid chromatography coupled to tandem mass spectrometry (HPLC-MS/MS) composed by Vanquish UPLC (VF-P20-A Pump, VF-A10-A Sample Module and VH-C10-A Column Compartment) and TSQ Altis Plus Mass Spectrometer, both from Thermo Scientific. The analysis employed a heated electrospray ionization (H-ESI) source in negative ionization mode, with spray voltage set to –2500 V, sheath gas flow of 50 arbitrary units, auxiliary gas at 10, sweep gas at 1, an ion transfer tube temperature of 325 °C, and a vaporizer temperature of 350 °C. Chromatographic separation was carried out on a ACQUITY UPLC BEH Amide Column (2.1 x 150 mm with 1.7 um particles) at a constant flow rate of 0.4 mL/min. The mobile phase consisted of two solvents: Water 10 mM Ammonium Formate + 0.15% FA (solvent A) and ACN + 0.05% FA + 2% Ammonium Formate (1 M) (solvent B). The gradient program was as follows: from 0.0 to 12.0 minutes, the elution profile went from 20% to 55% of solvent A; from 12.0 to 15.0 minutes, the flow was kept at 55% of A; from 15.0 to 15.1 minutes, it returned to 20% of A, which was maintained until 18.0 minutes when the run ended. The MS/MS method monitored multiple reaction monitoring (MRM) transitions for both GSH and GSSG over a scan window of 18 minutes. For reduced glutathione (GSH), two transitions were used. GSH1: m/z 308.1 to m/z 162.1 (collision energy of 16.59 V and RF lens voltage at 49 V), and GSH2: m/z 330.1 to m/z 201.1 (collision energy of 17 V and RF lens voltage at 69 V). For oxidized glutathione (GSSG), the following two transitions were monitored. GSSG1: m/z 613.2 to m/z 484.1 (collision energy of 15.36 V and RF lens voltage at 92 V) and GSSG2: m/z 613.2 to m/z 355.1 (collision energy of 21.47 V and RF lens voltage at 92 V) These parameters were optimized to achieve sensitive and specific detection of glutathione species under the described conditions.

bioRxiv preprint doi: https://doi.org/10.64898/2026.06.15.732246; this version posted June 15, 2026. The copyright holder for this preprint (which was not certified by peer review) is the author/funder, who has granted bioRxiv a license to display the preprint in perpetuity. It is made available under a CC-BY-NC-ND 4.0 International license.

### Nitroblue Tetrazolium (NBT) Staining for Superoxide Detection

Seven-day-old non-colonized and SA190-colonized *Arabidopsis thaliana* Col-0 seedlings were used for nitroblue tetrazolium (NBT) staining to detect superoxide accumulation, following the protocol described by Kumar et al. (2014) (54) with minor modifications. Seedlings were placed in 24-well plates and immersed in freshly prepared NBT staining solution. Plates were wrapped in aluminum foil and incubated overnight at room temperature. The following day, the staining solution was removed, and absolute ethanol was added to each well to decolorize the tissues. Plates were incubated in a boiling water bath for 10 minutes. Seedlings were then transferred onto microscope slides and mounted with 60% glycerol. Superoxide accumulation was visualized under a light microscope.

### Metabolite Analysis

Approximately 90 mg of shoot tissue and 40 mg of root tissue were extracted using a solvent mixture of $H_2O$:MeOH:$CHCl_3$ (1:2.5:1, v/v/v). Samples were vortexed and shaken for 6 minutes at 4 °C, followed by centrifugation for 5 minutes. The resulting supernatant was used for metabolite profiling by gas chromatography–mass spectrometry (GC-MS) using a 7200 GCQTOF system (Agilent Technologies, Santa Clara, CA, USA), as previously described (55). For quantification, peak areas were normalized to Ribitol used as internal standards.

### Generation of Marker-Free gshA and gshB Deletion Mutants

Marker-free deletion mutants of *GshA* and *GshB* were generated in SA190 using a two-step homologous recombination approach. For the construction of the deletion, ~500 bp region up- and downstream of gene of interest were generated by gene synthesis (GenScript, Singapore). The synthesized fragments were cloned into the suicide vector pK18mobsacB (56) via HindIII and XbaI restriction sites. Sequence of the resulting plasmids were verified by sequencing prior to their introduction into SA190 via electroporation. Transformants were selected on LB agar plates supplemented with 50 µg/mL kanamycin. For counterselection of double-crossover recombinants, colonies were plated onto LB agar containing 15% sucrose. Kanamycin sensitive and sucrose resistant clones were screened for the desired gene deletion by colony PCR and Sanger sequencing. Plasmids and primers used in this study are listed in Supplementary Tables 1 and 2.

### Statistical Analysis

All statistical analyses in this study were conducted using GraphPad Prism (Version 10.2.0). The plant assay was performed with three biological replicates and two technical replicates (n = 36). Colony-forming unit (CFU) data were generated from three independent biological replicates. Analysis of total fresh weight, primary root length, sulfate uptake, cysteine, GSH,

bioRxiv preprint doi: https://doi.org/10.64898/2026.06.15.732246; this version posted June 15, 2026. The copyright holder for this preprint (which was not certified by peer review) is the author/funder, who has granted bioRxiv a license to display the preprint in perpetuity. It is made available under a CC-BY-NC-ND 4.0 International license.

GSSG, GSH/GSSG and CFU levels was performed using two-way ANOVA with the post-hoc Tukey test. The heatmap were prepared using the MetaboAnalyst program (version 6.0). The plant assay plates were scanned using the EPSON scanner. The primary root length of the plants was measured using the ImageJ program (Version 1.53t). Letters on the graphs indicate statistically significant differences in mean values ($p < 0.05$). Data were presented in boxplot graphs, where whiskers represent the minimum and maximum values, and the horizontal line indicates the median.

## Acknowledgments

The authors would thank all members of Hirt lab, AG Kopriva, the CDA management team, and the Bioscience Core Labs in KAUST for the technical assistance and their help in many aspects of this work. The authors also thank Prof. Dr. Jörn Kalinowski, Center for Biotechnology (CeBiTec), Bielefeld University, Germany for donating the pK18mobsacB plasmid. The work was funded by KAUST fund BAS/1/1062-01-01 to H.H. as part of the DARWIN21 desert initiative (http://www.darwin21.org/). S.K. and B.E. are supported by the Deutsche Forschungsgemeinschaft (DFG) under Germany´s Excellence Strategy – EXC 2048/1 – project 390686111 and under Priority Programme "2125 Deconstruction and Reconstruction of Plant Microbiota (DECRyPT)", project 401836049. The authors acknowledge the use of ChatGPT for assistance with grammatical corrections and improved phrasing in this manuscript.

bioRxiv preprint doi: https://doi.org/10.64898/2026.06.15.732246; this version posted June 15, 2026. The copyright holder for this preprint (which was not certified by peer review) is the author/funder, who has granted bioRxiv a license to display the preprint in perpetuity. It is made available under a CC-BY-NC-ND 4.0 International license.

## References

1. Y. Zhou, H. M. Lam, J. Zhang, Inhibition of photosynthesis and energy dissipation induced by water and high light stresses in rice. *J. Exp. Bot.* **58**, 1207–1217 (2007).

2. G. Zinta, *et al.*, Physiological, biochemical, and genome-wide transcriptional analysis reveals that elevated CO2 mitigates the impact of combined heat wave and drought stress in Arabidopsis thaliana at multiple organizational levels. *Glob. Chang. Biol.* **20**, 3670–85 (2014).

3. H. G. Jones, Monitoring plant and soil water status: established and novel methods revisited and their relevance to studies of drought tolerance. *J. Exp. Bot.* **58**, 119–30 (2007).

4. M. Qiao, C. Hong, Y. Jiao, S. Hou, H. Gao, Impacts of Drought on Photosynthesis in Major Food Crops and the Related Mechanisms of Plant Responses to Drought. *Plants (Basel).* **13** (2024).

5. F. K. Choudhury, R. M. Rivero, E. Blumwald, R. Mittler, Reactive oxygen species, abiotic stress and stress combination. *Plant J.* **90**, 856–867 (2017).

6. M. H. Cruz de Carvalho, Drought stress and reactive oxygen species: Production, scavenging and signaling. *Plant Signal. Behav.* **3**, 156–65 (2008).

7. S. S. Gill, N. Tuteja, Reactive oxygen species and antioxidant machinery in abiotic stress tolerance in crop plants. *Plant Physiol. Biochem.* **48**, 909–30 (2010).

8. A. F. Alvi, N. Iqbal, M. Albaqami, N. A. Khan, The emerging key role of reactive sulfur species in abiotic stress tolerance in plants. *Physiol. Plant.* **175**, e13945 (2023).

9. H. Takahashi, F. Marsolais, A. Cuypers, S. Kopriva, Sulfur metabolism: actions for plant resilience and environmental adaptation. *J. Exp. Bot.* **74**, 3271–3275 (2023).

10. G. Creissen, *et al.*, Elevated glutathione biosynthetic capacity in the chloroplasts of transgenic tobacco plants paradoxically causes increased oxidative stress. *Plant Cell* **11**, 1277–92 (1999).

11. M. S. E. Suliman, *et al.*, Exogenous glutathione protected wheat seedling from high temperature and water deficit damages. *Sci. Rep.* **14**, 5304 (2024).

12. Y. ZHOU, *et al.*, Exogenous GSH protects tomatoes against salt stress by modulating photosystem II efficiency, absorbed light allocation and H2O2-scavenging system in chloroplasts. *J. Integr. Agric.* **17**, 2257–2272 (2018).

13. Z. Jakubowska, M. Gradowski, J. Dobrzyński, Role of plant growth-promoting bacteria (PGPB) in enhancing phenolic compounds biosynthesis and its relevance to abiotic stress tolerance in plants: a review. *Antonie Van Leeuwenhoek* **118**, 123 (2025).

14. S. Rani, A. Sogarwal, Gargi, S. Mishra, S. Kaur, Harnessing plant-bacterial interactions to enhance abiotic stress tolerance in plants: a review. *Discover Plants* **2**, 250 (2025).

15. W. Zhang, *et al.*, Drought stress responses in maize are diminished by Piriformospora indica. *Plant Signal. Behav.* **13**, e1414121 (2018).

bioRxiv preprint doi: https://doi.org/10.64898/2026.06.15.732246; this version posted June 15, 2026. The copyright holder for this preprint (which was not certified by peer review) is the author/funder, who has granted bioRxiv a license to display the preprint in perpetuity. It is made available under a CC-BY-NC-ND 4.0 International license.

16. A. de Zélicourt, *et al.*, Ethylene induced plant stress tolerance by Enterobacter sp. SA187 is mediated by 2-keto-4-methylthiobutyric acid production. *PLoS Genet.* **14** (2018).

17. F. F. Lafi, *et al.*, Draft genome sequence of the phosphate-solubilizing bacterium Pseudomonas argentinensis strain SA190 isolated from the desert plant Indigofera argentea. *Genome Announc.* **4** (2016).

18. K. M. Alwutayd, *et al.*, Microbe-induced drought tolerance by ABA-mediated root architecture and epigenetic reprogramming. *EMBO Rep.* **24**, e56754 (2023).

19. J. J. Vidmar, A. Tagmount, N. Cathala, B. Touraine, J. E. Davidian, Cloning and characterization of a root specific high-affinity sulfate transporter from Arabidopsis thaliana. *FEBS Lett.* **475**, 65–9 (2000).

20. N. Shibagaki, *et al.*, Selenate-resistant mutants of Arabidopsis thaliana identify Sultr1;2, a sulfate transporter required for efficient transport of sulfate into roots. *Plant J.* **29**, 475–86 (2002).

21. N. Yoshimoto, H. Takahashi, F. W. Smith, T. Yamaya, K. Saito, Two distinct highaffinity sulfate transporters with different inducibilities mediate uptake of sulfate in Arabidopsis roots. *Plant J.* **29**, 465–73 (2002).

22. C. S. Cobbett, M. J. May, R. Howden, B. Rolls, The glutathione-deficient, cadmiumsensitive mutant, cad2-1, of Arabidopsis thaliana is deficient in gammaglutamylcysteine synthetase. *Plant J.* **16**, 73–8 (1998).

23. M. Weber, M. Suter, C. Brunold, S. Kopriva, Sulfate assimilation in higher plants characterization of a stable intermediate in the adenosine 5'-phosphosulfate reductase reaction. *Eur. J. Biochem.* **267**, 3647–53 (2000).

24. N. Ahmad, M. Malagoli, M. Wirtz, R. Hell, Drought stress in maize causes differential acclimation responses of glutathione and sulfur metabolism in leaves and roots. *BMC Plant Biol.* **16** (2016).

25. M. Hasanuzzaman, K. Nahar, T. I. Anee, M. Fujita, Glutathione in plants: biosynthesis and physiological role in environmental stress tolerance. *Physiol. Mol. Biol. Plants* **23**, 249–268 (2017).

26. K. Aquilano, S. Baldelli, M. R. Ciriolo, Glutathione: new roles in redox signaling for an old antioxidant. *Front. Pharmacol.* **5**, 196 (2014).

27. C. Di Martino, S. Delfine, R. Pizzuto, F. Loreto, A. Fuggi, Free amino acids and glycine betaine in leaf osmoregulation of spinach responding to increasing salt stress. *New Phytologist* **158**, 455–463 (2003).

28. M. Han, *et al.*, l-Aspartate: An Essential Metabolite for Plant Growth and Stress Acclimation. *Molecules* **26** (2021).

29. A. A. M. Al-Mushhin, *et al.*, Exogenous Myo-Inositol Alleviates Salt Stress by Enhancing Antioxidants and Membrane Stability via the Upregulation of Stress Responsive Genes in Chenopodium quinoa L. *Plants (Basel).* **10** (2021).

30. L. Szabados, A. Savouré, Proline: a multifunctional amino acid. *Trends Plant Sci.* **15**, 89–97 (2010).

bioRxiv preprint doi: https://doi.org/10.64898/2026.06.15.732246; this version posted June 15, 2026. The copyright holder for this preprint (which was not certified by peer review) is the author/funder, who has granted bioRxiv a license to display the preprint in perpetuity. It is made available under a CC-BY-NC-ND 4.0 International license.

31. B. G. Forde, P. J. Lea, Glutamate in plants: metabolism, regulation, and signalling. *J. Exp. Bot.* **58**, 2339–58 (2007).

32. F. H. Haas, *et al.*, Mitochondrial serine acetyltransferase functions as a pacemaker of cysteine synthesis in plant cells. *Plant Physiol.* **148**, 1055–67 (2008).

33. S. C. Lu, Glutathione synthesis. *Biochim. Biophys. Acta* **1830**, 3143–53 (2013).

34. S. Kopriva, M. Malagoli, H. Takahashi, Sulfur nutrition: Impacts on plant development, metabolism, and stress responses. *J. Exp. Bot.* **70**, 4069–4073 (2019).

35. F. R. Capaldi, P. L. Gratão, A. R. Reis, L. W. Lima, R. A. Azevedo, Sulfur Metabolism and Stress Defense Responses in Plants. *Trop. Plant Biol.* **8**, 60–73 (2015).

36. M. J. Hawkesford, L. J. De Kok, Managing sulphur metabolism in plants. *Plant Cell Environ.* **29**, 382–95 (2006).

37. J. M. Ruiz, E. Blumwald, Salinity-induced glutathione synthesis in Brassica napus. *Planta* **214**, 965–969 (2002).

38. M. Azeem, *et al.*, Salinity stress improves antioxidant potential by modulating physiobiochemical responses in Moringa oleifera Lam. *Sci. Rep.* **13** (2023).

39. K. Patel, *et al.*, Effect of supplementing Sulphur-oxidizing bacteria with different Sulphur sources on the growth and development of chickpea (Cicer arietinum). *Plant Stress* **12**, 100433 (2024).

40. M. A. Kertesz, P. Mirleau, The role of soil microbes in plant sulphur nutrition. *J. Exp. Bot.* **55**, 1939–45 (2004).

41. G. Noctor, C. H. Foyer, ASCORBATE AND GLUTATHIONE: Keeping Active Oxygen Under Control. *Annu. Rev. Plant Physiol. Plant Mol. Biol.* **49**, 249–279 (1998).

42. O. Zitka, *et al.*, Redox status expressed as GSH:GSSG ratio as a marker for oxidative stress in paediatric tumour patients. *Oncol. Lett.* **4**, 1247–1253 (2012).

43. T. A. Abd El Mageed, *et al.*, Glutathione-mediated changes in productivity, photosynthetic efficiency, osmolytes, and antioxidant capacity of common beans (Phaseolus vulgaris) grown under water deficit. *PeerJ* **11**, e15343 (2023).

44. K. Nahar, M. Hasanuzzaman, M. M. Alam, M. Fujita, Glutathione-induced drought stress tolerance in mung bean: coordinated roles of the antioxidant defence and methylglyoxal detoxification systems. *AoB Plants* **7** (2015).

45. G. V Smirnova, O. N. Oktyabrsky, Glutathione in bacteria. *Biochemistry (Mosc).* **70**, 1199–211 (2005).

46. A. Meister, [3] Glutathione biosynthesis and its inhibition. *Methods Enzymol.* **252**, 26–30 (1995).

47. M. E. Anderson, Glutathione: an overview of biosynthesis and modulation. *Chem. Biol. Interact.* **111–112**, 1–14 (1998).

48. N. G. Cairns, M. Pasternak, A. Wachter, C. S. Cobbett, A. J. Meyer, Maturation of arabidopsis seeds is dependent on glutathione biosynthesis within the embryo. *Plant Physiol.* **141**, 446–55 (2006).

bioRxiv preprint doi: https://doi.org/10.64898/2026.06.15.732246; this version posted June 15, 2026. The copyright holder for this preprint (which was not certified by peer review) is the author/funder, who has granted bioRxiv a license to display the preprint in perpetuity. It is made available under a CC-BY-NC-ND 4.0 International license.

49. M. Pasternak, *et al.*, Restricting glutathione biosynthesis to the cytosol is sufficient for normal plant development. *Plant J.* **53**, 999–1012 (2008).

50. A. Kahnert, P. Mirleau, R. Wait, M. A. Kertesz, The LysR-type regulator SftR is involved in soil survival and sulphate ester metabolism in Pseudomonas putida. *Environ. Microbiol.* **4**, 225–37 (2002).

51. A. Mukherjee, *et al.*, A bacterial signal coordinates plant-microbe fitness trade-off to enhance sulfur deficiency tolerance in plants. *Cell Host Microbe* **33**, 1748-1764.e6 (2025).

52. M. Saad, A. de Zelicourt, E. Rolli, L. Synek, H. Hirt, Quantification of Root Colonizing Bacteria. *Bio. Protoc.* **8** (2018).

53. C. Dietzen, *et al.*, The Transcription Factor EIL1 Participates in the Regulation of Sulfur-Deficiency Response. *Plant Physiol.* **184**, 2120–2136 (2020).

54. D. Kumar, M. A. Yusuf, P. Singh, M. Sardar, N. B. Sarin, Histochemical detection of superoxide and H2O2 accumulation in Brassica juncea seedlings. *Bio. Protoc.* **4**, e1108–e1108 (2014).

55. U. Schlüter, *et al.*, Brassicaceae display variation in efficiency of photorespiratory carbon-recapturing mechanisms. *J. Exp. Bot.* **74**, 6631–6649 (2023).

56. A. Schäfer, *et al.*, Small mobilizable multi-purpose cloning vectors derived from the Escherichia coli plasmids pK18 and pK19: selection of defined deletions in the chromosome of Corynebacterium glutamicum. *Gene* **145**, 69–73 (1994).

bioRxiv preprint doi: https://doi.org/10.64898/2026.06.15.732246; this version posted June 15, 2026. The copyright holder for this preprint (which was not certified by peer review) is the author/funder, who has granted bioRxiv a license to display the preprint in perpetuity. It is made available under a CC-BY-NC-ND 4.0 International license.

## Figures

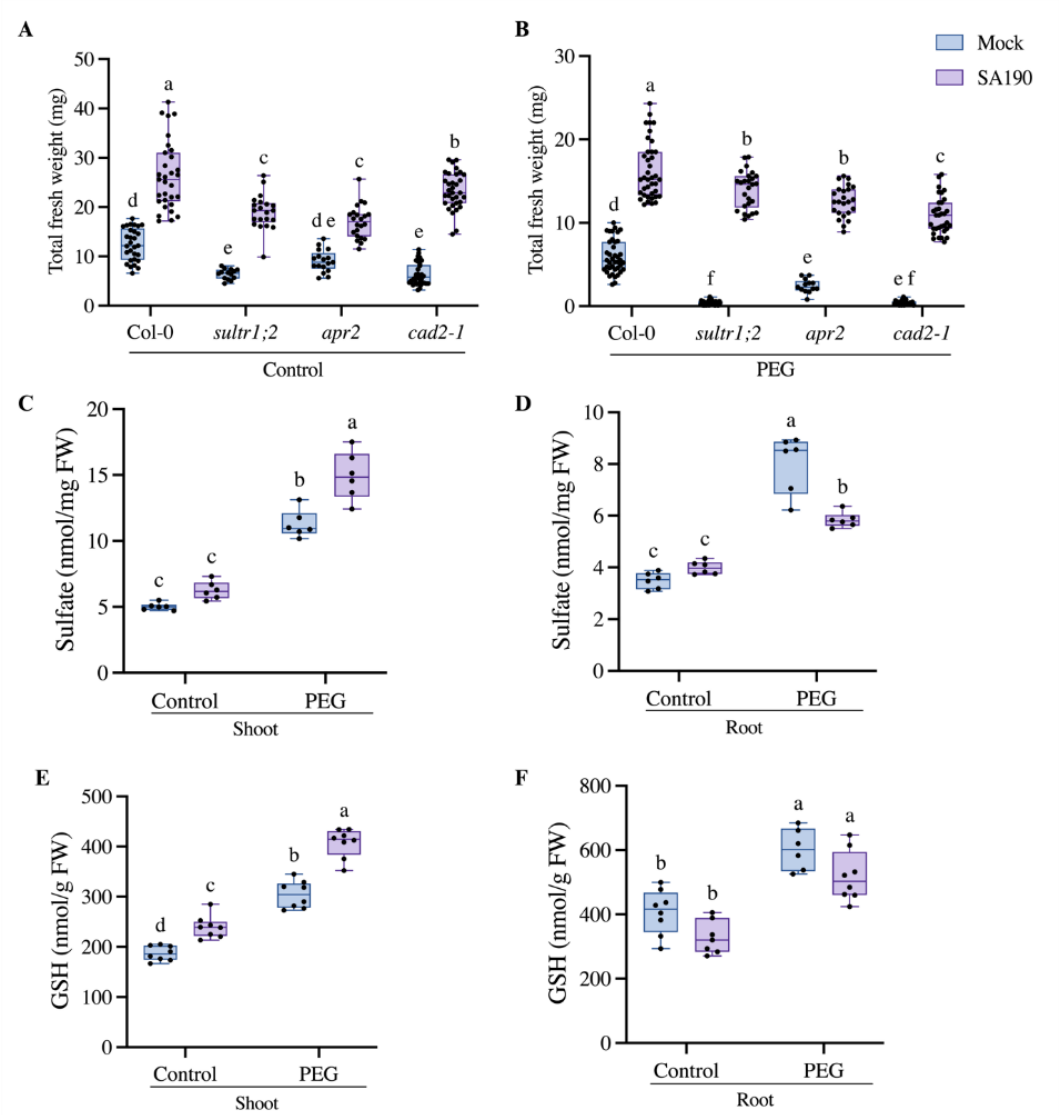



**Figure 1. Effect of *Pseudomonas argentinensis* SA190 on sulfur-deficient Arabidopsis mutants, sulfate uptake, and glutathione (GSH) levels under control (non-stress) and 25% PEG-induced drought stress conditions.** Total fresh weight of non-colonized (mock) and SA190-colonized *Arabidopsis thaliana* Col-0 grown on control (A) or 25% PEG-induced drought stress (B) for 15 days. Sulfate content in shoot (C) and root (D) samples under control and 25% PEG-induced drought stress conditions. GSH levels in shoot (E) and root (F) tissues of mock- and SA190-inoculated plants under the same conditions. The plant assay was performed in three biological replicates and two technical replicates (n=36). Whiskers represent minimum and maximum values, the horizontal line indicates the median. Different letters indicate statistically significant differences based on two-way ANOVA ($p < 0.05$).

bioRxiv preprint doi: https://doi.org/10.64898/2026.06.15.732246; this version posted June 15, 2026. The copyright holder for this preprint (which was not certified by peer review) is the author/funder, who has granted bioRxiv a license to display the preprint in perpetuity. It is made available under a CC-BY-NC-ND 4.0 International license.

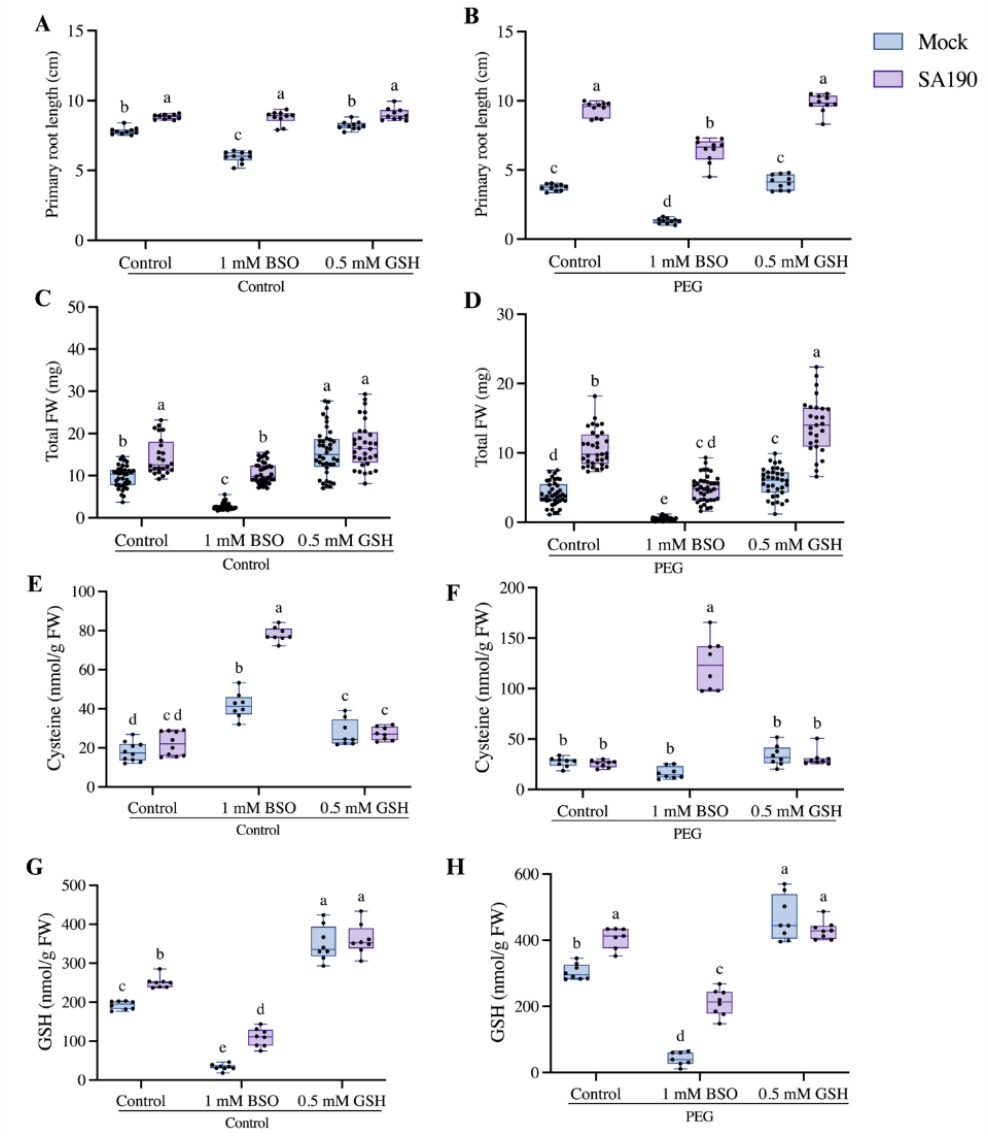



**Figure 2. Effect of *Pseudomonas argentinensis* SA190 on Arabidopsis growth in the presence of BSO and GSH under control (non-stress) and 25% PEG-induced drought stress conditions.** Primary root length of non-colonized and SA190-colonized *Arabidopsis thaliana* Col-0 under control, 1 mM BSO, and 0.5 mM GSH treatments on control (A) and 25% PEG-induced drought stress (B). Root length was measured using ImageJ (version 1.53t). Total fresh weight of non-colonized and SA190-colonized plants under the same treatments on control (C) and 25% PEG-induced drought stress (D) conditions. Cysteine levels in shoot tissue under the same treatments on control (E) and 25% PEG-induced drought stress (F). Glutathione (GSH) levels in shoot tissue under the same treatments on control (G) and 25% PEG-induced drought stress (H). The plant assay was performed in three biological replicates and two technical replicates (n=36). Whiskers represent minimum and maximum values, the horizontal line indicates the median. Different letters denote statistically significant differences based on two-way ANOVA ($p < 0.05$).

bioRxiv preprint doi: https://doi.org/10.64898/2026.06.15.732246; this version posted June 15, 2026. The copyright holder for this preprint (which was not certified by peer review) is the author/funder, who has granted bioRxiv a license to display the preprint in perpetuity. It is made available under a CC-BY-NC-ND 4.0 International license.

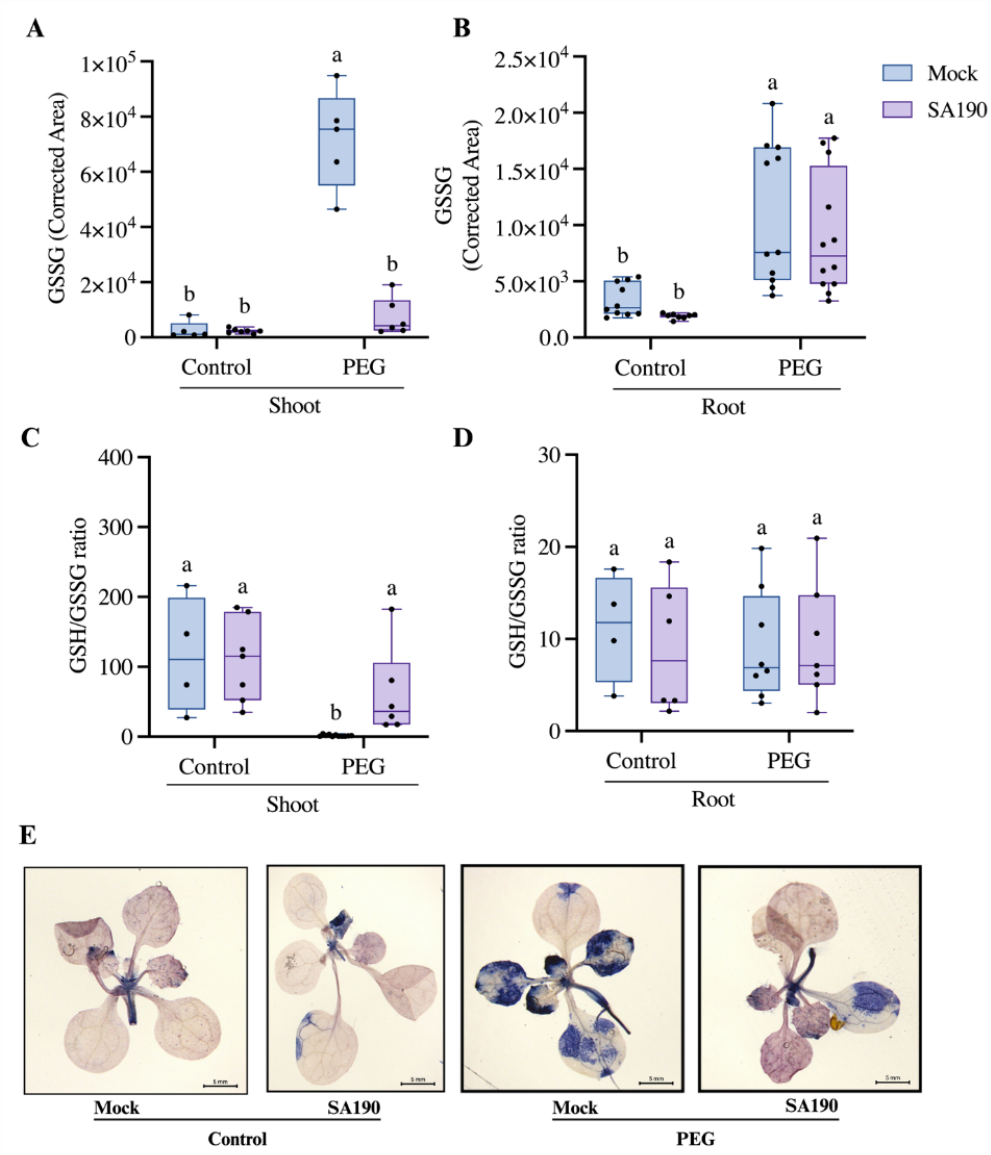



**Figure 3. Effect of *Pseudomonas argentinensis* SA190 on redox homeostasis under control (non-stress) and 25% PEG-induced drought stress conditions.** The GSSG level of non-colonized and SA190-colonized *Arabidopsis thaliana* Col-0 under control and 25% PEG induced drought stress conditions for the shoot (A), the GSH/GSSG ratio of non-colonized and SA190-colonized *Arabidopsis thaliana* Col-0 under control and 25% PEG stress conditions for the shoot (B), the GSSG level of non-colonized and SA190-colonized *Arabidopsis thaliana* Col0 under control and 25% PEG-induced drought stress conditions for the root (C), The GSH/GSSG ratio of non-colonized and SA190-colonized *Arabidopsis thaliana* Col-0 under control and 25% PEG stress conditions for the root (D). In the boxplot, the whiskers represent the minimum and maximum values, while the horizontal line represents the median. Different letters indicate statistical differences based on two-way ANOVA ($p < 0.05$). Effect of SA190 on superoxide accumulation in 7-day-old seedlings under control and 25% PEG-induced drought stress asessed by nitro blue tetrazolium (NBT) staining (E).

bioRxiv preprint doi: https://doi.org/10.64898/2026.06.15.732246; this version posted June 15, 2026. The copyright holder for this preprint (which was not certified by peer review) is the author/funder, who has granted bioRxiv a license to display the preprint in perpetuity. It is made available under a CC-BY-NC-ND 4.0 International license.

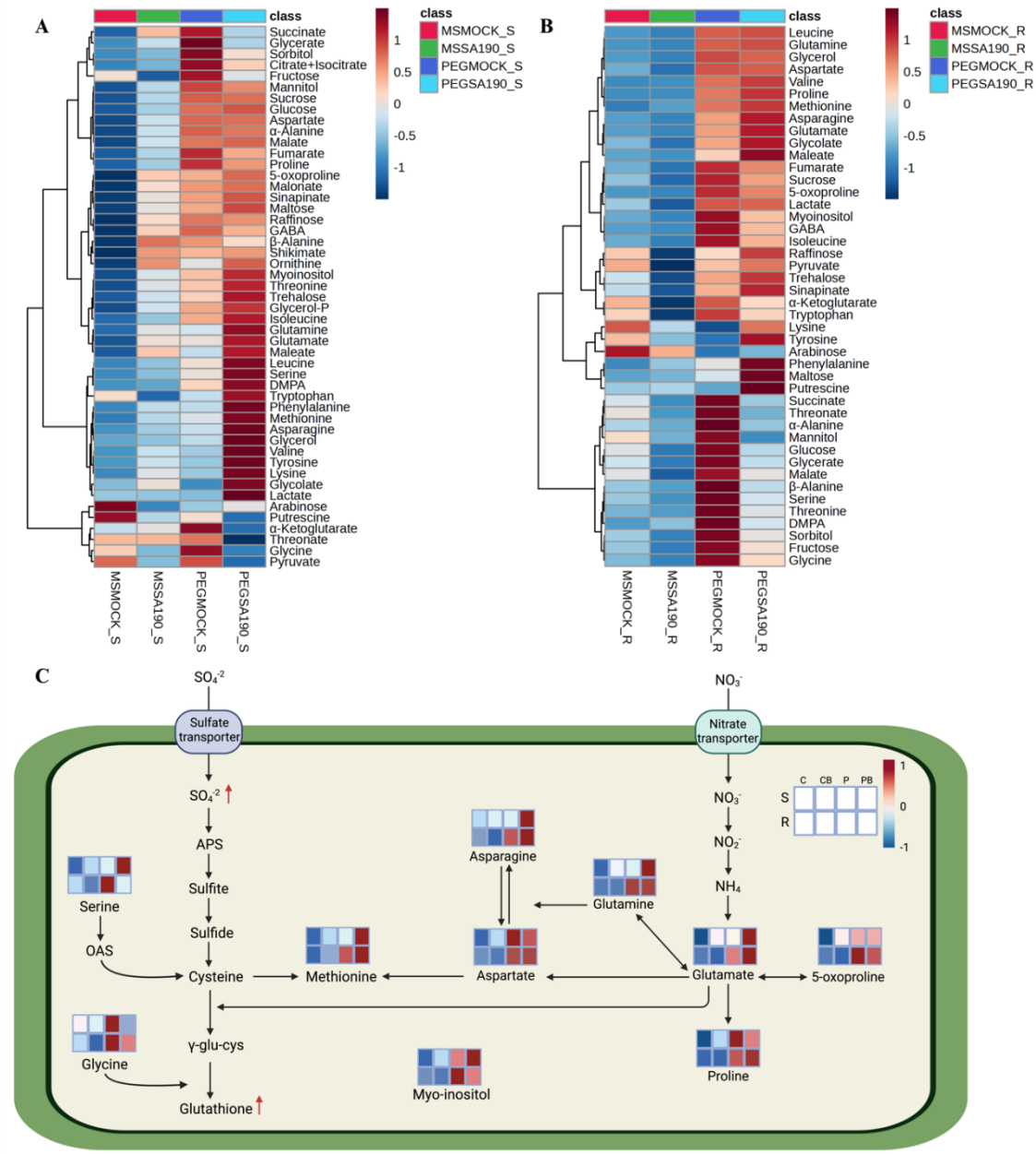



**Figure 4. *Pseudomonas argentinensis* SA190 modulates sulfur-related metabolites and glutathione biosynthesis pathways under control (non-stress) and 25% PEG-induced drought stress.** Heatmap of metabolites in shoot tissues of *Arabidopsis thaliana* treated with mock or SA190 under control (non-stress) and 25% PEG-induced drought stress conditions (A). Heatmap of metabolites in root tissues under the same conditions (B). Metabolic pathway map illustrating the connection between SA190-responsive metabolites involved in sulfur related and glutathione (GSH) biosynthesis (C). S, shoot; R, root; C, Control (non-stress); CB, bacterial treatment under control condition (non-stress); P, PEG stress; PB, bacterial treatment under PEG stress. Metabolite levels are color-coded based on statistical significance: red indicates significant up-regulation; blue indicates significant down-regulation. Metabolic pathway map was created using Biorender.com (https://BioRender.com/qr8pqwq).

bioRxiv preprint doi: https://doi.org/10.64898/2026.06.15.732246; this version posted June 15, 2026. The copyright holder for this preprint (which was not certified by peer review) is the author/funder, who has granted bioRxiv a license to display the preprint in perpetuity. It is made available under a CC-BY-NC-ND 4.0 International license.

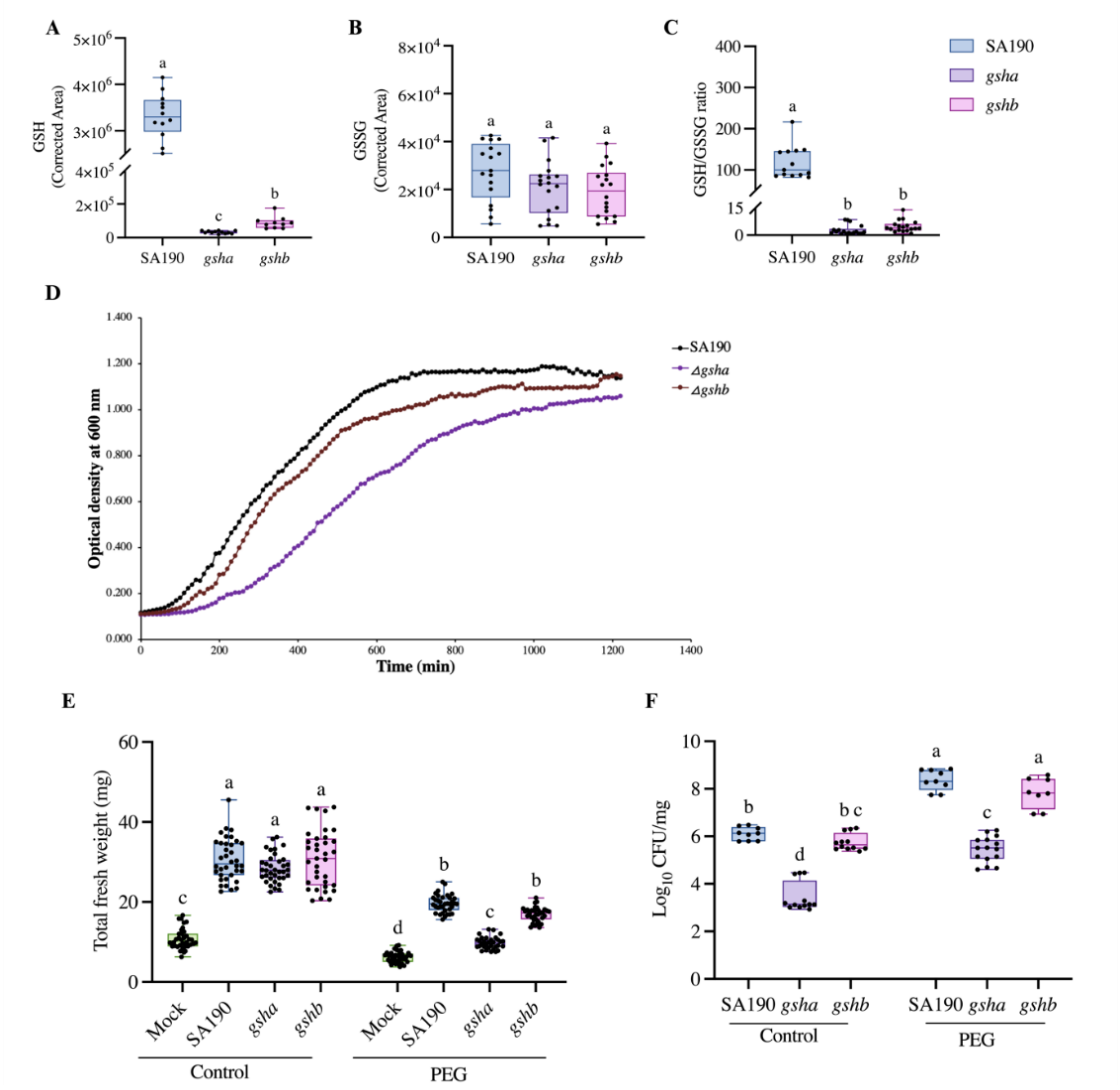



**Figure 5. Functional analysis of *Pseudomonas argentinensis* SA190 and glutathione deficient mutants.** Bacterial glutathione (GSH) levels in SA190 WT, Δ*gshA*, and Δ*gshB* mutants (A). Bacterial oxidized glutathione (GSSG) levels in SA190, Δ*gshA*, and Δ*gshB* (B). GSH/GSSG ratio in SA190 and the glutathione-deficient mutants (C). For panels A–C, six biological replicates were used. Different letters indicate statistical differences based on one way ANOVA ($p < 0.05$). Growth curves of SA190, Δ*gshA*, and Δ*gshB* in LB medium (D). Total fresh weight of *Arabidopsis thaliana* Col-0 plants inoculated with SA190, Δ*gshA*, or Δ*gshB*, or mock-inoculated, grown under control (non-stress) and 25% PEG-induced drought stress conditions (E). The plant assay was performed with three biological replicates and two technical replicates (n=36). Whiskers indicate minimum and maximum values, the horizontal line marks the median. Statistical differences were determined by two-way ANOVA ($p < 0.05$). Root colonization levels of SA190 and glutathione-deficient mutants. The boxplots show colony forming unit (CFU) data from three independent biological replicates, different letters indicate statistical differences based on two-way ANOVA ($p < 0.05$) (F).

bioRxiv preprint doi: https://doi.org/10.64898/2026.06.15.732246; this version posted June 15, 2026. The copyright holder for this preprint (which was not certified by peer review) is the author/funder, who has granted bioRxiv a license to display the preprint in perpetuity. It is made available under a CC-BY-NC-ND 4.0 International license.

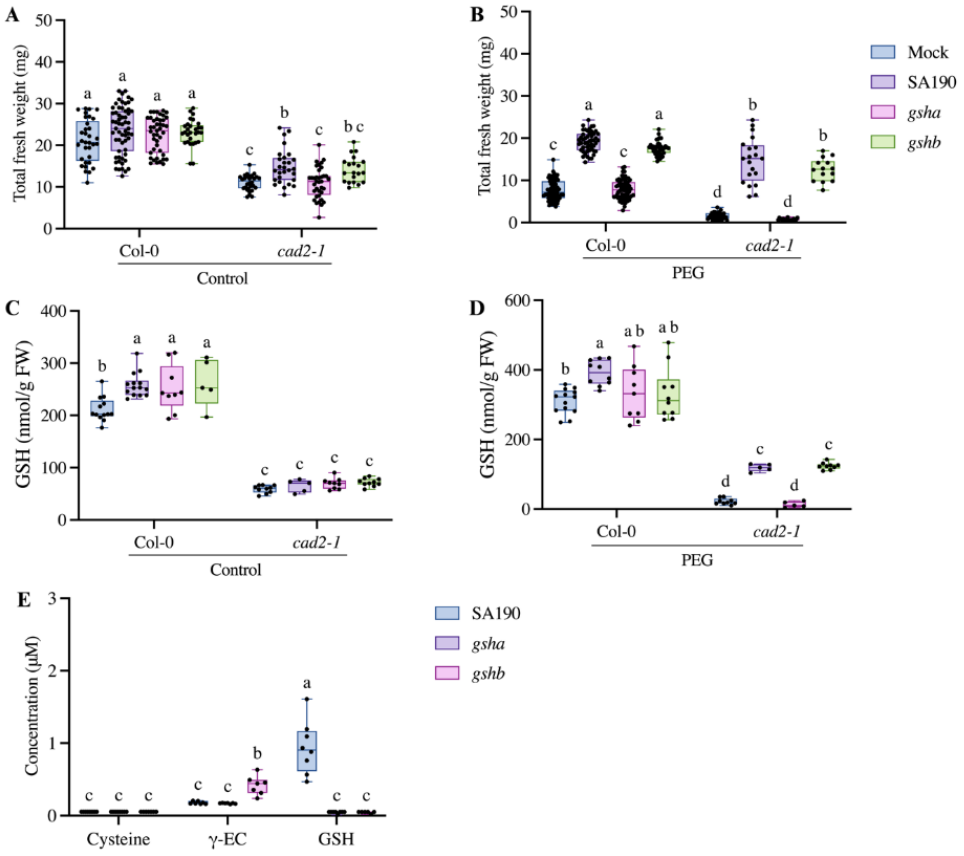



**Figure 6. Effects of *Pseudomonas argentinensis* SA190, Δ*gshA*, and Δ*gshB* on *cad2-1* biomass and GSH levels under control and 25% PEG-induced drought stress.** Total fresh weight of non-colonized plants, plants colonized with SA190, and plants colonized with Δ*gshA* or Δ*gshB* under control (A) and 25% PEG-induced drought stress (B). Plant assays were performed using three biological replicates with two technical replicates per treatment (n = 36). Boxplot whiskers represent minimum and maximum values, the horizontal line indicates the median. Different letters indicate statistically significant differences based on two-way ANOVA ($p < 0.05$). Glutathione (GSH) levels in shoot tissue under the same treatments in control (C) and 25% PEG-induced drought stress (D). Different letters indicate statistically significant differences based on two-way ANOVA ($p < 0.05$). Cysteine, γ-glutamylcysteine (γ-EC), and GSH levels in pellet of SA190 wild type, Δ*gshA*, and Δ*gshB* mutants grown in M9 medium (E). Seven biological replicates were analyzed. Different letters indicate statistically significant differences based on two-way ANOVA ($p < 0.05$).

## Discussion

This thesis aimed to identify key bacterial traits and mechanisms underlying the plant growth-promoting (PGP) activity of *Pseudomonas argentinensis* SA190. To achieve this, a transposon mutant library was constructed to elucidate the roles of key SA190 genes contributing to bacterial PGP activity. Since SA190 exerts its beneficial effects under drought stress, mutants were characterized under PEG-induced drought stress conditions. The mutant screen revealed that biofilm formation has a significant impact on SA190 colonization and its PGP activity under PEG-induced stress. As a final layer, we investigated how SA190 modulates the metabolism of *Arabidopsis thaliana* to exert its beneficial effects under PEG-induced drought stress, focusing particularly on sulfur metabolism.

### Plant growth-promoting traits of SA190

Global food demand is expected to increase substantially due to the growing world population (Duchenne-Moutien & Neetoo, 2021). This increasing demand creates pressure on agriculture, which is already challenged by climate change-induced stresses such as drought, heat waves, and flooding (Rizzo et al., 2021). These stresses reduce crop productivity and raise food security concerns (Tigchelaar et al., 2018; van Dijk et al., 2021). Although fertilizers are widely used to enhance yield under these conditions, their long-term application can lead to soil degradation and heavy metal accumulation (Wu et al., 2025). Therefore, sustainable alternatives, such as plant growth-promoting bacteria (PGPB), hold an indispensable place. PGPB solubilize phosphate, produce siderophores, indole-3-acetic acid (IAA), and 1-aminocyclopropane-1-carboxylate (ACC) deaminase, and modulate plant hormones (Lugtenberg & Kamilova, 2009; Orozco-Mosqueda et al., 2018). These traits contribute to improved plant growth and development by enhancing nutrient uptake (Lugtenberg & Kamilova, 2009).

Among PGPBs, the *Pseudomonas* genus is one of the dominant groups (Liang et al., 2024). Our model system, *Pseudomonas argentinensis* SA190, is capable of solubilizing phosphate and producing siderophores and IAA (Elkatmis, Parween, et al., 2025). While these traits indicate the functional potential of SA190 as a PGPB, they need to be evaluated in the context of plant interactions to determine their actual effects. Nevertheless, SA190's contribution to phosphate and iron uptake may support plant growth by enhancing physiological processes such as ATP production and photosynthesis. Previous studies on other PGPB have reported similar findings (Costa-Gutierrez et al., 2020; Goswami et al., 2013; Pieterse et al., 2021). For example, *Pseudomonas putida* KT2440 produces IAA, siderophores, and ACC deaminase, and

solubilizes phosphate (Costa-Gutierrez et al., 2020). It has also been reported to improve seed germination and root length in soybean and corn under salt stress (Costa-Gutierrez et al., 2020). Another well-described beneficial microbe, *Pseudomonas simiae* WCS417, possesses several PGP traits, such as siderophore production, VOC production, and biofilm formation (Pieterse et al., 2021). In addition, it has been shown to enhance plant tolerance to several stresses, including salt and drought stress (Pieterse et al., 2021). Also, *Pseudomonas spp*. olive green (OG) possesses PGP traits such as phosphate solubilization, IAA, siderophore, HCN, and catalase production (Goswami et al., 2013). In particular, inoculation with *Pseudomonas* spp. olive green (OG) has been reported to increase chickpea biomass (Goswami et al., 2013).

In addition to these traits, PGPB are also known to induce systemic resistance and enhance plant tolerance to abiotic stresses (Lugtenberg & Kamilova, 2009; Orozco-Mosqueda et al., 2018). SA190 demonstrated strong stress tolerance, surviving under high salt (up to 1 M NaCl) and osmotic stress conditions (10-20% PEG 8000) (Elkatmis, Parween, et al., 2025). However, the ability of SA190 to grow under these stress conditions does not necessarily translate into functional PGP effects. Therefore, the PGP effect of SA190 was further evaluated in a plant assay. SA190 inoculation significantly improved Arabidopsis growth under 25% PEG-induced drought stress (Alwutayd et al., 2023). PEG is commonly used to mimic drought stress under controlled conditions, as it creates a matrix on the agar surface that limits water availability to plant roots (Gonzalez et al., 2023). Therefore, it induces drought stress by reducing the osmotic potential and creating osmotic stress (Gonzalez et al., 2023). Taken together, these findings suggest that SA190 not only possesses key PGP traits but also maintains functional activity under PEG stress conditions. However, the ability of endophytic bacteria, including SA190, to exert these beneficial effects and confer stress tolerance depends on their successful colonization of the plant roots.

**Role of biofilm formation in SA190 root colonization and plant growth promotion**

Soil provides a dynamic environment for microbial activity, largely shaped by the region surrounding the root, known as the rhizosphere (Bardgett & Van Der Putten, 2014; Bulgarelli et al., 2013). This zone is continuously influenced by root-derived signals and exudates that recruit diverse microbial communities (Bardgett & Van Der Putten, 2014; Bulgarelli et al., 2013; Ma et al., 2022). Within these communities, the ability of bacteria to successfully attach to and colonize plant roots is a determinant of their capacity to influence plant growth and health (Knights et al., 2021). Several key microbial traits support and maintain this colonization process (Knights et al., 2021). Motility is one of these essential traits that allows PGPB to move

toward and respond to root exudates (Lucero et al., 2020). In this way, it facilitates effective root colonization and interaction with the host plant (Lucero et al., 2020; Yang et al., 2024). In addition to motility, biofilm formation enables stable attachment to the root surface (Bhattacharyya et al., 2023; Morcillo & Manzanera, 2021). This trait becomes particularly important under drought stress conditions, as it can create a protective microenvironment that enhances bacterial survival and persistence (Bhattacharyya et al., 2023; Karimi et al., 2022; Morcillo & Manzanera, 2021). Since SA190 is a root endophyte that enhances plant growth under PEG-induced drought stress, successful root colonization is a prerequisite for establishing a beneficial interaction with the host.

Focusing on microbial traits essential for the Arabidopsis-SA190 interaction, we constructed an SA190 transposon library and screened it for mutants in biofilm formation (Elkatmis, Parween, et al., 2025). This approach allowed us to identify candidate genes potentially involved in root colonization and the establishment of beneficial interactions. We found that *wspC*::Tn5, *rpoE*::Tn5, and *fliD*::Tn5 mutants exhibited reduced biofilm formation (Elkatmis, Parween, et al., 2025). Although disruption of these genes did not affect overall bacterial fitness, the mutants displayed significantly reduced root colonization under PEG-induced drought stress (Elkatmis, Parween, et al., 2025). These mutants also showed a diminished plant growth-promoting effect, suggesting a direct link between biofilm formation, efficient root colonization, and stress tolerance in Arabidopsis. These findings indicate that biofilm formation is not only critical for stable root colonization by endophytic SA190 but also enables SA190 to influence host physiology and exert beneficial effects. Reduced biofilm formation diminished SA190's ability to maintain close interaction with the host, thereby limiting colonization efficiency and plant growth-promoting effects.

We then applied a root surface sterilization step to remove epiphytic bacteria and to investigate the contribution of loosely and stably attached colonization to the PGP effect. This approach allowed us to link the effects of biofilm-related mutants to the stable colonization ability of SA190 and to evaluate the importance of attachment strength for its PGP activity. The reduction in colonization after this treatment suggests that these genes contribute to stable root attachment under PEG-induced drought stress conditions. Their disruption weakens bacterial adherence to the Arabidopsis root surface. This interpretation is supported by the functional roles of these genes. The *fliD* gene is associated with motility (Huang et al., 2019; Ratthawongjirakul et al., 2016), *rpoE* with stress response (Gao et al., 2016), and *wspC* with chemotaxis and biofilm

regulation (Li et al., 2024; O'Neal et al., 2022). Together, these functions highlight the need for coordinated regulation of movement and surface attachment for successful colonization. Consistent with our findings, a study in other PGPB reported a similar relationship between biofilm formation and colonization (Budiharjo et al., 2014). For example, in *Bacillus amyloliquefaciens* ssp. *plantarum* FZB42, disruption of the *degU* gene impaired biofilm formation and reduced bacterial colonization of lettuce roots (Budiharjo et al., 2014). Taken together, these results indicate that biofilm formation is a key microbial trait required for successful root colonization and SA190-mediated plant growth promotion under PEG-induced drought stress conditions.

Although our findings demonstrate the importance of bacterial traits for successful root colonization, colonization is not determined only by bacterial factors. Since colonization represents a bidirectional interaction between the host and the bacteria, host-derived factors can also play an important role in shaping bacterial colonization in the root. For example, a study on *Pseudomonas simiae* WCS417 showed that Arabidopsis mutants deficient in root defense barriers, including cutin, suberin, callose, and lignin deposition, showed altered bacterial root colonization and growth-promotion responses (Zhou et al., 2025). These findings suggest that successful root colonization depends on a complex interplay between host and bacterial factors.

In conclusion, in this thesis, we identified biofilm-related genes involved in SA190 root colonization and plant growth promotion under PEG-induced drought stress. However, further investigation of both bacterial and host factors is necessary to achieve a more comprehensive understanding of colonization and this beneficial interaction.

**Role of sulfur metabolism in SA190-mediated drought tolerance**

Despite the essential role of colonization and biofilm formation in SA190-mediated plant growth promotion, these factors alone cannot fully explain the increase in plant biomass under PEG stress. This suggests that SA190 may modulate metabolic and physiological processes in Arabidopsis, thereby contributing to the observed drought tolerance. In this context, we focused on sulfur metabolism, as sulfur metabolism contributes to plant stress tolerance through the production of several important molecules, including glutathione (GSH), hydrogen sulfide ($H_2S$), and PAP (3'-phosphoadenosine 5'-phosphate), a signaling molecule generated during sulfation reactions (Noctor et al., 2011, Kopriva, 2006; Liu et al., 2021; Gigolashvili et al., 2012; Estavillo et al., 2011). GSH functions as a critical antioxidant and redox buffer (Noctor et al., 2011, Kopriva, 2006). It protects cells from oxidative damage by detoxifying reactive

oxygen species and maintaining cellular redox homeostasis (Kopriva, 2006). $H_2S$ acts as a signaling molecule that affects stress tolerance by regulating antioxidant defenses, stomatal closure, and stress-responsive gene expression (Liu et al., 2021). On the other hand, PAP plays a role in retrograde signaling from the chloroplast to the nucleus and accumulates during drought stress (Estavillo et al., 2011; Gigolashvili et al., 2012). In this way, it inhibits exoribonucleases to modulate the expression of stress-responsive genes (Estavillo et al., 2011; Gigolashvili et al., 2012). Consequently, mutants in SAL1 phosphatase accumulate PAP and show incresed tolerance to drought stress (Estavillo et al., 2011). Together, these molecules highlight the role of sulfur metabolism in coordinating antioxidant defense, cellular signaling, and stress adaptation.

We, therefore, investigated sulfur metabolism mutants and found that *sultr1;2*, *apr2*, and *cad2-1* exhibit reduced biomass under PEG-induced drought stress. The increased drought sensitivity of these mutants highlights the critical role of sulfur metabolism in plant adaptation to drought stress. The sulfate transporter mutant *sultr1;2* exhibited significantly reduced biomass under PEG-induced drought stress. This finding is consistent with its established role in high-affinity sulfate uptake from the rhizosphere (Vidmar et al., 2000). Impaired sulfate uptake in *sultr1;2* restricts sulfur availability for downstream metabolic processes (Shibagaki et al., 2002; Vidmar et al., 2000), thereby limiting the synthesis of sulfur-containing compounds required for stress adaptation. Similarly, the *apr2* mutant, defective in APS reductase activity (Weber et al., 2000), showed growth inhibition under PEG stress conditions. This finding suggests that sulfate reduction may contribute to plant stress tolerance by supporting the production of downstream sulfur-containing compounds such as cysteine and glutathione under PEG stress conditions. Notably, the *cad2-1* mutant, carrying a loss-of-function allele of the γ-glutamylcysteine synthetase gene (*GSH1*) (Cobbett et al., 1998), displayed severe growth reduction under PEG stress. This phenotype is consistent with the central role of GSH in plant stress tolerance, as mentioned above. Therefore, reduced GSH biosynthesis in *cad2-1* likely compromises the plant's ability to cope with PEG-induced oxidative stress, resulting in increased sensitivity to PEG treatment.

Collectively, the enhanced drought sensitivity observed in *sultr1;2, apr2*, and *cad2-1* indicates that an intact sulfur metabolic pathway, from sulfate uptake and assimilation to glutathione biosynthesis, is essential for maintaining growth and stress resilience under PEG-induced drought stress conditions. These findings are consistent with previous studies linking sulfur

nutrition and glutathione metabolism to abiotic stress tolerance (Andrés-Barrao et al., 2021; Mukherjee et al., 2025; Shekhawat et al., 2024) and further support a central role for sulfur metabolism in PEG-induced drought stress adaptation in *Arabidopsis thaliana*.

Treatment with SA190 rescued the phenotype and enhanced the biomass of these mutants under PEG stress. These findings suggest that SA190 positively influences sulfur metabolism and/or downstream antioxidant pathways in the host plant. Supporting this result, SA190 treatment led to increased GSH levels and an elevated GSH/GSSG ratio under PEG stress, indicating improved redox balance. Chemical inhibition of GSH synthesis using BSO and genetic impairment in the *cad2-1* mutant reduced GSH levels in Arabidopsis, whereas SA190 treatment enhanced GSH accumulation under PEG stress conditions. These findings suggest that SA190 contributes to maintaining cellular homeostasis by promoting GSH biosynthesis or regeneration. In addition, these results are consistent with increased sulfate accumulation in shoots under PEG stress. This observation suggests that SA190 may enhance host sulfur assimilation and redirect metabolic flux toward GSH biosynthesis, thereby contributing to improved antioxidant capacity and stress tolerance. In this way, SA190 may improve ROS detoxification capacity under PEG stress. Consistent with these observations, beneficial microbes have been shown to regulate sulfur metabolism and antioxidant responses in plants under abiotic stress (Azeem et al., 2025; Koźmińska et al., 2024). For example, sulfur-oxidizing bacteria (SOB), such as *Halothiobacillus halophilus*, enhance sulfur accumulation in *Plantago coronopus* under drought and high salinity (300 mM NaCl) (Koźmińska et al., 2024). SOB treatment also increased GSH levels under salt stress, suggesting that microbe-mediated sulfur metabolism can contribute to improved redox homeostasis (Koźmińska et al., 2024). Another study showed that inoculation with *Pseudomonas* strains (*P. monteilii* SHA_AHK, *P. aeruginosa* PS3, *P. aeruginosa* SAHK, *P. putida* AHK_SHA007) increased GSH accumulation in sorghum under salt stress, further supporting the role of beneficial microbes in strengthening the plant antioxidant machinery (Azeem et al., 2025). Together, our findings support the idea that SA190-mediated enhancement of drought tolerance may involve modulation of sulfur metabolism and GSH-dependent redox regulation.

As shown in our model and supported by examples in the literature, PGPB can modulate sulfur metabolism and GSH levels in plants under stress conditions. To dissect the contribution of bacterial GSH metabolism to the Arabidopsis-SA190 interaction, we generated bacterial knockout mutants in *gshA* and *gshB*. Similar to Arabidopsis, SA190 possesses a two-step GSH

biosynthesis pathway. The first step is the production of γ-glutamylcysteine (γ-EC), the rate-limiting step, catalyzed by γ-glutamylcysteine synthetase (γ-ECS), encoded by *gshA* (Forman et al., 2009). The second step is the conversion of γ-EC to GSH, catalyzed by glutathione synthetase (GS), encoded by *gshB* (Forman et al., 2009). When these mutants were tested in the *cad2-1* plant mutant under PEG-induced drought stress, treatment with the *gshA* mutant resulted in reduced biomass and lower GSH levels compared to wild-type SA190. In contrast, the *gshB* mutant showed biomass and GSH levels comparable to SA190 under PEG stress. These results suggest that the intermediate molecule γ-EC may play an important role in drought stress tolerance. The observed increase in GSH levels in *cad2-1* plants treated with the *gshB* mutant may be explained by the supply of γ-EC from the bacteria. Since the second step of GSH biosynthesis remains functional in *cad2-1*, the plant can convert γ-EC into GSH. Accordingly, *gshB* treatment in *cad2-1* result in GSH levels comparable to those observed with SA190 treatment. These findings underscore the functional importance of the *gshA* gene in the plant growth-promoting effect of SA190. The importance of the *gshA* gene is also highlighted in another study (Mukherjee et al., 2025). In that study, the generation of a *gshA* mutant from *Pseudomonas* sp. 6A2 reduced biomass under sulfur-deficient conditions (Mukherjee et al., 2025). These findings also support that sulfur metabolism, particularly GSH, is a key component of plant-microbe interactions (Mukherjee et al., 2025).

Taken together, our findings in this thesis highlight that SA190 employs multi-layered mechanisms to exert its PGP activity. First, phosphate solubilization, IAA and siderophore production, and the stress tolerance of SA190 contribute to its PGP activity. Second, transposon library screening and analysis of biofilm mutants under PEG stress revealed that biofilm formation is essential for SA190 colonization and its ability to exert beneficial effects under PEG stress. Finally, we investigated how SA190 influences host metabolism and physiology to enhance PEG stress tolerance. Our results indicate that SA190 may modulate host sulfur metabolism, leading to enhanced GSH-mediated redox homeostasis under PEG stress. These findings highlight the importance of integrating microbial traits with host metabolic pathways to fully understand plant-microbe interactions under stress conditions.

**Limitations and future directions**

This thesis highlights the multilayered mechanisms underlying the PGP activity of *Pseudomonas argentinensis* SA190, including transposon library construction, biofilm formation analysis, and the investigation of sulfur metabolism during plant-microbe interactions under PEG-induced drought stress. Although these findings provide important

insights into the beneficial interaction between SA190 and *Arabidopsis thaliana*, several limitations remain and provide important directions for future research.

***Experimental limitations and ecological relevance***

This study was primarily conducted using a PEG-based agar plate system. PEG-induced osmotic stress is widely used to mimic drought conditions because it reduces water availability to plant roots under controlled experimental conditions (Gonzalez et al., 2023). The PEG plate system offers several advantages, including easy monitoring of root architecture, precise control of water availability, and high reproducibility between experiments. However, PEG-based plate systems cannot fully reproduce the complexity of soil drought conditions. Therefore, this represents a major limitation of the present study. To determine whether our findings are consistent under soil conditions, future studies should validate these results in soil-based drought experiments to better assess the ecological relevance of SA190-mediated drought tolerance. In addition, validating SA190-mediated drought tolerance in crop plants under soil-based conditions could also provide essential data bridging the gap between controlled laboratory findings and real-world agricultural applications. These data could represent a key step toward establishing SA190 as a potential bioinoculant for sustainable crop protection under drought stress.

***Unresolved mechanisms of sulfur metabolism in the Arabidopsis-SA190 interaction***

One of the main findings of this thesis is that sulfur metabolism is one of the components of the beneficial interaction between Arabidopsis and SA190. Mutant analyses and metabolite measurements suggest that GSH or γ-EC contributes to SA190-mediated PEG stress protection. However, the precise mechanism by which GSH and/or γ-EC contribute to PEG stress protection remains unresolved.

SA190 is an endophytic bacterium that colonizes internal root tissues, which makes it technically difficult to monitor the direct supply of sulfur-containing compounds to plant tissues. This technical challenge is the second main limitation of this project. Although our physiological and genetic data strongly suggest the involvement of bacterial sulfur metabolism in enhancing plant stress tolerance, direct molecular evidence for GSH or γ-EC transfer is still lacking.

Future work should focus on isotope-labeling approaches, such as feeding SA190 with stable isotope-labeled sulfur or labeled γ-EC/GSH precursors. Feeding experiments using isotope-

labeled sulfate, cysteine, γ-EC, or GSH could provide insights into which sulfur-containing molecules are transferred from SA190 to the plant. Therefore, combining isotope labeling with genetic analyses and targeted metabolite measurements may help elucidate the role of sulfur-containing compounds during the Arabidopsis-SA190 interaction.

***Sulfur flux analysis and future perspectives***

In this thesis, we quantified thiol and sulfate contents in samples treated with SA190. However, these measurements represent only snapshots of metabolite pools at specific time points. Therefore, they do not provide information about sulfur flux, and it remains unclear whether SA190 affects sulfur redistribution between roots and shoots. Future studies should employ isotope-labeling approaches to quantify sulfur flux and trace the incorporation of sulfur into cysteine, GSH, and other sulfur-containing metabolites in roots and shoots. These experiments could provide a deeper understanding of how SA190 reshapes host sulfur metabolism to enhance PEG-induced drought stress tolerance.

***Future directions for biofilm and colonization studies***

Another important finding of this thesis was the identification of genes contributing to biofilm formation and root colonization in SA190. Characterization of the Tn5 transposon mutants revealed that stable root attachment is critical for the beneficial effects of SA190. Through plant assays under PEG-induced drought stress, we demonstrated that *wspC*, *rpoE*, and *fliD* are important for SA190-mediated drought stress tolerance (Elkatmis, Parween, et al., 2025). However, the molecular mechanisms underlying the contribution of these genes to plant growth promotion and stress tolerance remain unclear. Future studies should investigate how these biofilm-related genes affect bacterial persistence, nutrient exchange, and signaling processes at the root-microbe interface. Comparative transcriptomic and metabolomic analyses of plants colonized by SA190 and these biofilm mutants could help identify the bacterial pathways required for efficient root attachment and beneficial plant-microbe interactions.

***Conclusion***

Overall, this thesis provides a framework for understanding how microbial colonization traits and sulfur-mediated redox regulation contribute to plant stress resilience. Future studies integrating soil and isotope-labeling experiments will further advance our understanding of the mechanistic basis of beneficial plant-microbe interactions under abiotic stress conditions.

## References


Albanesi, D., Mansilla, M. C., Schujman, G. E., & de Mendoza, D. (2005). Bacillus subtilis cysteine synthetase is a global regulator of the expression of genes involved in sulfur assimilation. *Journal of Bacteriology*, *187*(22), 7631–7638. https://doi.org/10.1128/JB.187.22.7631-7638.2005

Ali, S., Tahir, S., Hassan, S. S., Lu, M., Wang, X., Quyen, L. T. Q., Zhang, W., & Chen, S. (2025). The Role of Phytohormones in Mediating Drought Stress Responses in Populus Species. *International Journal of Molecular Sciences*, *26*(8). https://doi.org/10.3390/ijms26083884

Alwutayd, K. M., Rawat, A. A., Sheikh, A. H., Almeida-Trapp, M., Veluchamy, A., Jalal, R., Karampelias, M., Froehlich, K., Alzaed, W., Tabassum, N., Schley, T. R., Schäffner, A. R., Daur, I., Saad, M. M., & Hirt, H. (2023). Microbe-induced drought tolerance by ABA-mediated root architecture and epigenetic reprogramming. *EMBO Reports*, *24*(8), e56754. https://doi.org/10.15252/embr.202256754

Andrés-Barrao, C., Alzubaidy, H., Jalal, R., Mariappan, K. G., de Zélicourt, A., Bokhari, A., Artyukh, O., Alwutayd, K., Rawat, A., Shekhawat, K., Almeida-Trapp, M., Saad, M. M., & Hirt, H. (2021). Coordinated bacterial and plant sulfur metabolism in Enterobacter sp. SA187-induced plant salt stress tolerance. *Proceedings of the National Academy of Sciences of the United States of America*, *118*(46). https://doi.org/10.1073/pnas.2107417118

Aroca, R., Porcel, R., & Ruiz-Lozano, J. M. (2012). Regulation of root water uptake under abiotic stress conditions. In *Journal of Experimental Botany* (Vol. 63, Number 1, pp. 43–57). https://doi.org/10.1093/jxb/err266

Azeem, M., Sultana, R., Ahmed, N., Abbasi, M. W., Hasan, K. A., Dong, R., Alamri, S., & Alfagham, A. T. (2025). Salinity Stress Resilience in Sorghum bicolor through Pseudomonas-Mediated Modulation of Growth, Antioxidant System, and Eco-Physiological Adaptations. *ACS Omega*, *10*(1), 940–954. https://doi.org/10.1021/acsomega.4c08110

Bali, A. S. (2025). Integrating ROS and plant hormone signaling in response to abiotic stress. *Discover Plants*, *2*(1). https://doi.org/10.1007/s44372-025-00440-9

Bardgett, R. D., & Van Der Putten, W. H. (2014). Belowground biodiversity and ecosystem functioning. In *Nature* (Vol. 515, Number 7528, pp. 505–511). Nature Publishing Group. https://doi.org/10.1038/nature13855

Batool, T., Ali, S., Seleiman, M. F., Naveed, N. H., Ali, A., Ahmed, K., Abid, M., Rizwan, M., Shahid, M. R., Alotaibi, M., Al-Ashkar, I., & Mubushar, M. (2020). Plant growth promoting rhizobacteria alleviates drought stress in potato in response to suppressive oxidative stress and antioxidant enzymes activities. *Scientific Reports*, *10*(1), 16975. https://doi.org/10.1038/s41598-020-73489-z

Bhattacharyya, A., Mavrodi, O., Bhowmik, N., Weller, D., Thomashow, L., & Mavrodi, D. (2023). Bacterial biofilms as an essential component of rhizosphere plant-microbe

interactions. *Methods in Microbiology*, *53*, 3–48. https://doi.org/10.1016/bs.mim.2023.05.006

Bose Mazumdar, A., & Chattopadhyay, S. (2025). Glutathione Pathways and Gene Networks: Central Players in Crop Adaptation to Environmental Stresses. In *Plant Growth Regulation* (Vol. 105, Number 6, pp. 1927–1948). Springer Science and Business Media B.V. https://doi.org/10.1007/s10725-025-01375-7

Budiharjo, A., Chowdhury, S. P., Dietel, K., Beator, B., Dolgova, O., Fan, B., Bleiss, W., Ziegler, J., Schmid, M., Hartmann, A., & Borriss, R. (2014). Transposon mutagenesis of the plant-associated Bacillus amyloliquefaciens ssp. plantarum FZB42 revealed that the nfrA and RBAM17410 genes are involved in plant-microbe-interactions. *PloS One*, *9*(5), e98267. https://doi.org/10.1371/journal.pone.0098267

Bulgarelli, D., Schlaeppi, K., Spaepen, S., Van Themaat, E. V. L., & Schulze-Lefert, P. (2013). Structure and functions of the bacterial microbiota of plants. In *Annual Review of Plant Biology* (Vol. 64, pp. 807–838). https://doi.org/10.1146/annurev-arplant-050312-120106

Carbonero, F., Benefiel, A. C., Alizadeh-Ghamsari, A. H., & Gaskins, H. R. (2012). Microbial pathways in colonic sulfur metabolism and links with health and disease. *Frontiers in Physiology*, *3*, 448. https://doi.org/10.3389/fphys.2012.00448

Chaudhary, S., Sindhu, S. S., Dhanker, R., & Kumari, A. (2023). Microbes-mediated sulphur cycling in soil: Impact on soil fertility, crop production and environmental sustainability. In *Microbiological Research* (Vol. 271). Elsevier GmbH. https://doi.org/10.1016/j.micres.2023.127340

Chen, Z., Yang, G., Hao, X., Samak, N. A., Jia, Y., Peh, S., Mu, T., Yang, M., & Xing, J. (2021). Recent advances in microbial capture of hydrogen sulfide from sour gas via sulfur-oxidizing bacteria. *Engineering in Life Sciences*, *21*(10), 693–708. https://doi.org/10.1002/elsc.202100006

Chew, O., Whelan, J., & Millar, A. H. (2003). Molecular Definition of the Ascorbate-Glutathione Cycle in Arabidopsis Mitochondria Reveals Dual Targeting of Antioxidant Defenses in Plants. *Journal of Biological Chemistry*, *278*(47), 46869–46877. https://doi.org/10.1074/JBC.M307525200

Chieb, M., & Gachomo, E. W. (2023). The role of plant growth promoting rhizobacteria in plant drought stress responses. *BMC Plant Biology*, *23*(1), 407. https://doi.org/10.1186/s12870-023-04403-8

Cobbett, C. S., May, M. J., Howden, R., & Rolls, B. (1998). The glutathione-deficient, cadmium-sensitive mutant, cad2-1, of Arabidopsis thaliana is deficient in gamma-glutamylcysteine synthetase. *The Plant Journal : For Cell and Molecular Biology*, *16*(1), 73–78. https://doi.org/10.1046/j.1365-313x.1998.00262.x

Cohen, A. C., Travaglia, C. N., Bottini, R., & Piccoli, P. N. (2009). Participation of abscisic acid and gibberellins produced by endophytic Azospirillum in the alleviation of drought effects in maize. *Botany*, *87*(5), 455–462. https://doi.org/10.1139/B09-023

Costa-Gutierrez, S. B., Lami, M. J., Santo, M. C. C.-D., Zenoff, A. M., Vincent, P. A., Molina-Henares, M. A., Espinosa-Urgel, M., & de Cristóbal, R. E. (2020). Plant growth promotion

by Pseudomonas putida KT2440 under saline stress: role of eptA. *Applied Microbiology and Biotechnology*, *104*(10), 4577–4592. https://doi.org/10.1007/s00253-020-10516-z

de Zelicourt, A., Al-Yousif, M., & Hirt, H. (2013). Rhizosphere microbes as essential partners for plant stress tolerance. *Molecular Plant*, *6*(2), 242–245. https://doi.org/10.1093/mp/sst028

Dietz, K. J., Zörb, C., & Geilfus, C. M. (2021). Drought and crop yield. In *Plant Biology* (Vol. 23, Number 6, pp. 881–893). John Wiley and Sons Inc. https://doi.org/10.1111/plb.13304

Duchenne-Moutien, R. A., & Neetoo, H. (2021). Climate change and emerging food safety issues: A review. In *Journal of Food Protection* (Vol. 84, Number 11, pp. 1884–1897). International Association for Food Protection. https://doi.org/10.4315/JFP-21-141

Elkatmis, B., Alkhateeb, R. S., Mannes, C., Jalal, R., Trapp, M., Westhoff, P., Ozkan, C., Thelen, G. M., Han, B., Saad, M. M., Kopriva, S., & Hirt, H. (2026). *Root endophyte sulfur metabolites enhance redox balance and drought tolerance in Arabidopsis*. https://doi.org/10.64898/2026.06.15.732246

Elkatmis, B., Han, B., Parween, S., Kopriva, S., Hirt, H., & Saad, M. M. (2025). Comprehensive Mapping of EZ-Tn5 Transposon Insertion Sites in Pseudomonas argentinensis SA190 Using RATE-PCR. *Bio-Protocol*, *15*(14), e5389. https://doi.org/10.21769/BioProtoc.5389

Elkatmis, B., Parween, S., Eida, A. A., Jalal, R., Lafi, F., Alam, I., Kopriva, S., Hirt, H., & Saad, M. M. (2025). Integrated genomic and mutagenesis analysis of Pseudomonas argentinensis SA190 reveals mechanisms of plant root colonization and stress resilience. *BMC Microbiology*, *25*(1), 785. https://doi.org/10.1186/s12866-025-04495-2

Estavillo, G. M., Crisp, P. A., Pornsiriwong, W., Wirtz, M., Collinge, D., Carrie, C., Giraud, E., Whelan, J., David, P., Javot, H., Brearley, C., Hell, R., Marin, E., & Pogson, B. J. (2011). Evidence for a SAL1-PAP chloroplast retrograde pathway that functions in drought and high light signaling in Arabidopsis. *The Plant Cell*, *23*(11), 3992–4012. https://doi.org/10.1105/tpc.111.091033

Eswaran, S. U. D., Sundaram, L., Perveen, K., Bukhari, N. A., & Sayyed, R. Z. (2024). Osmolyte-producing microbial biostimulants regulate the growth of Arachis hypogaea L. under drought stress. *BMC Microbiology*, *24*(1). https://doi.org/10.1186/s12866-024-03320-6

Fang, Y., & Xiong, L. (2015). General mechanisms of drought response and their application in drought resistance improvement in plants. *Cellular and Molecular Life Sciences : CMLS*, *72*(4), 673–689. https://doi.org/10.1007/s00018-014-1767-0

Fidler, J., Graska, J., Gietler, M., Nykiel, M., Prabucka, B., Rybarczyk-Płońska, A., Muszyńska, E., Morkunas, I., & Labudda, M. (2022). PYR/PYL/RCAR Receptors Play a Vital Role in the Abscisic-Acid-Dependent Responses of Plants to External or Internal Stimuli. *Cells*, *11*(8). https://doi.org/10.3390/cells11081352

Forman, H. J., Zhang, H., & Rinna, A. (2009). Glutathione: overview of its protective roles, measurement, and biosynthesis. *Molecular Aspects of Medicine*, *30*(1–2), 1–12. https://doi.org/10.1016/j.mam.2008.08.006

Gahan, J., & Schmalenberger, A. (2014). The role of bacteria and mycorrhiza in plant sulfur supply. *Frontiers in Plant Science*, *5*(DEC). https://doi.org/10.3389/fpls.2014.00723

Gao, S., Wu, H., Yu, X., Qian, L., & Gao, X. (2016). Swarming motility plays the major role in migration during tomato root colonization by Bacillus subtilis SWR01. *Biological Control*, *98*, 11–17. https://doi.org/10.1016/j.biocontrol.2016.03.011

García, J. E., Maroniche, G., Creus, C., Suárez-Rodríguez, R., Ramirez-Trujillo, J. A., & Groppa, M. D. (2017). In vitro PGPR properties and osmotic tolerance of different Azospirillum native strains and their effects on growth of maize under drought stress. *Microbiological Research*, *202*, 21–29. https://doi.org/10.1016/j.micres.2017.04.007

Ghosh, D., Sen, S., & Mohapatra, S. (2017). Modulation of proline metabolic gene expression in Arabidopsis thaliana under water-stressed conditions by a drought-mitigating Pseudomonas putida strain. *Annals of Microbiology*, *67*(10), 655–668. https://doi.org/10.1007/s13213-017-1294-y

Gigolashvili, T., Geier, M., Ashykhmina, N., Frerigmann, H., Wulfert, S., Krueger, S., Mugford, S. G., Kopriva, S., Haferkamp, I., & Flügge, U.-I. (2012). The Arabidopsis thylakoid ADP/ATP carrier TAAC has an additional role in supplying plastidic phosphoadenosine 5'-phosphosulfate to the cytosol. *The Plant Cell*, *24*(10), 4187–4204. https://doi.org/10.1105/tpc.112.101964

Gigolashvili, T., & Kopriva, S. (2014). Transporters in plant sulfur metabolism. *Frontiers in Plant Science*, *5*, 442. https://doi.org/10.3389/fpls.2014.00442

Gill, S. S., & Tuteja, N. (2010). Reactive oxygen species and antioxidant machinery in abiotic stress tolerance in crop plants. *Plant Physiology and Biochemistry : PPB*, *48*(12), 909–930. https://doi.org/10.1016/j.plaphy.2010.08.016

Glick, B. R. (2012). Plant growth-promoting bacteria: mechanisms and applications. *Scientifica*, *2012*, 963401. https://doi.org/10.6064/2012/963401

Glick, B. R. (2014). Bacteria with ACC deaminase can promote plant growth and help to feed the world. *Microbiological Research*, *169*(1), 30–39. https://doi.org/10.1016/j.micres.2013.09.009

Gonzalez, S., Swift, J., Xu, J., Illouz-Eliaz, N., Nery, J. R., & Ecker, J. R. (2023). *Mimicking genuine drought responses using a high throughput plate assay*. https://doi.org/10.7554/eLife.84747.1

Goswami, D., Vaghela, H., Parmar, S., Dhandhukia, P., & Thakker, J. N. (2013). Plant growth promoting potentials of Pseudomonas spp. strain OG isolated from marine water. *Journal of Plant Interactions*, *8*(4), 281–290. https://doi.org/10.1080/17429145.2013.768360

Gupta, A., Mishra, R., Rai, S., Bano, A., Pathak, N., Fujita, M., Kumar, M., & Hasanuzzaman, M. (2022). Mechanistic Insights of Plant Growth Promoting Bacteria Mediated Drought and Salt Stress Tolerance in Plants for Sustainable Agriculture. *International Journal of Molecular Sciences*, *23*(7). https://doi.org/10.3390/ijms23073741

Haghpanah, M., Hashemipetroudi, S., Arzani, A., & Araniti, F. (2024). Drought Tolerance in Plants: Physiological and Molecular Responses. *Plants (Basel, Switzerland)*, *13*(21). https://doi.org/10.3390/plants13212962

Hasanuzzaman, M., Bhuyan, M. H. M. B., Zulfiqar, F., Raza, A., Mohsin, S. M., Mahmud, J. Al, Fujita, M., & Fotopoulos, V. (2020). Reactive Oxygen Species and Antioxidant Defense in Plants under Abiotic Stress: Revisiting the Crucial Role of a Universal Defense Regulator. *Antioxidants (Basel, Switzerland)*, *9*(8). https://doi.org/10.3390/antiox9080681

Hasanuzzaman, M., Nahar, K., Anee, T. I., & Fujita, M. (2017). Glutathione in plants: biosynthesis and physiological role in environmental stress tolerance. *Physiology and Molecular Biology of Plants : An International Journal of Functional Plant Biology*, *23*(2), 249–268. https://doi.org/10.1007/s12298-017-0422-2

Hewedy, O. A., Ali, M. G., El-Meihy, R. M., Teiba, I. I., Santos-Villalobos, S. de los, Rastogi, A., Wu, H., Hajiyev, A. M., Zadneprovskaya, E. V., Pashkovskiy, P., Kumar, R., Elsheery, N. I., & Allakhverdiev, S. I. (2026). The dual role of ethylene in plant growth and abiotic stress: Mechanisms, regulation, and mitigation through ACC deaminase. *Plant Science*, *362*, 112858. https://doi.org/10.1016/J.PLANTSCI.2025.112858

Huang, Z., Pan, X., Xu, N., & Guo, M. (2019). Bacterial chemotaxis coupling protein: Structure, function and diversity. In *Microbiological Research* (Vol. 219, pp. 40–48). Elsevier GmbH. https://doi.org/10.1016/j.micres.2018.11.001

Imran, M., Mpovo, C. L., Aaqil Khan, M., Shaffique, S., Ninson, D., Bilal, S., Khan, M., Kwon, E.-H., Kang, S.-M., Yun, B.-W., & Lee, I.-J. (2023). Synergistic Effect of Melatonin and Lysinibacillus fusiformis L. (PLT16) to Mitigate Drought Stress via Regulation of Hormonal, Antioxidants System, and Physio-Molecular Responses in Soybean Plants. *International Journal of Molecular Sciences*, *24*(10). https://doi.org/10.3390/ijms24108489

Jakubowska, Z., Gradowski, M., & Dobrzyński, J. (2025). Role of plant growth-promoting bacteria (PGPB) in enhancing phenolic compounds biosynthesis and its relevance to abiotic stress tolerance in plants: a review. *Antonie van Leeuwenhoek*, *118*(9), 123. https://doi.org/10.1007/s10482-025-02130-8

Jarin, A., Ghosh, U. K., Hossain, Md. S., Mahmud, A., & Khan, Md. A. R. (2024). Glycine betaine in plant responses and tolerance to abiotic stresses. *Discover Agriculture*, *2*(1). https://doi.org/10.1007/s44279-024-00152-w

Javot, H., & Maurel, C. (2002). The role of aquaporins in root water uptake. *Annals of Botany*, *90*(3), 301–313. https://doi.org/10.1093/aob/mcf199

Jiang, H., Zeng, Y.-Y., Liu, X.-D., Corpas, F. J., Hasan, M. M., Li, F.-P., Tian, X.-Q., Zhang, Y.-H., He, R.-Y., & Fang, X.-W. (2026). Rooting for survival: ABA-mediated hormonal integration driving primary root elongation under drought stress. *Journal Of Plant Ecology*, *19*(2). https://doi.org/10.1093/jpe/rtaf172

Karimi, E., Aliasgharzad, N., Esfandiari, E., Hassanpouraghdam, M. B., Neu, T. R., Buscot, F., Reitz, T., Breitkreuz, C., & Tarkka, M. T. (2022). Biofilm forming rhizobacteria affect the physiological and biochemical responses of wheat to drought. *AMB Express*, *12*(1). https://doi.org/10.1186/s13568-022-01432-8

Kertesz, M. A. (2000). Riding the sulfur cycle--metabolism of sulfonates and sulfate esters in gram-negative bacteria. *FEMS Microbiology Reviews*, *24*(2), 135–175. https://doi.org/10.1016/S0168-6445(99)00033-9

Khan, N. (2025). Molecular Insights into ABA-Mediated Regulation of Stress Tolerance and Development in Plants. *International Journal of Molecular Sciences*, *26*(16). https://doi.org/10.3390/ijms26167872

Kim, Y.-T., Kwon, J.-G., O'Sullivan, D. J., & Lee, J.-H. (2024). Regulatory mechanism of cysteine-dependent methionine biosynthesis in Bifidobacterium longum: insights into sulfur metabolism in gut microbiota. *Gut Microbes*, *16*(1), 2419565. https://doi.org/10.1080/19490976.2024.2419565

Knights, H. E., Jorrin, B., Haskett, T. L., & Poole, P. S. (2021). Deciphering bacterial mechanisms of root colonization. In *Environmental Microbiology Reports* (Vol. 13, Number 4, pp. 428–444). John Wiley and Sons Inc. https://doi.org/10.1111/1758-2229.12934

Kooyers, N. J. (2015). The evolution of drought escape and avoidance in natural herbaceous populations. *Plant Science*, *234*, 155–162. https://doi.org/10.1016/J.PLANTSCI.2015.02.012

Kopriva, S. (2006). Regulation of sulfate assimilation in Arabidopsis and beyond. *Annals of Botany*, *97*(4), 479–495. https://doi.org/10.1093/aob/mcl006

Kopriva, S., Malagoli, M., & Takahashi, H. (2019). Sulfur nutrition: Impacts on plant development, metabolism, and stress responses. *Journal of Experimental Botany*, *70*(16), 4069–4073. https://doi.org/10.1093/jxb/erz319

Kopriva, S., Mugford, S. G., Baraniecka, P., Lee, B.-R., Matthewman, C. A., & Koprivova, A. (2012). Control of sulfur partitioning between primary and secondary metabolism in Arabidopsis. *Frontiers in Plant Science*, *3*, 163. https://doi.org/10.3389/fpls.2012.00163

Koprivova, A., & Kopriva, S. (2016). Sulfation pathways in plants. *Chemico-Biological Interactions*, *259*(Pt A), 23–30. https://doi.org/10.1016/j.cbi.2016.05.021

Kováč, J., Vítězová, M., & Kushkevych, I. (2018). Metabolic Activity of Sulfate-Reducing Bacteria from Rodents with Colitis. *Open Medicine (Warsaw, Poland)*, *13*, 344–349. https://doi.org/10.1515/med-2018-0052

Koźmińska, A., Hassan, M. Al, Halecki, W., Kruszyna, C., & Hanus-Fajerska, E. (2024). Beneficial Microorganisms: Sulfur-Oxidizing Bacteria Modulate Salt and Drought Stress Responses in the Halophyte Plantago coronopus L. *Sustainability (Switzerland)*, *16*(24). https://doi.org/10.3390/su162410866

Kumar, U., Panneerselvam, P., Gupta, V. V. S. R., Manjunath, M., Priyadarshinee, P., Sahoo, A., Dash, S. R., Kaviraj, M., & Annapurna, K. (2018). Diversity of Sulfur-Oxidizing and Sulfur-Reducing Microbes in Diverse Ecosystems. In *Microorganisms for Sustainability* (Vol. 3, pp. 65–89). Springer. https://doi.org/10.1007/978-981-10-6178-3_4

Kushkevych, I., Cejnar, J., Treml, J., Dordević, D., Kollar, P., & Vítězová, M. (2020). Recent Advances in Metabolic Pathways of Sulfate Reduction in Intestinal Bacteria. *Cells*, *9*(3). https://doi.org/10.3390/cells9030698

Lafi, F. F., Alam, I., Geurts, R., Bisseling, T., Bajic, V. B., Hirt, H., & Saad, M. M. (2016). Draft genome sequence of the phosphate-solubilizing bacterium Pseudomonas

argentinensis strain SA190 isolated from the desert plant Indigofera argentea. *Genome Announcements*, *4*(6). https://doi.org/10.1128/genomeA.01431-16

Laxa, M., Liebthal, M., Telman, W., Chibani, K., & Dietz, K.-J. (2019). The Role of the Plant Antioxidant System in Drought Tolerance. *Antioxidants (Basel, Switzerland)*, *8*(4). https://doi.org/10.3390/antiox8040094

LeBoeuf, E. N., & Grove, A. (2025). CysB in the Multiverse of Functions: Regulatory Roles in Cysteine Biosynthesis and Beyond. In *Frontiers in Bioscience - Landmark* (Vol. 30, Number 8). IMR Press Limited. https://doi.org/10.31083/FBL36563

Li, Y., Narayanan, M., Shi, X., Chen, X., Li, Z., & Ma, Y. (2024). Biofilms formation in plant growth-promoting bacteria for alleviating agro-environmental stress. *The Science of the Total Environment*, *907*, 167774. https://doi.org/10.1016/j.scitotenv.2023.167774

Li, Y., Wen, S., Li, Z., Liu, R., Zhang, Z., Li, Y., Lyu, D., & Jian, H. (2025). The evolution of the aquaporin gene family and drought tolerance mechanisms in green plants. *Horticulture Research*, *12*(11), uhaf209. https://doi.org/10.1093/hr/uhaf209

Liang, J., Liu, B., Christensen, M. J., Li, C., Zhang, X., & Nan, Z. (2024). The effects of Pseudomonas strains isolated from Achnatherum inebrians on plant growth: A genomic perspective. *Environmental Microbiology Reports*, *16*(5), e70011. https://doi.org/10.1111/1758-2229.70011

Lim, J., Lim, C. W., & Lee, S. C. (2022). Core Components of Abscisic Acid Signaling and Their Post-translational Modification. *Frontiers in Plant Science*, *13*, 895698. https://doi.org/10.3389/fpls.2022.895698

Liu, H., Wang, J., Liu, J., Liu, T., & Xue, S. (2021). Hydrogen sulfide (H2S) signaling in plant development and stress responses. *ABIOTECH*, *2*(1), 32–63. https://doi.org/10.1007/s42994-021-00035-4

Liu, S., Lv, Z., Liu, Y., Li, L., & Zhang, L. (2018). Network analysis of ABA-dependent and ABA-independent drought responsive genes in Arabidopsis thaliana. *Genetics and Molecular Biology*, *41*(3), 624–637. https://doi.org/10.1590/1678-4685-gmb-2017-0229

Lou, L., Li, X., Chen, J., Li, Y., Tang, Y., & Lv, J. (2018). Photosynthetic and ascorbate-glutathione metabolism in the flag leaves as compared to spikes under drought stress of winter wheat (Triticum aestivum L.). *PloS One*, *13*(3), e0194625. https://doi.org/10.1371/journal.pone.0194625

Lu, X., Liu, S.-F., Yue, L., Zhao, X., Zhang, Y.-B., Xie, Z.-K., & Wang, R.-Y. (2018). Epsc Involved in the Encoding of Exopolysaccharides Produced by Bacillus amyloliquefaciens FZB42 Act to Boost the Drought Tolerance of Arabidopsis thaliana. *International Journal of Molecular Sciences*, *19*(12). https://doi.org/10.3390/ijms19123795

Lu, Y., Duursma, R. A., Farrior, C. E., Medlyn, B. E., & Feng, X. (2020). Optimal stomatal drought response shaped by competition for water and hydraulic risk can explain plant trait covariation. *New Phytologist*, *225*(3), 1206–1217. https://doi.org/10.1111/nph.16207

Lucero, C. T., Lorda, G. S., Ludueña, L. M., Anzuay, M. S., & Taurian, T. (2020). Motility and biofilm production involved in the interaction of phosphate solubilizing endophytic strains

with peanut, maize and soybean plants. *Rhizosphere*, *15*, 100228. https://doi.org/10.1016/J.RHISPH.2020.100228

Lugtenberg, B., & Kamilova, F. (2009). Plant-growth-promoting rhizobacteria. *Annual Review of Microbiology*, *63*, 541–556. https://doi.org/10.1146/annurev.micro.62.081307.162918

Ma, W., Tang, S., Dengzeng, Z., Zhang, D., Zhang, T., & Ma, X. (2022). Root exudates contribute to belowground ecosystem hotspots: A review. In *Frontiers in Microbiology* (Vol. 13). Frontiers Media S.A. https://doi.org/10.3389/fmicb.2022.937940

Mansilla, M. C., Albanesi, D., & de Mendoza, D. (2000). Transcriptional control of the sulfur-regulated cysH operon, containing genes involved in L-cysteine biosynthesis in Bacillus subtilis. *Journal of Bacteriology*, *182*(20), 5885–5892. https://doi.org/10.1128/JB.182.20.5885-5892.2000

Mendes, R., Garbeva, P., & Raaijmakers, J. M. (2013). The rhizosphere microbiome: Significance of plant beneficial, plant pathogenic, and human pathogenic microorganisms. In *FEMS Microbiology Reviews* (Vol. 37, Number 5, pp. 634–663). https://doi.org/10.1111/1574-6976.12028

Mirleau, P., Wogelius, R., Smith, A., & Kertesz, M. A. (2005). Importance of organosulfur utilization for survival of Pseudomonas putida in soil and rhizosphere. *Applied and Environmental Microbiology*, *71*(11), 6571–6577. https://doi.org/10.1128/AEM.71.11.6571-6577.2005

Moormann, J., Heinemann, B., Angermann, C., Koprivova, A., Armbruster, U., Kopriva, S., & Hildebrandt, T. M. (2025). Cysteine Signalling in Plant Pathogen Response. *Plant, Cell & Environment*, *48*(10), 7107–7122. https://doi.org/10.1111/pce.70017

Morcillo, R. J. L., & Manzanera, M. (2021). The Effects of Plant-Associated Bacterial Exopolysaccharides on Plant Abiotic Stress Tolerance. *Metabolites*, *11*(6). https://doi.org/10.3390/metabo11060337

Muhammad Aslam, M., Waseem, M., Jakada, B. H., Okal, E. J., Lei, Z., Saqib, H. S. A., Yuan, W., Xu, W., & Zhang, Q. (2022). Mechanisms of Abscisic Acid-Mediated Drought Stress Responses in Plants. *International Journal of Molecular Sciences*, *23*(3). https://doi.org/10.3390/ijms23031084

Mukherjee, A., Mazumder, M., Verma, A., Tikariha, H., Bhattacharya, R., Ooi, Q. E., & Swarup, S. (2025). A bacterial signal coordinates plant-microbe fitness trade-off to enhance sulfur deficiency tolerance in plants. *Cell Host & Microbe*. https://doi.org/10.1016/j.chom.2025.09.007

Nadarajah, K. K. (2020). Ros homeostasis in abiotic stress tolerance in plants. In *International Journal of Molecular Sciences* (Vol. 21, Number 15, pp. 1–29). MDPI AG. https://doi.org/10.3390/ijms21155208

Narayan, O. P., Kumar, P., Yadav, B., Dua, M., & Johri, A. K. (2023). Sulfur nutrition and its role in plant growth and development. *Plant Signaling & Behavior*, *18*(1), 2030082. https://doi.org/10.1080/15592324.2022.2030082

Naseem, H., Ahsan, M., Shahid, M. A., & Khan, N. (2018). Exopolysaccharides producing rhizobacteria and their role in plant growth and drought tolerance. *Journal of Basic Microbiology*, *58*(12), 1009–1022. https://doi.org/10.1002/jobm.201800309

O'Neal, L., Baraquet, C., Suo, Z., Dreifus, J. E., Peng, Y., Raivio, T. L., Wozniak, D. J., Harwood, C. S., & Parsek, M. R. (2022). The Wsp system of Pseudomonas aeruginosa links surface sensing and cell envelope stress. *Proceedings of the National Academy of Sciences of the United States of America*, *119*(18), e2117633119. https://doi.org/10.1073/pnas.2117633119

Orozco-Mosqueda, M. del C., Glick, B. R., & Santoyo, G. (2020). ACC deaminase in plant growth-promoting bacteria (PGPB): An efficient mechanism to counter salt stress in crops. In *Microbiological Research* (Vol. 235). Elsevier GmbH. https://doi.org/10.1016/j.micres.2020.126439

Orozco-Mosqueda, M. del C., Rocha-Granados, M. del C., Glick, B. R., & Santoyo, G. (2018). Microbiome engineering to improve biocontrol and plant growth-promoting mechanisms. In *Microbiological Research* (Vol. 208, pp. 25–31). Elsevier GmbH. https://doi.org/10.1016/j.micres.2018.01.005

Pérez-Montaño, F., Aparicio, N., Arenas, F., Arjona, J. M., Camacho, M., Fernández-García, N., García-Fraile, P., Goicoechea, N., Macías-Naranjo, S., Matías, J., Montero-Calasanz, M. D. C., Morte, A., Olmos, E., Pueyo, J. J., Quiñones, M. A., Rey, L., & Reguera, M. (2025). Emerging crops and plant growth-promoting bacteria (PGPB): a synergistic approach to climate-resilient agriculture. *Microbiome*, *13*(1), 228. https://doi.org/10.1186/s40168-025-02225-4

Pieterse, C. M. J., Berendsen, R. L., de Jonge, R., Stringlis, I. A., Van Dijken, A. J. H., Van Pelt, J. A., Van Wees, S. C. M., Yu, K., Zamioudis, C., & Bakker, P. A. H. M. (2021). Pseudomonas simiae WCS417: star track of a model beneficial rhizobacterium. In *Plant and Soil* (Vol. 461, Numbers 1–2, pp. 245–263). Springer Science and Business Media Deutschland GmbH. https://doi.org/10.1007/s11104-020-04786-9

Pishchik, V. N., Chizhevskaya, E. P., Chebotar, V. K., Mirskaya, G. V, Khomyakov, Y. V, Vertebny, V. E., Kononchuk, P. Y., Kudryavtcev, D. V, Bortsova, O. A., Lapenko, N. G., & Tikhonovich, I. A. (2024). PGPB Isolated from Drought-Tolerant Plants Help Wheat Plants to Overcome Osmotic Stress. *Plants (Basel, Switzerland)*, *13*(23). https://doi.org/10.3390/plants13233381

Plugge, C. M., Zhang, W., Scholten, J. C. M., & Stams, A. J. M. (2011). Metabolic flexibility of sulfate-reducing bacteria. *Frontiers in Microbiology*, *2*, 81. https://doi.org/10.3389/fmicb.2011.00081

Qiao, M., Hong, C., Jiao, Y., Hou, S., & Gao, H. (2024). Impacts of Drought on Photosynthesis in Major Food Crops and the Related Mechanisms of Plant Responses to Drought. *Plants (Basel, Switzerland)*, *13*(13). https://doi.org/10.3390/plants13131808

Ratthawongjirakul, P., Thongkerd, V., & Chaicumpa, W. (2016). The impacts of a fliD mutation on the biofilm formation of Helicobacter pylori. *Asian Pacific Journal of Tropical Biomedicine*, *6*(12), 1008–1014. https://doi.org/10.1016/j.apjtb.2016.10.005

Rizzo, D. M., Lichtveld, M., Mazet, J. A. K., Togami, E., & Miller, S. A. (2021). Plant health and its effects on food safety and security in a One Health framework: four case studies. *One Health Outlook*, *3*(1). https://doi.org/10.1186/s42522-021-00038-7

Sánchez-Bermúdez, M., del Pozo, J. C., & Pernas, M. (2022). Effects of Combined Abiotic Stresses Related to Climate Change on Root Growth in Crops. In *Frontiers in Plant Science* (Vol. 13). Frontiers Media S.A. https://doi.org/10.3389/fpls.2022.918537

Saradadevi, R., Palta, J. A., & Siddique, K. H. M. (2017). ABA-Mediated Stomatal Response in Regulating Water Use during the Development of Terminal Drought in Wheat. *Frontiers in Plant Science*, *8*, 1251. https://doi.org/10.3389/fpls.2017.01251

Sato, H., Mizoi, J., Shinozaki, K., & Yamaguchi-Shinozaki, K. (2024). Complex plant responses to drought and heat stress under climate change. In *Plant Journal* (Vol. 117, Number 6, pp. 1873–1892). John Wiley and Sons Inc. https://doi.org/10.1111/tpj.16612

Shahbaz, U., Videau, P., Coulonnier, E., Papon, C., Navarro-Payá, D., Valenzuela, A. V., Matus, J. T., Malnoy, M., Zekri, O., Fiorani, F., Faralli, M., & Dalla Costa, L. (2025). Reduced stomatal density improves water-use efficiency in grapevine under climate scenarios of decreased water availability. *Plant Cell Reports*, *44*(9), 195. https://doi.org/10.1007/s00299-025-03577-9

Sharma, S., Bennett, M. J., & Mehra, P. (2025). Roles of hormones in regulating root growth-water interactions. *Journal of Experimental Botany*, *76*(7), 1987–1995. https://doi.org/10.1093/jxb/eraf063

Shavrukov, Y., Kurishbayev, A., Jatayev, S., Shvidchenko, V., Zotova, L., Koekemoer, F., de Groot, S., Soole, K., & Langridge, P. (2017). Early Flowering as a Drought Escape Mechanism in Plants: How Can It Aid Wheat Production? *Frontiers in Plant Science*, *8*, 1950. https://doi.org/10.3389/fpls.2017.01950

Shekhawat, K., Veluchamy, A., Fatima, A., García-Ramírez, G. X., Reichheld, J. P., Artyukh, O., Fröhlich, K., Polussa, A., Parween, S., Nagarajan, A. P., Rayapuram, N., & Hirt, H. (2024). Microbe-induced coordination of plant iron–sulfur metabolism enhances high-light-stress tolerance of Arabidopsis. *Plant Communications*, *5*(11), 101012. https://doi.org/10.1016/J.XPLC.2024.101012

Shibagaki, N., Rose, A., McDermott, J. P., Fujiwara, T., Hayashi, H., Yoneyama, T., & Davies, J. P. (2002). Selenate-resistant mutants of Arabidopsis thaliana identify Sultr1;2, a sulfate transporter required for efficient transport of sulfate into roots. *The Plant Journal : For Cell and Molecular Biology*, *29*(4), 475–486. https://doi.org/10.1046/j.0960-7412.2001.01232.x

Singh, M., Kumar, J., Singh, S., Singh, V. P., & Prasad, S. M. (2015). Roles of osmoprotectants in improving salinity and drought tolerance in plants: a review. In *Reviews in Environmental Science and Biotechnology* (Vol. 14, Number 3, pp. 407–426). Kluwer Academic Publishers. https://doi.org/10.1007/s11157-015-9372-8

Sinha, A. K., Jaggi, M., Raghuram, B., & Tuteja, N. (2011). Mitogen-activated protein kinase signaling in plants under abiotic stress. *Plant Signaling & Behavior*, *6*(2), 196–203. https://doi.org/10.4161/psb.6.2.14701

Sohag, A. A. M., Tahjib-Ul-Arif, M., Polash, M. A. S., Belal Chowdhury, M., Afrin, S., Burritt, D. J., Murata, Y., Hossain, M. A., & Afzal Hossain, M. (2020). Exogenous Glutathione-Mediated Drought Stress Tolerance in Rice (Oryza sativa L.) is Associated with Lower Oxidative Damage and Favorable Ionic Homeostasis. *Iranian Journal of Science and Technology, Transaction A: Science*, *44*(4), 955–971. https://doi.org/10.1007/s40995-020-00917-0

Takahashi, H., Marsolais, F., Cuypers, A., & Kopriva, S. (2023). Sulfur metabolism: actions for plant resilience and environmental adaptation. *Journal of Experimental Botany*, *74*(11), 3271–3275. https://doi.org/10.1093/jxb/erad164

Thompson, A. J., Andrews, J., Mulholland, B. J., McKee, J. M. T., Hilton, H. W., Horridge, J. S., Farquhar, G. D., Smeeton, R. C., Smillie, I. R. A., Black, C. R., & Taylor, I. B. (2007). Overproduction of abscisic acid in tomato increases transpiration efficiency and root hydraulic conductivity and influences leaf expansion. *Plant Physiology*, *143*(4), 1905–1917. https://doi.org/10.1104/pp.106.093559

Tigchelaar, M., Battisti, D. S., Naylor, R. L., & Ray, D. K. (2018). Future warming increases probability of globally synchronized maize production shocks. *Proceedings of the National Academy of Sciences of the United States of America*, *115*(26), 6644–6649. https://doi.org/10.1073/pnas.1718031115

van Dijk, M., Morley, T., Rau, M. L., & Saghai, Y. (2021). A meta-analysis of projected global food demand and population at risk of hunger for the period 2010–2050. *Nature Food*, *2*(7), 494–501. https://doi.org/10.1038/s43016-021-00322-9

Vidmar, J. J., Tagmount, A., Cathala, N., Touraine, B., & Davidian, J. E. (2000). Cloning and characterization of a root specific high-affinity sulfate transporter from Arabidopsis thaliana. *FEBS Letters*, *475*(1), 65–69. https://doi.org/10.1016/s0014-5793(00)01615-x

Wang, D.-C., Jiang, C.-H., Zhang, L.-N., Chen, L., Zhang, X.-Y., & Guo, J.-H. (2019). Biofilms Positively Contribute to Bacillus amyloliquefaciens 54-induced Drought Tolerance in Tomato Plants. *International Journal of Molecular Sciences*, *20*(24). https://doi.org/10.3390/ijms20246271

Wang, S., Zhou, H., He, Z., Ma, D., Sun, W., Xu, X., & Tian, Q. (2024). Effects of Drought Stress on Leaf Functional Traits and Biomass Characteristics of Atriplex canescens. *Plants (Basel, Switzerland)*, *13*(14). https://doi.org/10.3390/plants13142006

Weber, M., Suter, M., Brunold, C., & Kopriva, S. (2000). Sulfate assimilation in higher plants characterization of a stable intermediate in the adenosine 5'-phosphosulfate reductase reaction. *European Journal of Biochemistry*, *267*(12), 3647–3653. https://doi.org/10.1046/j.1432-1327.2000.01394.x

Wu, G., Tian, N., She, F., Cao, A., Wu, W., Zheng, S., & Yang, N. (2023). Characteristics analysis of Early Responsive to Dehydration genes in Arabidopsis thaliana (AtERD). *Plant Signaling & Behavior*, *18*(1), 2105021. https://doi.org/10.1080/15592324.2022.2105021

Wu, S., Li, K., Diao, T., Sun, Y., Sun, T., & Wang, C. (2025). Influence of continuous fertilization on heavy metals accumulation and microorganism communities in greenhouse

soils under 22 years of long-term manure organic fertilizer experiment. *Science of The Total Environment*, *959*, 178294. https://doi.org/10.1016/J.SCITOTENV.2024.178294

Yang, L., Qian, X., Zhao, Z., Wang, Y., Ding, G., & Xing, X. (2024). Mechanisms of rhizosphere plant-microbe interactions: molecular insights into microbial colonization. In *Frontiers in Plant Science* (Vol. 15). Frontiers Media SA. https://doi.org/10.3389/fpls.2024.1491495

Yao, T., Zhang, J., Xie, M., Yuan, G., Tschaplinski, T. J., Muchero, W., & Chen, J.-G. (2020). Transcriptional Regulation of Drought Response in Arabidopsis and Woody Plants. *Frontiers in Plant Science*, *11*, 572137. https://doi.org/10.3389/fpls.2020.572137

Zhou, J., Uribe Acosta, M., Stassen, M. J. J., Qi, R., de Jonge, R., White, F., Kramer, G., Dong, L., Pieterse, C. M. J., & Stringlis, I. A. (2025). Arabidopsis root defense barriers support beneficial interactions with rhizobacterium Pseudomonas simiae WCS417. *The New Phytologist*, *248*(4), 2021–2039. https://doi.org/10.1111/nph.70549

Zhou, Y., Lam, H. M., & Zhang, J. (2007). Inhibition of photosynthesis and energy dissipation induced by water and high light stresses in rice. *Journal of Experimental Botany*, *58*(5), 1207–1217. https://doi.org/10.1093/jxb/erl291

Zia, R., Nawaz, M. S., Siddique, M. J., Hakim, S., & Imran, A. (2021). Plant survival under drought stress: Implications, adaptive responses, and integrated rhizosphere management strategy for stress mitigation. *Microbiological Research*, *242*, 126626. https://doi.org/10.1016/j.micres.2020.126626

Zinta, G., AbdElgawad, H., Domagalska, M. A., Vergauwen, L., Knapen, D., Nijs, I., Janssens, I. A., Beemster, G. T. S., & Asard, H. (2014). Physiological, biochemical, and genome-wide transcriptional analysis reveals that elevated CO2 mitigates the impact of combined heat wave and drought stress in Arabidopsis thaliana at multiple organizational levels. *Global Change Biology*, *20*(12), 3670–3685. https://doi.org/10.1111/gcb.12626

## Author contributions

**Elkatmis B**, Parween S, Eida AA, Jalal R, Lafi F, Alam I, Kopriva S, Hirt H, Saad MM. (2025) Integrated genomic and mutagenesis analysis of *Pseudomonas argentinensis* SA190 reveals mechanisms of plant root colonization and stress resilience. BMC Microbiology 25, 785. https://doi.org/10.1186/s12866-025-04495-2

- **B.E.**: Data curation, investigation, validation, methodology development, writing—original draft, and writing—review and editing. S.P., A.A.E., R.J., F.L., and I.A.: Methodology refinement and data curation. S.K.: Conceptualization, supervision, and manuscript review and editing. H.H.: Funding acquisition, project supervision, and writing—review and editing. M.M.S.: Project ideation and conceptualization, supervision of experimental design, protocol tuning, validation, and manuscript writing—review and editing.

**Elkatmis B**, Han B, Parween S, Kopriva S, Hirt H, Saad MM (2025) Comprehensive mapping of EZ-Tn5 transposon insertion sites in *Pseudomonas argentinensis* SA190 using RATE-PCR. Bio-protocol 15: e5389. https://doi.org/10.21769/BioProtoc.5389

- **B.E.** data curation, investigation, validation, methodology, writing—original draft, and writing—review and editing; B.H. methodology, data curation, S.P. methodology, data curation; S.K. conceptualization, supervision and review and editing. H.H. funding acquisition, supervision, and writing—review and editing; M.M.S. methodology establishment, conceptualization, supervision, validation, and writing—review and editing.

**Elkatmis B**, Alkhateeb RS, Mannes C, Jalal R, Trapp M, Westhoff P, Ozkan C, Thelen GM, Han B, Saad MM, Kopriva S, Hirt H. (2026) Root endophyte sulfur metabolites enhance redox balance and drought tolerance in Arabidopsis. bioRxiv 2026.06.15.732246. https://doi.org/10.64898/2026.06.15.732246

- M.M.S., S.K., and H.H., supervised the project; **B.E.**, S.K., and H.H. conceptualized the project; **B.E.**, S.K., and H.H. designed experiments; Experimental works were mainly carried out by **B.E.** with help of R.S.A, C.M., R.J., C.O., and G.M.T.; **B.E.** analyzed the data and generated figures; M.T. performed the HPLC-MS/MS; P.W. performed GC-

MS and analyzed metabolite profiles; **B.E.** and B.H. generated the mutants; **B.E.** and R.S.A. drafted the manuscript, all authors read, edited, and aproved the final manuscript.

## Acknowledgements

First and foremost, I would like to express my deepest gratitude to my supervisors, Prof. Dr. Stan Kopriva and Prof. Dr. Heribert Hirt, for giving me the opportunity to pursue my PhD within this collaborative project between the University of Cologne and KAUST. I am sincerely grateful for their continuous support, guidance, and encouragement throughout my doctoral studies. I greatly enjoyed our scientific discussions, which helped shape both this project and my development as a researcher.

I would also like to extend my sincere thanks to Dr. Maged Saad for his supervision, support, and guidance from the very beginning of this project. His advice, encouragement, and scientific input were invaluable throughout my PhD journey.

I am grateful to Prof. Dr. Vera Göhre for being a member of my Thesis Advisory Committee and for providing insightful discussions, constructive feedback, and valuable guidance throughout my doctoral studies. I would also like to thank Prof. Dr. Tatjana Hildebrandt and Prof. Dr. Andreas Beyer for serving as members of my thesis committee.

My sincere thanks go to the CEPLAS Graduate School for providing me with the opportunity to pursue my PhD in such a stimulating and inspiring scientific environment. I am especially grateful to the CEPLAS Graduate School coordinators, particularly Dr. Nadine Rademacher and Dr. Juliane Schmid, for their continuous support with administrative matters and for always patiently answering my questions, making every process much smoother and easier.

I would also like to thank the Visiting Student Onboarding Team at KAUST, especially Ting Zhang, for arranging the logistics and paperwork for my visits and for providing valuable support throughout the administrative process.

I would also like to acknowledge our collaborators. I am grateful to Dr. Philipp Westhoff for the collaboration on GC-MS analyses. I would like to thank Prof. Dr. Andreas Meyer for valuable scientific discussions, for providing plant material, and for giving me access to his facilities. I am also grateful to Dr. Stephan Wagner for his assistance and guidance with confocal microscopy.

I feel incredibly fortunate to have spent part of my PhD at KAUST and to have worked in a second research environment with outstanding colleagues and friends. This experience was both scientifically and personally enriching.

I would like to sincerely thank Dr. Rabeaa Alkhateeb for her supervision, support, and guidance throughout my time at KAUST. She helped me tremendously with the project and made my first days in the laboratory much easier by introducing me to the group and helping me settle in. Beyond her scientific support, I am grateful to have gained a wonderful friend.

I am also deeply grateful to Dr. Rewaa Jalal for her help with numerous plant experiments, especially the transfers to PEG plates, which would have been much more challenging without her support. I would like to thank Dr. Marilia Trapp for her assistance with LC-MS measurements of thiols and Dr. Baoda Han for her help with the project and for always patiently answering my questions. My sincere thanks also go to Eneroliza for arranging everything in the laboratory and for the fun moments we shared outside the lab, especially at the swimming pool. I am also grateful to Carlos for his assistance with ICP-OES analyses.

I would also like to thank my friends at KAUST, especially Waad and Anam, for their friendship, support, our small trips, and all the memorable pizza nights by the Red Sea. Special thanks go to Katja for being such a wonderful friend and for making my integration into the KAUST community so easy. I am grateful for the many hiking trips, movie nights, game nights, coffee discussions, and for her constant support throughout the years. I would also like to thank Tanja for our conversations about books and life and for always being there as a supportive friend. I am also grateful to Hasna for her friendship and support.

My sincere thanks go to my colleagues and friends at the University of Cologne. I would like to thank Dr. Anna Koprivova for her help and support with the project. I am grateful to our technicians, Bastian, Sabine, and Irene, for their assistance in the laboratory. I would also like to thank the students who contributed to this work, Catherine, Ceyda, and Marie. It was a pleasure working with you and sharing this scientific journey. A special thank you goes to Varsa and Raissa for their friendship, support, and all the enjoyable moments we shared throughout this journey.

Beyond academia, I would like to thank my childhood friends, Ayşenur and Sema, for their unwavering friendship, support, and for all the wonderful memories and trips we have shared over the years.

Finally, and most importantly, I would like to thank my parents and my brother. Their endless support, encouragement, and belief in me have been the foundation of everything I have achieved.

## Erklärung

Hiermit versichere ich an Eides statt, dass ich die vorliegende Dissertation selbstständig und ohne die Benutzung anderer als der angegebenen Hilfsmittel und Literatur angefertigt habe. Alle Stellen, die wörtlich oder sinngemäß aus veröffentlichten und nicht veröffentlichten Werken dem Wortlaut oder dem Sinn nach entnommen wurden, sind als solche kenntlich gemacht. Ich versichere an Eides statt, dass diese Dissertation noch keiner anderen Fakultät oder Universität zur Prüfung vorgelegen hat; dass sie -abgesehen von den oben angegebenen Teilpublikationennoch nicht veröffentlicht worden ist sowie, dass ich eine Veröffentlichung der Dissertation vor Abschluss der Promotion nicht ohne Genehmigung des Promotionsausschusses vornehmen werde. Die Bestimmungen dieser Ordnung sind mir bekannt. Darüber hinaus erkläre ich hiermit, dass ich die Ordnung zur Sicherung guter wissenschaftlicher Praxis und zum Umgang mit wissenschaftlichem Fehlverhalten der Universität zu Köln gelesen und sie bei der Durchführung der Dissertation zugrundeliegenden Arbeiten und der schriftlich verfassten Dissertation beachtet habe und verpflichte mich hiermit, die dort genannten Vorgaben bei allen wissenschaftlichen Tätigkeiten zu beachten und umzusetzen. Ich versichere, dass die eingereichte elektronische Fassung der eingereichten Druckfassung vollständig entspricht.

Die von mir vorgelegte Dissertation ist von Prof. Stanislav Kopriva betreut worden.

Köln, 01.07.2026



Büsra Elkatmis

# Appendix

# Chapter 1

## Integrated genomic and mutagenesis analysis of *Pseudomonas argentinensis* SA190 reveals mechanisms of plant root colonization and stress resilience

**Elkatmis B,** Parween S, Eida AA, Jalal R, Lafi F, Alam I, Kopriva S, Hirt H, Saad MM (2025)

BMC Microbiology 25, 785. https://doi.org/10.1186/s12866-025-04495-2

## Supplementary material

**Supplementary Table 1.** The primers used in the project.

**Supplementary Table 2.** Validation of insertion sites in SA190 mutants by HiSeq Sequencing technology.

**Supplementary Table 3.** Average nucleotide identity (ANI) of Type Strain Genome Server (TYGS).

**Supplementary Table 4.** Average Amino Acid identity (AAI) from EzAAI (V.1.2.2).

**Supplementary Table 5.** The API 50 CH analysis of *Pseudomonas argentinensis* SA190.

**Supplementary Figure 1.** Phosphate solubilization (A) and siderophore production (B) in *Pseudomonas argentinensis* SA190.

**Supplementary Figure 2.** AntiSMASH analysis (version 8.0.4) of *Pseudomonas argentinensis* SA190.

**Supplementary Figure 3.** MIBiG comparisons of regions 1, 2, and 3 generated using antiSMASH (version 8.0.4). (A) Region 1, (B) Region 2, and (C) Region 3.

**Supplementary Figure 4.** MIBiG comparison was shown for the regions 4, 5 and 6 by using antiSMASH (version 8.0.4). (A) Region 4, (B) Region 5, and (C) Region 6.

**Supplementary Figure 5.** MIBiG comparison was shown for the regions 7 and 8 by using antiSMASH (version 8.0.4). (A) Region 7 and (B) Region 8.

**Supplementary Figure 6.** Growth curves of SA190 and the *wspC*::Tn5, *rpoE*::Tn5, and *fliD*::Tn5 mutants.

## Supplementary Data

**Supplementary Table 1.** The primers used in the project.

| The name of the primer | Sequence |
|---|---|
| Inv-1 | ATGGCTCATAACACCCCTTGTATTA |
| Inv-2 | GAACTTTTGCTGAGTTGAAGGATCA |
| KAN-2-F | ACCTACAACAAAGCTCTCATCAACC |
| KAN-2-R | GCAATGTAACATCAGAGATTTTGAG |

**Supplementary Table 2.** Validation of insertion sites in SA190 mutants by HiSeq Sequencing technology.

| qseqid | Sample ID | sseqid | Percentage of identical matches | Alignment length | mismatch | gapopen | qstart | qend | sstart | send | evalue | bitscore |
|---|---|---|---|---|---|---|---|---|---|---|---|---|
| tn5 | B5 | NODE_2_length_497665_cov_160.085036 | 100 | 108 | 0 | 0 | 1 | 108 | 3E+05 | 349728 | 9.2E-52 | 200 |
| tn5 | B4 | NODE_20_length_79072_cov_144.562517 | 100 | 108 | 0 | 0 | 1 | 108 | 60797 | 60690 | 9.2E-52 | 200 |
| tn5 | B3 | NODE_19_length_79072_cov_140.973758 | 100 | 108 | 0 | 0 | 1 | 108 | 18276 | 18383 | 9.2E-52 | 200 |
| tn5 | B2 | NODE_1_length_497665_cov_196.568265 | 100 | 108 | 0 | 0 | 1 | 108 | 3E+05 | 317551 | 9.2E-52 | 200 |
| tn5 | B1 | NODE_1_length_680816_cov_194.442609 | 100 | 108 | 0 | 0 | 1 | 108 | 2E+05 | 214575 | 9.2E-52 | 200 |

**Supplementary Table 3.** Average nucleotide identity (ANI) of Type Strain Genome Server (TYGS).

| Query strain | Subject strain | dDDH (d0, in %) | C.I. (d0, in %) | dDDH (d4, in %) | C.I. (d4, in %) | dDDH (d6, in %) | C.I. (d6, in %) | G+C content difference (in %) |
|---|---|---|---|---|---|---|---|---|
| SA190 | Pseudomonas argentinensis LMG 22563 | 75 | [71.0 - 78.6] | 40.1 | [37.6 - 42.6] | 67.5 | [64.1 - 70.8] | 0.43 |
| SA190 | Pseudomonas punonensis CECT 8089 | 67.7 | [63.8 - 71.3] | 34.3 | [31.9 - 36.9] | 59.1 | [55.8 - 62.2] | 2.18 |
| SA190 | Pseudomonas straminea JCM 2783 | 66.9 | [63.0 - 70.5] | 38.4 | [36.0 - 41.0] | 60.5 | [57.2 - 63.7] | 0.78 |
| SA190 | Pseudomonas seleniipraecipitans LMG 25475 | 54.4 | [50.8 - 57.8] | 28.1 | [25.8 - 30.6] | 46.3 | [43.3 - 49.4] | 2.49 |
| SA190 | Pseudomonas flavescens LMG 18387 | 46.2 | [42.8 - 49.6] | 30 | [27.6 - 32.5] | 41.4 | [38.4 - 44.4] | 0.54 |
| SA190 | Pseudomonas daroniae FRB 228 | 45 | [41.6 - 48.4] | 29.9 | [27.5 - 32.4] | 40.5 | [37.5 - 43.5] | 1.98 |
| SA190 | Pseudomonas dryadis FRB 230 | 35.8 | [32.4 - 39.3] | 28.1 | [25.7 - 30.6] | 33 | [30.1 - 36.1] | 0.97 |
| SA190 | Pseudomonas guguanensis JCM 18416 | 25.4 | [22.1 - 29.0] | 24.2 | [21.9 - 26.7] | 24.1 | [21.2 - 27.2] | 0.21 |
| SA190 | Pseudomonas hydrolytica DSWY01 | 24.6 | [21.3 - 28.3] | 24.4 | [22.1 - 26.8] | 23.5 | [20.6 - 26.6] | 0.46 |
| SA190 | Pseudomonas yangonensis JCM 33396 | 24.4 | [21.1 - 28.1] | 24.1 | [21.8 - 26.5] | 23.3 | [20.4 - 26.3] | 1.09 |
| SA190 | Pseudomonas parafulva DSM 17004 | 18.6 | [15.5 - 22.2] | 21.4 | [19.1 - 23.8] | 18.2 | [15.6 - 21.2] | 1.52 |
| SA190 | Pseudomonas turukhanskensis VKM B-2935 | 18.3 | [15.2 - 21.9] | 21.4 | [19.2 - 23.9] | 18 | [15.3 - 21.0] | 3.42 |
| SA190 | Pseudomonas fulva DSM 17717 | 17.6 | [14.5 - 21.1] | 21.5 | [19.2 - 23.9] | 17.4 | [14.8 - 20.4] | 2.24 |

**Supplementary Table 4.** Average Amino Acid identity (AAI) from EzAAI (V.1.2.2).

| Label 1 | Label 2 | AAI | CDS count 1 | CDS count 2 | Matched coun | Proteome cov. | ID param. | Cov. param. |
|---|---|---|---|---|---|---|---|---|
| SA190 | Pseudomonas argentinensis LMG 22563 | 93.526839 | 4545 | 4648 | 3970 | 0.863701 | 0.4 | 0.5 |
| SA190 | Pseudomonas straminea JCM 2783 | 93.084034 | 4545 | 4588 | 3808 | 0.833899 | 0.4 | 0.5 |
| SA190 | Pseudomonas punonensis CECT 8089 | 92.321749 | 4545 | 4485 | 3745 | 0.829457 | 0.4 | 0.5 |
| SA190 | Pseudomonas seleniipraecipitans LMG 25475 | 88.842435 | 4545 | 4224 | 3556 | 0.811039 | 0.4 | 0.5 |
| SA190 | Pseudomonas daroniae FRB 228 | 88.733516 | 4545 | 4943 | 3552 | 0.748735 | 0.4 | 0.5 |
| SA190 | Pseudomonas flavescens LMG 18387 | 88.392457 | 4545 | 5326 | 3679 | 0.745416 | 0.4 | 0.5 |
| SA190 | Pseudomonas dryadis FRB 230 | 84.733416 | 4545 | 5006 | 3407 | 0.713433 | 0.4 | 0.5 |
| SA190 | Pseudomonas guguanensis JCM 18416 | 77.722042 | 4545 | 4609 | 2958 | 0.646275 | 0.4 | 0.5 |
| SA190 | Pseudomonas yangonensis JCM 33396 | 77.565477 | 4545 | 4909 | 3011 | 0.636979 | 0.4 | 0.5 |
| SA190 | Pseudomonas hydrolytica DSWY01 | 77.563802 | 4545 | 4853 | 2938 | 0.625239 | 0.4 | 0.5 |
| SA190 | Pseudomonas turukhanskensis VKM B-2935 | 74.818816 | 4545 | 5380 | 2931 | 0.59063 | 0.4 | 0.5 |
| SA190 | Pseudomonas fulva DSM 17717 | 73.013539 | 4545 | 4325 | 2707 | 0.610372 | 0.4 | 0.5 |
| SA190 | Pseudomonas parafulva DSM 17004 | 73.009593 | 4545 | 4499 | 2726 | 0.602831 | 0.4 | 0.5 |

**Supplementary Table 5.** The API 50 CH analysis of *Pseudomonas argentinensis* SA190.

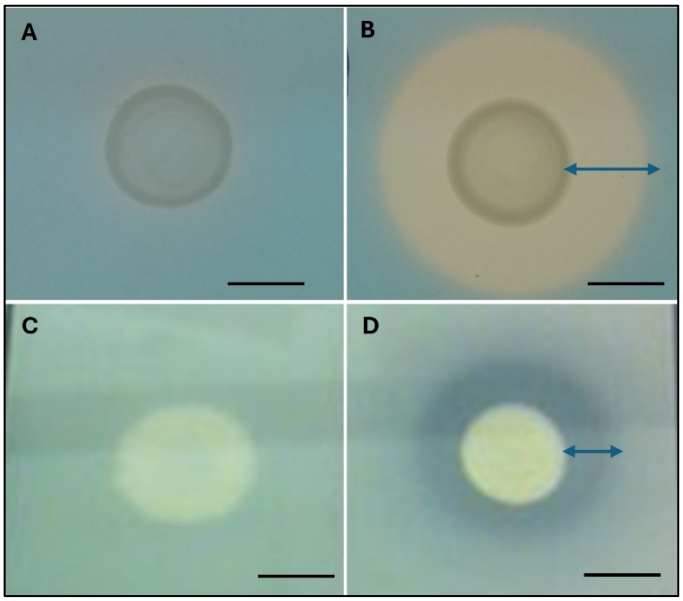
| Reaction | Suger | Suger type |
|---|---|---|
| 1 | D-Arabinose | Monosacharides |
| 1 | L-Arabinose | |
| 1 | D-Ribose | |
| 3 | D-Xylose | |
| 3 | L-Xylose | |
| 3 | D-Galactose | |
| 1 | D-Glucose | |
| 1 | D-Fructose | |
| 1 | D-Mannose | |
| 3 | L-Sorbose | |
| 3 | L-Rhamnose | |
| 3 | N-Acetylglucosamine | |
| 3 | D-Lyxose | |
| 1 | D-Tagatose | |
| 3 | D-Fucose | |
| 3 | L-Fucose | |
| 1 | Methyl-beta-D-xylopyranoside | Mono-Derivatives |
| 3 | Methyl-alpha-D-mannopyranoside | |
| 3 | Methyl-alpha-D-glucopyranoside | |
| 1 | D-Cellobiose | Disaacharides |
| 1 | D-Maltose | |
| 3 | D-Lactose (bovine origin) | |
| 1 | D-Melibiose | |
| 3 | D-Saccharose (sucrose) | |
| 3 | D-Trehalose | |
| 3 | Gentiobiose | |
| 3 | D-Turanose | |
| 3 | Amygdalin | Glycosides |
| 2 | Arbutin | |
| 3 | Esculin /ferric citrate | |
| 3 | Salicin | |
| 3 | Inulin | Polysacharides |
| 1 | D-Melezitose | |
| 1 | D-Raffinose | |
| 3 | Amidon (starch) | |
| 1 | Glycogen | |
| 1 | Glycerol | Polyols |
| 1 | Erythritol | |
| 3 | D-Adonitol | |
| 3 | Dulcitol | |
| 1 | Inositol | |
| 1 | D-Mannitol | |
| 2 | D-Sorbitol | |
| 1 | Xylitol | |
| 1 | D-Arabitol | |
| 1 | L-Arabitol | |
| 2 | Potassium gluconate | Salts |
| 1 | Potassium 2-ketogluconate | |
| 1 | Potassium 5-ketogluconate | |

**Supplementary Figure 1. Phosphate solubilization and siderophore production by *Pseudomonas argentinensis* SA190.**

**(A–B)** Siderophore production on Chrome Azurol S (CAS) agar.
(A) Control bacteria without siderophore activity.
(B) SA190 inoculated on CAS agar showing a distinct orange halo (blue arrow) around the colony, demonstrating siderophore secretion and iron-chelating activity

**(C–D)** Phosphate solubilization on Pikovskaya (PVK) agar.
(C) Control bacteria without visible halo.
(D) SA190 inoculated on PVK agar showing a clear halo zone around the colony (blue arrow), indicating inorganic phosphate solubilization.

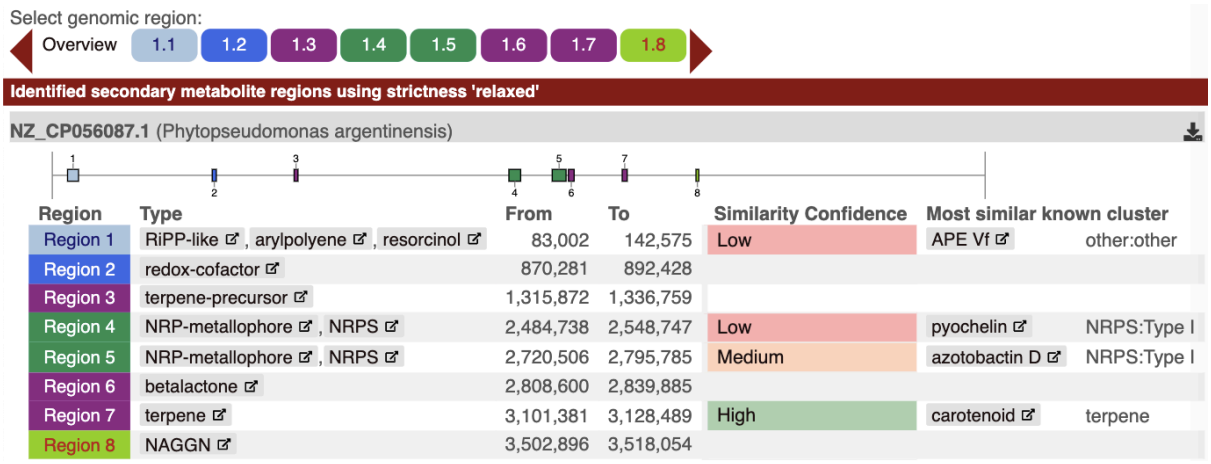
**Scale bars** = 0.5 cm.



**Supplementary Figure 2. Secondary metabolite biosynthetic gene clusters (BGCs) predicted in *Pseudomonas argentinensis* SA190 using antiSMASH** analysis (version 8.0.4)

Eight secondary metabolite biosynthetic gene clusters (Regions 1–8) were identified in the complete genome of *P. argentinensis* SA190 using antiSMASH (v6.0) under "relaxed" detection strictness. The BGCs span diverse classes of metabolites, including:

- **Region 1:** RiPP-like, arylpolyene, and resorcinol biosynthesis, with low similarity to known APE (aryl polyene) clusters.
- **Region 2:** Redox cofactor cluster, with no close match to known references.
- **Region 3:** Terpene-precursor pathway, with undefined similarity.
- **Region 4 & 5:** NRPS-metallophore hybrid clusters, including pyochelin-like (low confidence) and azotobactin D-like (medium confidence) siderophore-related BGCs.
- **Region 6:** Betalactone-type cluster.
- **Region 7:** Terpene cluster, similar to carotenoid biosynthesis pathways (high similarity).
- **Region 8:** NAGGN-like BGC with unknown functional annotation.




| Region | Type | From | To | Similarity Confidence | Most similar known cluster | |
|---|---|---|---|---|---|---|
| Region 1 | RiPP-like, arylpolyene, resorcinol | 83,002 | 142,575 | Low | APE Vf | other:other |
| Region 2 | redox-cofactor | 870,281 | 892,428 | | | |
| Region 3 | terpene-precursor | 1,315,872 | 1,336,759 | | | |
| Region 4 | NRP-metallophore, NRPS | 2,484,738 | 2,548,747 | Low | pyochelin | NRPS:Type I |
| Region 5 | NRP-metallophore, NRPS | 2,720,506 | 2,795,785 | Medium | azotobactin D | NRPS:Type I |
| Region 6 | betalactone | 2,808,600 | 2,839,885 | | | |
| Region 7 | terpene | 3,101,381 | 3,128,489 | High | carotenoid | terpene |
| Region 8 | NAGGN | 3,502,896 | 3,518,054 | | | |

**Supplementary Figure 3.** MIBiG comparisons of regions 1, 2, and 3 generated using antiSMASH (version 8.0.4). (A) Region 1, (B) Region 2, and (C) Region 3.

**A** Region 1

| Reference | RiPP-like | arylpolyene | resorcinol | Similarity score | Type | Compound(s) | Organism |
|---|---|---|---|---|---|---|---|
| BGC0002341.2 | | | | 0.89 | other (other) | 3,5-dibromo-p-anisic acid | Planctomycetales bacterium 10988 |
| BGC0001244.3 | | | | 0.52 | PKS | (-)-Mellein | Parastagonospora nodorum |
| BGC0002008.3 | | | | 0.46 | other (other) | aryl polyenes | Xenorhabdus doucetiae |
| BGC0000836.5 | | | | 0.45 | other (other) | APE Ec | Escherichia coli CFT073 |
| BGC0001197.5 | | | | 0.34 | PKS | frankiamicin | Frankia sp. EAN1pec |
| BGC0000840.5 | | | | 0.33 | other (other) | xanthomonadin I | Xanthomonas oryzae pv. oryzae |
| BGC0001526.4 | | | | 0.33 | other (other) | bartoloside E, bartoloside F, bartoloside G, bartoloside H, bartoloside I, bartoloside J, bartoloside K | Synechocystis salina LEGE 06099 |
| BGC0001525.3 | | | | 0.33 | other (other) | bartoloside B, bartoloside C, bartoloside D | Synechocystis salina LEGE 06155 |
| BGC0002711.2 | | | | 0.32 | PKS | nostovalerolactone, 9-dehydronostovalerolactone | Nostoc punctiforme PCC 73102 |
| BGC0001987.2 | | | | 0.32 | PKS | koreenceine A, koreenceine B, koreenceine C, koreenceine D | Pseudomonas koreensis |

**B** Region 2

| Reference | redox-cofactor | Similarity score | Type | Compound(s) | Organism |
|---|---|---|---|---|---|
| BGC0001227.3 | | 0.39 | terpene | isorenieratene | Streptomyces collinus Tu 365 |
| BGC0000906.3 | | 0.36 | other (other) | heme D1 | Heliophilum fasciatum |
| BGC0001100.5 | | 0.36 | NRPS, PKS | lankacidin C | Streptomyces rochei |
| BGC0001789.3 | | 0.35 | ribosomal | suicin 90-1330 | Streptococcus suis |
| BGC0001441.5 | | 0.33 | other (other) | belactosin A, belactosin C | Streptomyces sp. |
| BGC0002339.3 | | 0.33 | terpene | 2-hydroxysorangiadenosine | Vitiosangium cumulatum |
| BGC0001753.3 | | 0.32 | ribosomal | radamycin, globimycin | Streptomyces globisporus subsp. globisporus |
| BGC0000147.5 | | 0.32 | PKS | soraphen A | Sorangium cellulosum |
| BGC0002300.2 | | 0.32 | NRPS | albomycin delta2, albomycin delta1, albomycin epsilon | Streptomyces sp. ATCC 700974 |
| BGC0002545.3 | | 0.32 | PKS | sungeidine C, sungeidine B, sungeidine D, sungeidine H, sungeidine A, sungeidine E, sungeidine F, sungeidine G | Micromonospora sp. |

**C** Region 3

| Reference | terpene-precursor | Similarity score | Type | Compound(s) | Organism |
|---|---|---|---|---|---|
| BGC0001361.3 | | 0.50 | terpene | sodorifen | Serratia plymuthica 4Rx13 |
| BGC0002283.2 | | 0.50 | terpene | sodorifen | Serratia plymuthica |
| BGC0002397.2 | | 0.47 | terpene | astallatene | Arabidopsis thaliana |
| BGC0000016.4 | | 0.44 | other (other) | amphotericin B | Streptomyces nodosus |
| BGC0002400.2 | | 0.44 | terpene | boleracene | Brassica oleracea var. oleracea |
| BGC0000927.3 | | 0.43 | other (flavin) | roseoflavin | Streptomyces davaonensis JCM 4913 |
| BGC0001475.4 | | 0.41 | terpene | aspterric acid | Aspergillus terreus NIH2624 |
| BGC0001594.3 | | 0.40 | other (other) | fischerindole L | Fischerella muscicola UTEX 1829 |
| BGC0000665.5 | | 0.39 | other (other), terpene | xiamycin, indosespene, sespenine, dixiamycin A, dixiamycin B, sulfadixiamycin A, sulfadixiamycin B, sulfadixiamycin C | Streptomyces sp. HKI0576 |
| BGC0001501.5 | | 0.39 | other (other) | ambiguine P | Fischerella sp. TAU |

**Supplementary Figure 4.** MIBiG comparison was shown for the regions 4, 5 and 6 by using antiSMASH (version 8.0.4). (A) Region 4, (B) Region 5, and (C) Region 6.

**A** **Region 4**

| Reference | NRP-metallophore / NRPS | Similarity score | Type | Compound(s) | Organism |
|---|---|---|---|---|---|
| BGC0001833.4 | | 0.61 | NRPS | icosalide A, icosalide B | Burkholderia gladioli |
| BGC0002286.3 | | 0.60 | NRPS | ririwpeptide A, ririwpeptide B, ririwpeptide C | Photorhabdus laumondii subsp. laumondii TTO1 |
| BGC0001758.4 | | 0.60 | NRPS | rhizomide A, rhizomide B, rhizomide C | Paraburkholderia rhizoxinica HKI 454 |
| BGC0001825.4 | | 0.60 | NRPS | xenematide | Xenorhabdus nematophila AN6/1 |
| BGC0001641.4 | | 0.60 | NRPS | kolossin | Photorhabdus laumondii subsp. laumondii TTO1 |
| BGC0001128.4 | | 0.60 | NRPS | gamexpeptide C | Photorhabdus laumondii subsp. laumondii TTO1 |
| BGC0002075.3 | | 0.59 | NRPS | pyreudione A, pyreudione B, pyreudione C, pyreudione D, pyreudione E | Pseudomonas fluorescens |
| BGC0000412.5 | | 0.59 | NRPS | pyochelin | Pseudomonas aeruginosa PAO1 |
| BGC0001135.5 | | 0.59 | NRPS | bicornutin A1, bicornutin A2 | Xenorhabdus budapestensis |
| BGC0002135.2 | | 0.59 | NRPS | bovienimide A | Xenorhabdus bovienii SS-2004 |

**B** **Region 5**

| Reference | NRP-metallophore / NRPS | Similarity score | Type | Compound(s) | Organism |
|---|---|---|---|---|---|
| BGC0002135.2 | | 0.92 | NRPS | bovienimide A | Xenorhabdus bovienii SS-2004 |
| BGC0001833.4 | | 0.85 | NRPS | icosalide A, icosalide B | Burkholderia gladioli |
| BGC0001128.4 | | 0.84 | NRPS | gamexpeptide C | Photorhabdus laumondii subsp. laumondii TTO1 |
| BGC0002286.3 | | 0.83 | NRPS | ririwpeptide A, ririwpeptide B, ririwpeptide C | Photorhabdus laumondii subsp. laumondii TTO1 |
| BGC0001135.5 | | 0.82 | NRPS | bicornutin A1, bicornutin A2 | Xenorhabdus budapestensis |
| BGC0001166.5 | | 0.81 | NRPS | HC-toxin | Alternaria jesenskae |
| BGC0001132.4 | | 0.80 | NRPS | xenotetrapeptide | Xenorhabdus nematophila ATCC 19061 |
| BGC0001825.4 | | 0.79 | NRPS | xenematide | Xenorhabdus nematophila AN6/1 |
| BGC0001261.3 | | 0.79 | NRPS | AM-toxin | Alternaria alternata |
| BGC0001133.4 | | 0.78 | NRPS | taxIllaid A | Xenorhabdus bovienii SS-2004 |

**C** **Region 6**

| Reference | betalactone | Similarity score | Type | Compound(s) | Organism |
|---|---|---|---|---|---|
| BGC0001286.3 | | 0.42 | other (other) | itaconic acid | Ustilago maydis |
| BGC0000513.3 | | 0.41 | ribosomal | Ery-9, Ery-6, Ery-8, Ery-7, Ery-5, Ery-4, Ery-3 | Saccharopolyspora erythraea NRRL 2338 |
| BGC0000889.5 | | 0.41 | other (other) | bagremycin A, bagremycin B | Streptomyces sp. WK-5344 |
| BGC0000410.5 | | 0.41 | NRPS | pseudomonine | Pseudomonas fluorescens |
| BGC0001075.5 | | 0.41 | PKS, terpene | aurachin RE | Rhodococcus erythropolis |
| BGC0001592.5 | | 0.41 | other (other) | ferroverdin, bagremycin | Streptomyces lunaelactis |
| BGC0001392.5 | | 0.40 | ribosomal | pinensins | Chitinophaga pinensis DSM 2588 |
| BGC0000892.4 | | 0.40 | other (other) | caryoynencin | Burkholderia gladioli BSR3 |
| BGC0002110.3 | | 0.39 | ribosomal | birimositide | Streptomyces rimosus subsp. rimosus WC-3908 |
| BGC0002496.3 | | 0.39 | NRPS | serratiochelin A, serratiochelin C, serratiochelin B | Serratia plymuthica |

**Supplementary Figure 5.** MIBiG comparison was shown for the regions 7 and 8 by using antiSMASH (version 8.0.4). (A) Region 7 and (B) Region 8.

**A**

**Region 7**

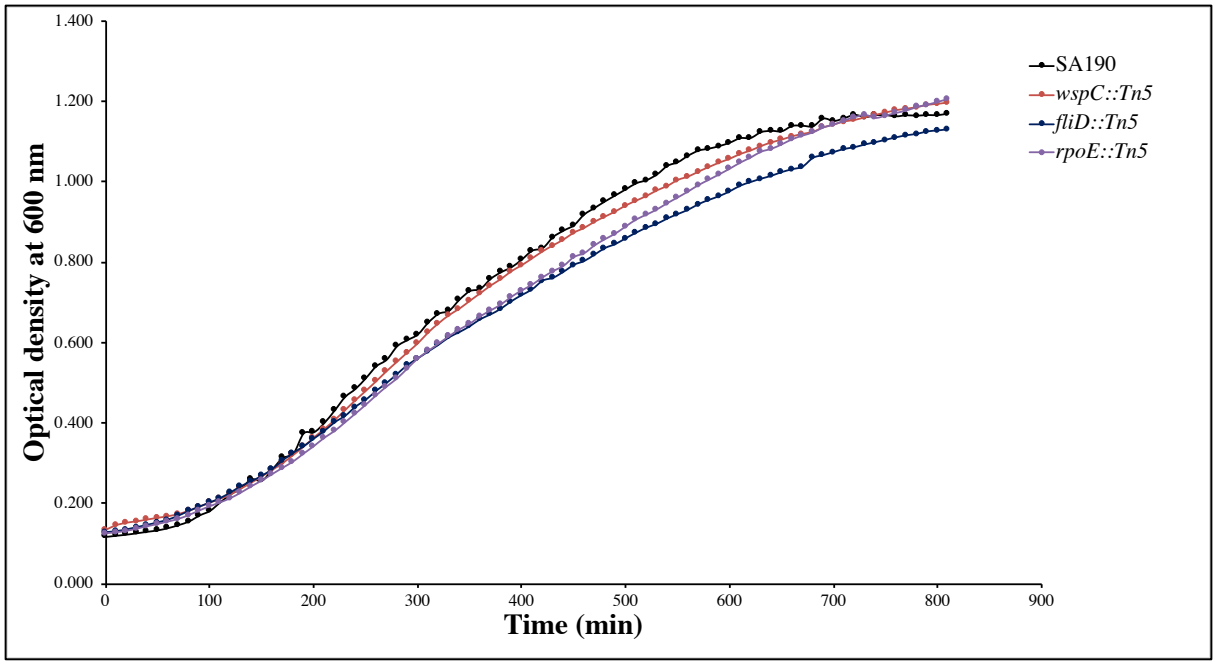
| Reference | terpene | Similarity score | Type | Compound(s) | Organism |
|---|---|---|---|---|---|
| BGC0000656.5 | | 0.81 | terpene | zeaxanthin | Xanthobacter autotrophicus Py2 |
| BGC0000647.3 | | 0.78 | terpene | carotenoid | Rhodobacter sphaeroides |
| BGC0000642.3 | | 0.77 | terpene | carotenoid | Enterobacteriaceae bacterium DC413 |
| BGC0000638.3 | | 0.76 | terpene | carotenoid | Pantoea ananatis |
| BGC0000641.3 | | 0.76 | terpene | carotenoid | Enterobacteriaceae bacterium DC416 |
| BGC0000640.3 | | 0.74 | terpene | carotenoid | Enterobacteriaceae bacterium DC404 |
| BGC0000639.3 | | 0.74 | terpene | carotenoid | Enterobacteriaceae bacterium DC260 |
| BGC0000630.3 | | 0.68 | terpene | (2R,3S,3'S)-2-hydroxyastaxanthin | Paracoccus haeundaensis |
| BGC0000643.3 | | 0.58 | terpene | carotenoid | Brevundimonas vesicularis |
| BGC0000646.5 | | 0.57 | terpene | β-carotein | uncultured bacterium |

**B**

**Region 8**

| Reference | NAGGN | Similarity score | Type | Compound(s) | Organism |
|---|---|---|---|---|---|
| BGC0001880.3 | | 0.44 | ribosomal | scytodecamide | Scytonema sp. UIC 10036 |
| BGC0000781.3 | | 0.42 | saccharide | O-antigen | Pseudomonas aeruginosa |
| BGC0000885.3 | | 0.42 | other (other) | 4-hydroxy-3-nitrosobenzamide | Streptomyces murayamaensis |
| BGC0000846.5 | | 0.42 | other (other) | tabtoxin | Pseudomonas syringae |
| BGC0000784.3 | | 0.37 | saccharide | O-antigen | Pseudomonas aeruginosa |
| BGC0001747.3 | | 0.36 | other (other) | pseudaminic acid | Tannerella forsythia |
| BGC0001395.5 | | 0.35 | other (other) | teichomycin A1 | Actinoplanes teichomyceticus |
| BGC0000937.5 | | 0.35 | other (other) | fosfazinomycin A, fosfazinomycin B | Streptomyces sp. WM6372 |
| BGC0001739.3 | | 0.34 | other (other) | phosphonoacetic Acid | Streptomyces sp. NRRL F-525 |
| BGC0001374.5 | | 0.34 | other (other) | thienodolin | Streptomyces albogriseolus |

**Supplementary Figure 6. Growth curves of SA190 and the *wspC*::Tn5, *rpoE*::Tn5, and *fliD*::Tn5 mutants.** SA190 and the biofilm mutants were grown in LB medium, and the optical density at 600 nm ($OD_{600}$) was measured every 10 minutes.



# Chapter 3

## Root endophyte sulfur metabolites enhance redox balance and drought tolerance in Arabidopsis

**Elkatmis B**, Alkhateeb RS, Mannes C, Jalal R, Trapp M, Westhoff P, Ozkan C, Thelen GM, Han B, Saad MM, Kopriva S, Hirt H (2026)

bioRxiv 2026.06.15.732246. https://doi.org/10.64898/2026.06.15.732246

## Supplementary material

**Supplementary Table 1.** Plasmids used in this study

**Supplementary Table 2.** Primers used for the generation of marker-free *gshA* and *gshB* deletion mutants

**Supplementary Figure 1.** Effect of *Pseudomonas argentinensis* SA190 on Arabidopsis *sultr1;2*, *apr2*, and *cad2-1* mutants under control (non-stress) conditions.

**Supplementary Figure 2.** Effect of *Pseudomonas argentinensis* SA190 on Arabidopsis *sultr1;2*, *apr2*, and *cad2-1* mutants under 25% PEG-induced drought stress conditions.

**Supplementary Figure 3.** Effect of *Pseudomonas argentinensis* SA190 on sulfate uptake in *Arabidopsis thaliana* Col-0 and sulfur pathway-deficient Arabidopsis mutants under control and 25% PEG-induced drought stress conditions.

**Supplementary Figure 4.** Effect of *Pseudomonas argentinensis* SA190 under 1 mM buthionine sulfoximine (BSO) and 0.5 mM glutathione (GSH) treatments in control (non-stress) conditions.

**Supplementary Figure 5.** Effect of *Pseudomonas argentinensis* SA190 on Arabidopsis under 1 mM buthionine sulfoximine (BSO) and 0.5 mM glutathione (GSH) under 25% PEG-induced drought stress conditions.

**Supplementary Figure 6.** Effect of buthionine sulfoximine (BSO) on the growth of *Pseudomonas argentinensis* SA190.

**Supplementary Figure 7.** Effect of *Pseudomonas argentinensis* SA190 on glutathione (GSH) levels in Arabidopsis *cad2-1* mutant under control (non-stress) and 25% PEG-induced drought stress conditions.

**Supplementary Figure 8.** Effect of *Pseudomonas argentinensis* SA190 glutathione deficient mutants on Arabidopsis *cad2-1* mutant under control (non-stress) conditions.

**Supplementary Figure 9.** Effect of *Pseudomonas argentinensis* SA190 glutathione deficient mutants on Arabidopsis *cad2-1* mutants under 25% PEG-induced drought stress conditions.

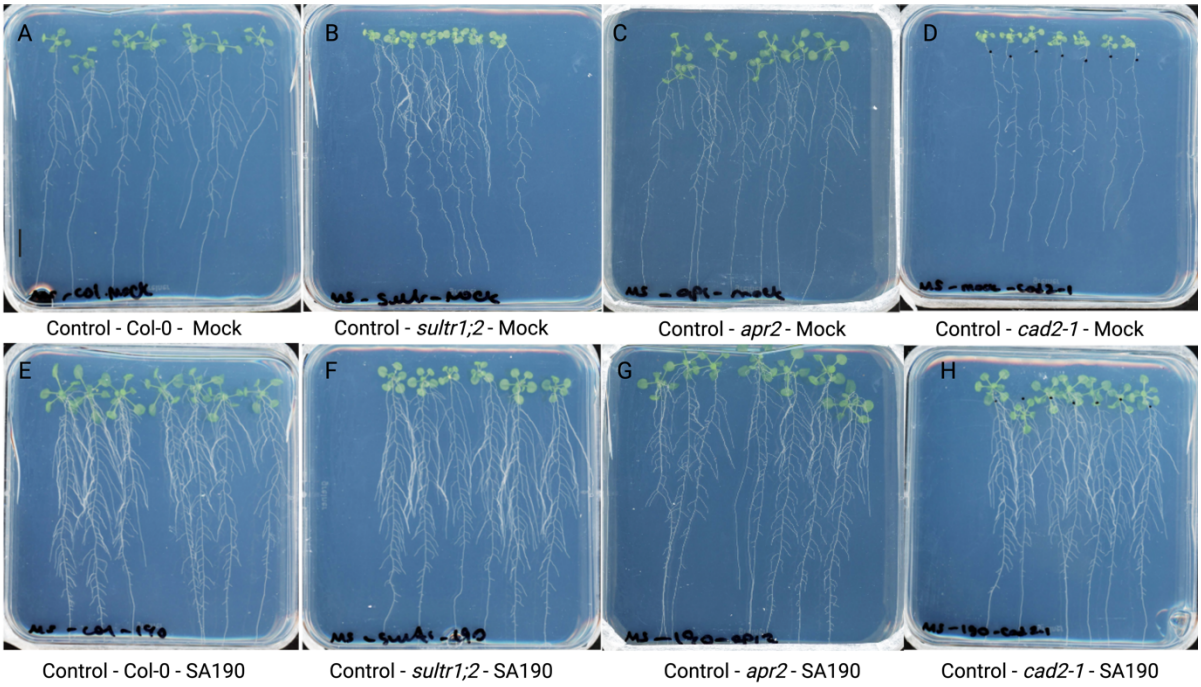
**Supplementary Data**

**Supplementary Table 1.** Plasmids used in this study

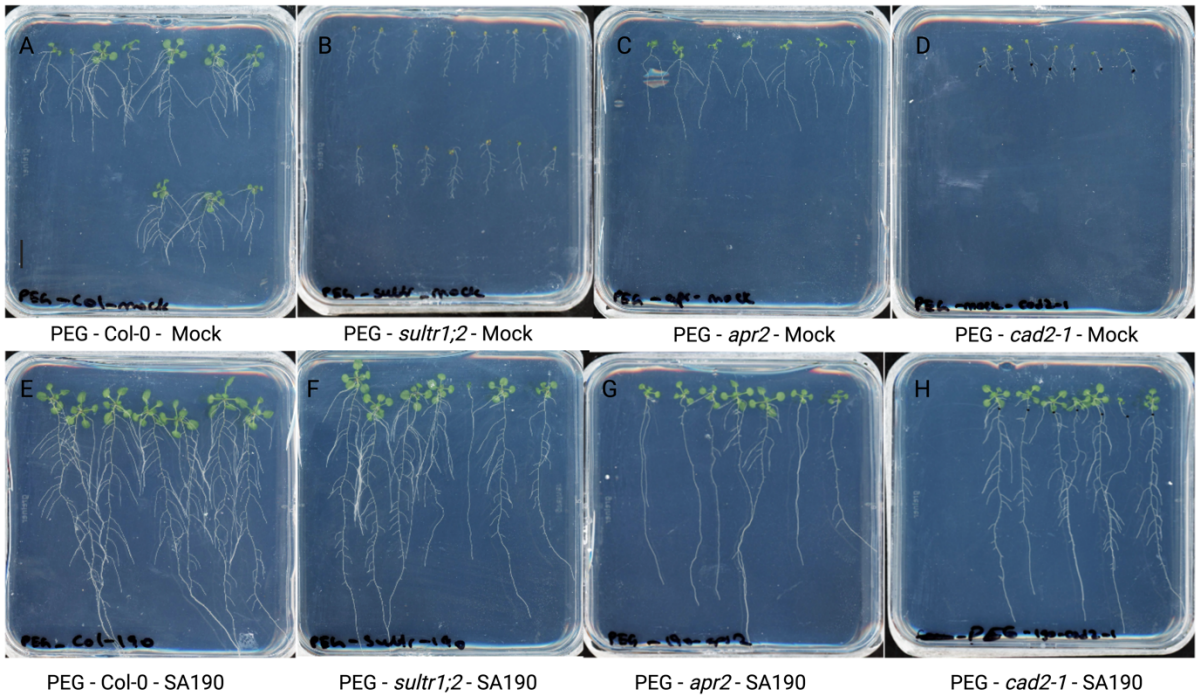
| Plasmids | Characteristics | Reference |
|---|---|---|
| pK18mobsacB | Suicide and narrow-broad-host vector | (Schäfer *et al*., 1994) |

**Supplementary Table 2.** Primers used for the generation of marker-free *gshA* and *gshB* deletion mutants

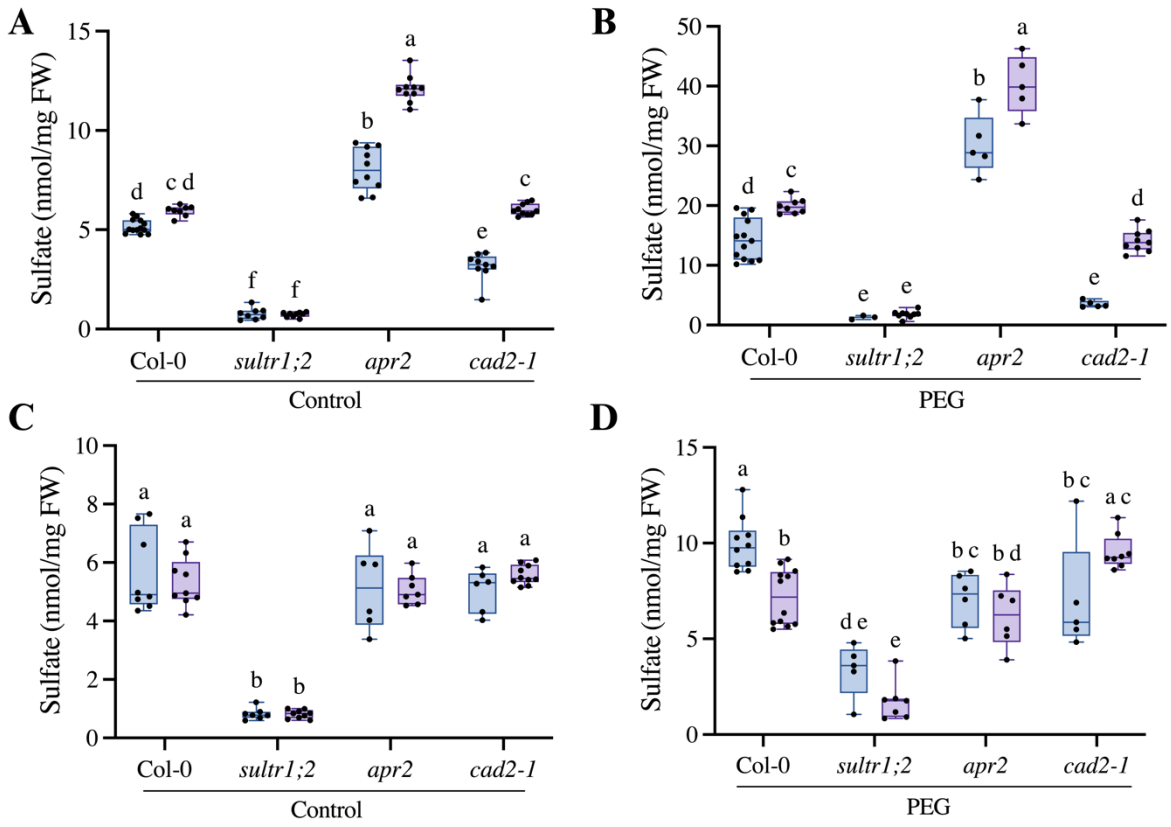
| Primers | Sequence (5'-3') | Usage |
|---|---|---|
| *gsha*_iF | GCCATTCGCCGTCTTTCTTG | |
| *gsha*_iR | CTGCCTGAAGAGGAGGTCAT | |
| *gsha*_oR | GCGACGTGGTCAAGGTCAAG | Deletion of *gsha* |
| *gsha*_oF | GATCACCATGGCGGTGAATT | |
| *gsha*_sF | GTGCTTGCAATCCATCCTAG | |
| *gshb*_iF | GGCACCCTGGTGGTCAAC | |
| *gshb*_iR | CCGCGCATTGAGCTTTTCG | |
| *gshb*_oR | GGACAACTGCGCGCTGTC | Deletion of *gshb* |
| *gshb*_oF | CGGTCGGCGAGTCATCAA | |
| *gshb*_sF | GAAACCAATGGGCCCGGC | |



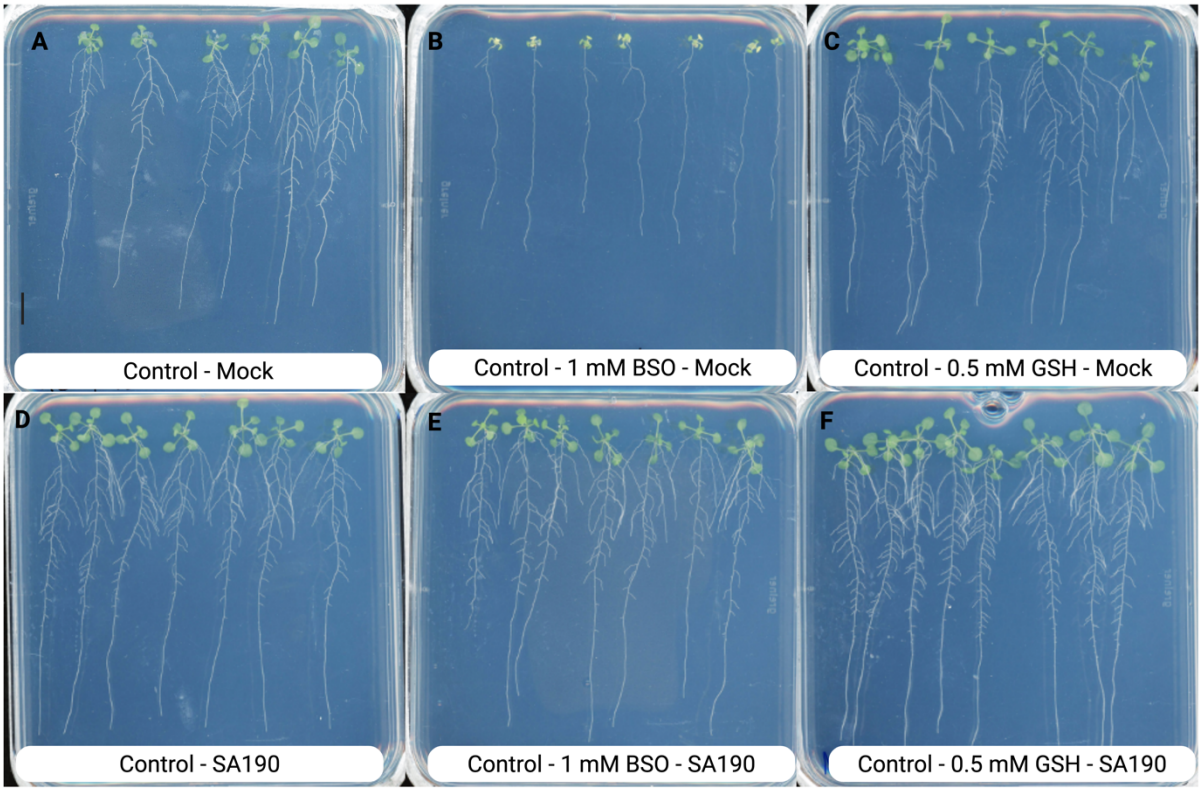

**Supplementary Figure 1. Effect of *Pseudomonas argentinensis* SA190 on Arabidopsis *sultr1;2, apr2*, and *cad2-1* mutants under control (non-stress) conditions.** Representative phenotypes of *Arabidopsis thaliana* Col-0 seedlings and the mutants after 15 days of growth under control conditions: non-colonized *Arabidopsis thaliana* Col-0, mock (A), non-colonized *sultr1;2,* mock (B), non-colonized *apr2,* mock (C), non-colonized *cad2-1,* mock (D), SA190-colonized *Arabidopsis thaliana* Col-0 (E), SA190-colonized *sultr1;2* (F), SA190-colonized *apr2* (G), SA190-colonized *cad2-1* (H). The scale bar is 1 cm.



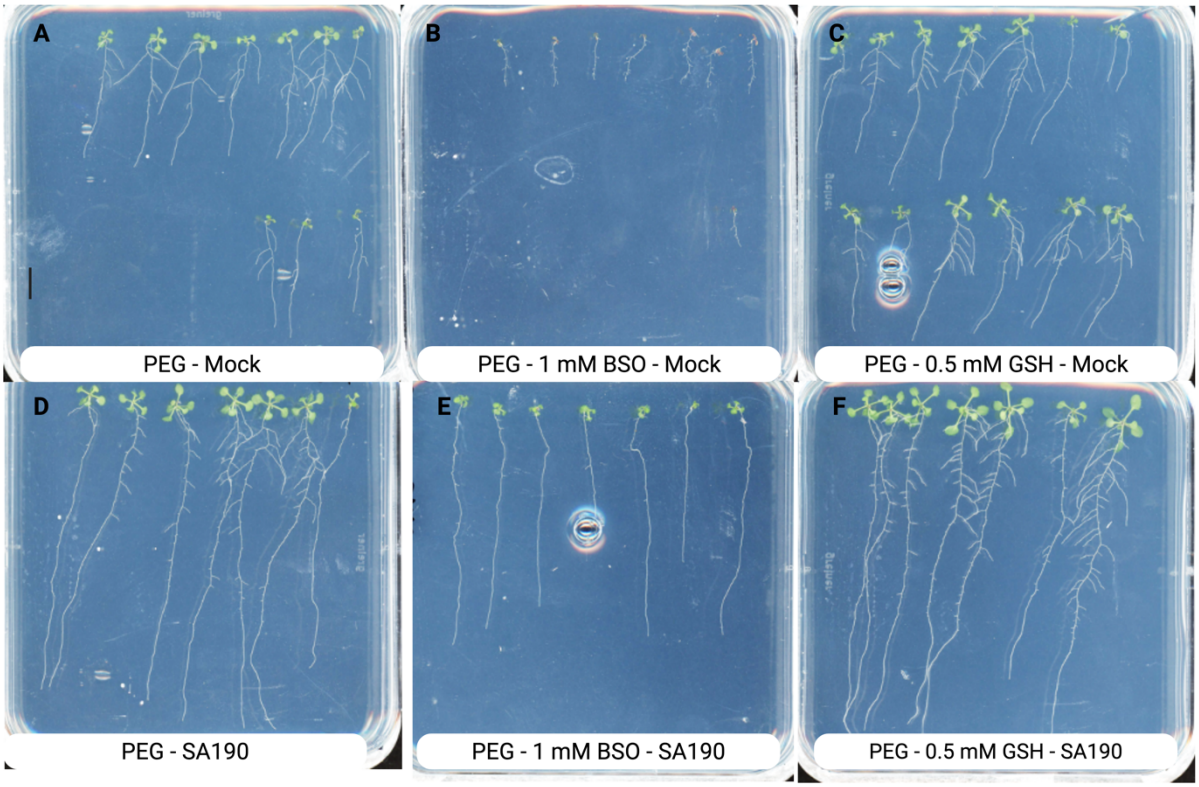

**Supplementary Figure 2. Effect of *Pseudomonas argentinensis* SA190 on Arabidopsis *sultr1;2, apr2*, and *cad2-1* mutants under 25% PEG-induced drought stress conditions.** Representative phenotypes of *Arabidopsis thaliana* Col-0 seedlings and the mutants after 15 days of growth under 25% PEG-induced drought stress: non-colonized *Arabidopsis thaliana* Col-0, mock (A), non-colonized *sultr1;2*, mock (B), non-colonized *apr2*, mock (C), non-colonized *cad2-1*, mock (D), SA190-colonized *Arabidopsis thaliana* Col-0 (E), SA190-colonized *sultr1;2* (F), SA190-colonized *apr2* (G), SA190-colonized *cad2-1* (H). The scale bar is 1 cm.



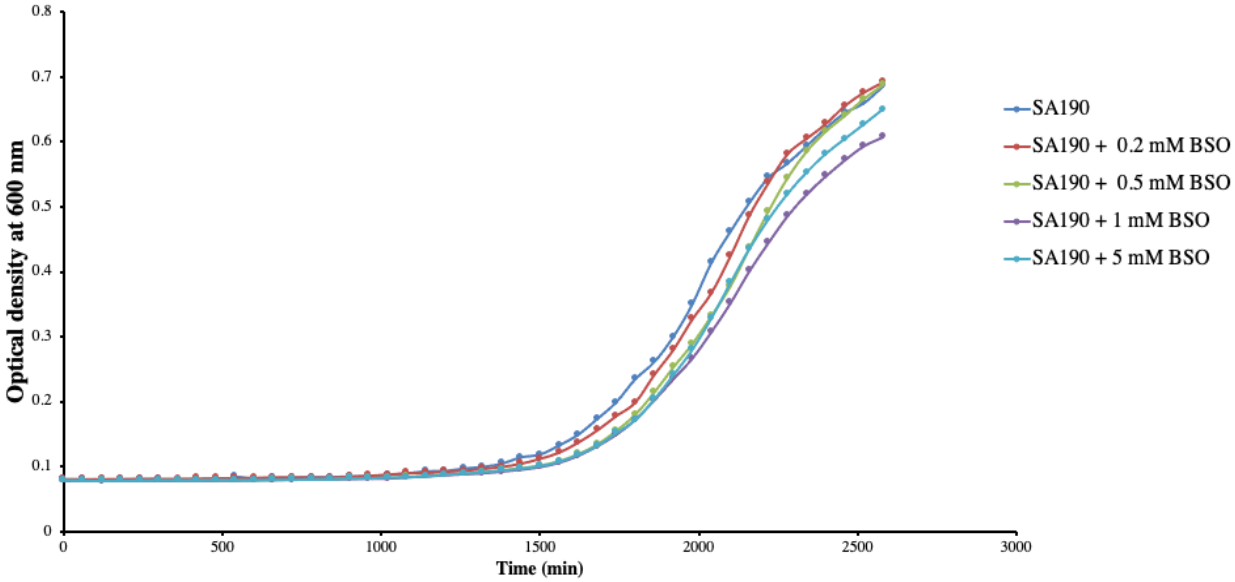

**Supplementary Figure 3. Effect of *Pseudomonas argentinensis* SA190 on sulfate uptake in *Arabidopsis thaliana* Col-0 and sulfur pathway-deficient Arabidopsis mutants under control and 25% PEG-induced drought stress conditions.** Sulfate content in shoot samples of Arabidopsis Col-0 and the *sultr1;2*, *apr2*, and *cad2-1* mutants under control conditions (A) and 25% PEG-induced drought stress conditions (B). Sulfate content in root samples of Arabidopsis Col-0 and the *sultr1;2*, *apr2*, and *cad2-1* mutants under control conditions (C) and 25% PEG-induced drought stress conditions (D). Whiskers represent minimum and maximum values, the horizontal line indicates the median. Different letters indicate statistically significant differences based on two-way ANOVA ($p < 0.05$).



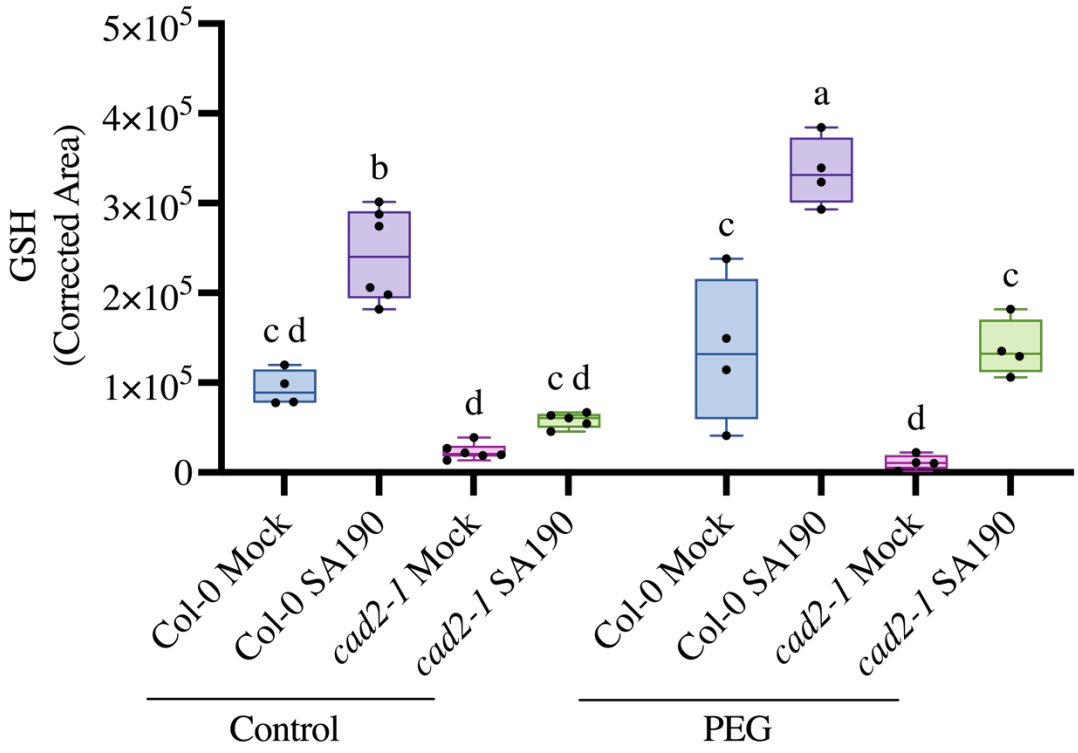

**Supplementary Figure 4. Effect of *Pseudomonas argentinensis* SA190 under 1 mM buthionine sulfoximine (BSO) and 0.5 mM glutathione (GSH) treatments in control (non-stress) conditions.** Representative phenotypes of *Arabidopsis thaliana* Col-0 seedlings after 12 days of growth under control conditions: non-colonized control (A), non-colonized + 1 mM BSO (B), non-colonized + 0.5 mM GSH (C), SA190-colonized (D), SA190-colonized + 1 mM BSO (E), and SA190-colonized + 0.5 mM GSH (F). The scale bar is 1 cm.



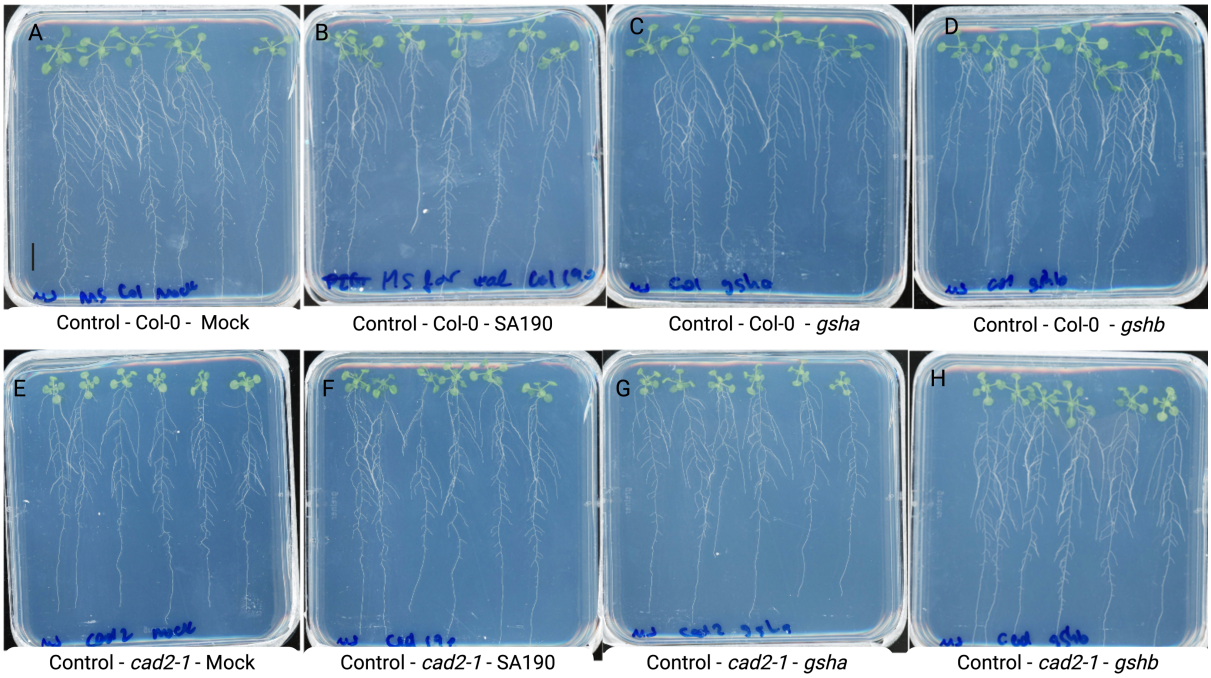

**Supplementary Figure 5. Effect of *Pseudomonas argentinensis* SA190 on Arabidopsis under 1 mM buthionine sulfoximine (BSO) and 0.5 mM glutathione (GSH) under 25% PEG-induced drought stress conditions.** Representative phenotypes of *Arabidopsis thaliana* Col-0 seedlings after 12 days of growth under 25% PEG-induced drought stress conditions: non-colonized control (A), non-colonized + 1 mM BSO (B), non-colonized + 0.5 mM GSH (C), SA190-colonized (D), SA190-colonized + 1 mM BSO (E), and SA190-colonized + 0.5 mM GSH (F). The scale bar is 1 cm.



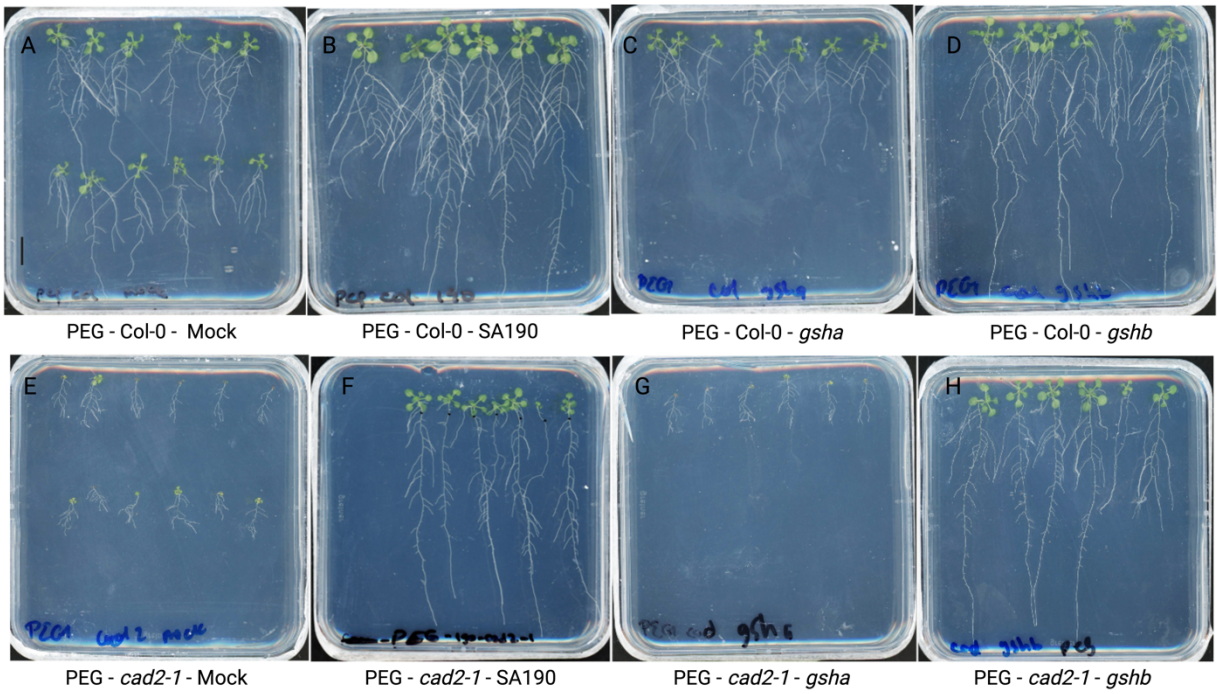

**Supplementary Figure 6. Effect of buthionine sulfoximine (BSO) on the growth of *Pseudomonas argentinensis* SA190.** BSO stock solution was added to SA190 liquid cultures to achieve final concentrations of 0.2 mM, 0.5 mM, 1 mM, and 5 mM in M9 medium. Bacterial growth was monitored every 10 minutes using a TECAN plate reader (Infinite M200 pro).




**Supplementary Figure 7. Effect of *Pseudomonas argentinensis* SA190 on glutathione (GSH) levels in Arabidopsis *cad2-1* mutant under control (non-stress) and 25% PEG-induced drought stress conditions.** GSH concentrations measured in shoot tissues of *Arabidopsis thaliana cad2-1* seedlings, non-colonized or colonized with SA190, grown under control (non-stress) and 25% PEG-induced drought stress conditions. Boxplots show data from two technical replicates. Whiskers represent minimum and maximum values, the horizontal line indicates the median. Different letters denote statistically significant differences based on two-way ANOVA ($p < 0.05$).




**Supplementary Figure 8. Effect of *Pseudomonas argentinensis* SA190 glutathione deficient mutants on Arabidopsis *cad2-1* mutant under control (non-stress) conditions.** Representative phenotypes of *Arabidopsis thaliana* Col-0 and *cad2-1* mutant seedlings after 15 days of growth under control conditions: non-colonized *Arabidopsis thaliana* Col-0, mock (A), SA190-colonized Col-0 (B), Δ*gsha*-colonized Col-0 (C), Δ*gshb*-colonized Col-0 (D), non-colonized *cad2-1*, mock (E), SA190-colonized *cad2-1* (F), Δ*gsha*-colonized *cad2-1* (G), Δ*gshb*-colonized *cad2-1* (H). The scale bar is 1 cm.




**Supplementary Figure 9. Effect of *Pseudomonas argentinensis* SA190 glutathione deficient mutants on Arabidopsis *cad2-1* mutants under 25% PEG-induced drought stress conditions.** Representative phenotypes of *Arabidopsis thaliana* Col-0 and *cad2-1* mutant seedlings after 15 days of growth under PEG stress conditions: non-colonized *Arabidopsis thaliana* Col-0, mock (A), SA190-colonized Col-0 (B), Δ*gsha*-colonized Col-0 (C), Δ*gshb*-colonized Col-0 (D), non-colonized *cad2-1*, mock (E), SA190-colonized *cad2-1* (F), Δ*gsha*-colonized *cad2-1* (G), Δ*gshb*-colonized *cad2-1* (H). The scale bar is 1 cm.